PhD degree in Molecular Medicine

European School of Molecular Medicine (SEMM),

University of Milan and University of Naples "Federico II"

Faculty of Medicine

Settore disciplinare: MED/04

The role of CD133 in the identification and maintenance of cancer stem cells derived from human glioblastoma

Brescia Paola

IFOM-IEO Campus, Milan

Matricola n. R07949

Supervisor: Prof. Pelicci Giuliana

IFOM-IEO Campus, Milan

Anno accademico 2010-2011

Your time is limited, so don't waste it living someone else's life. Don't be trapped by dogma, which is living with the results of other people's thinking. Don't let the noise of others' opinions drown out your own inner voice. And most important, have the courage to follow your heart and intuition. They somehow already know what you truly want to become.

TABLE OF CONTENTS

LIST OF ABBREVIATIONS

Amp	Amplified
BMP	Bone Morphogenic Protein
BSA	Bovine Serum Albumin
CDK	Cyclin-Dependent Kinase
CGH	Comparative Genomic Analysis
Chk	Checkpoint Protein
CNS	Central Nervous System
CSC	Cancer Stem Cell
Ct	Computer Tomography
DAPI	4,6-diamidino-2-phenylindole
DNA	Desoxyribonucleic acid
EDTA	Ethylenediaminetetraacetic acid
EGF(R)	Epidermal Growth Factor (Receptor)
FACS	Fluorescence Activated Cell Sorting
FFPE	Formalin-Fixed Paraffin-Embedded
FGF	Fibroblast Growth Factor
FSC	Forward Scatter
GBM	Glioblastoma
G-CIMP	Glioma-CpG Island Methylator Phenotype
GFP	Green Fluorescent Protein
GSC	Glioma Stem Cell
H&E	Hematoxylin and Eosin
HGF(R)	Hepatocyte Growth Factor (Receptor)
HPRT1	Hypoxanthine PhosphoRibosylTransferase 1
IDH	Isocitrate Dehydrogenase
IGF	Insulin-like Growth Factor
LOH	Loss Of Heterozigosity
mAb	monoclonal Antibody
MAPK	Ras-Mitogen-Activated Protein Kinase
MDR	Multi-Drug Resistance
MGMT	O-6-MethylGuanine-DNA MethylTransferase
MRI	Magnetic Resonance Imaging
mRNA	Messenger Ribonucleic Acid
mTOR	Mammalian Target Of Rapamycin
MTS/PMS	3-(4,5-dimethylthiazol-2-yl)-5-(3-carboxymethoxyphenyl)-2/phenazine methosulfate
Mut	Mutated
ND	Not Determinated
NF	NeuroFibromatosis
NSC	Neural Stem Cell
NT	Not Targeting
OE	Over-Expressed
PBS	Phosphate Buffered Saline
PDGF(R)	Platelet-derived Growth Factor (Receptor)
PET	Positron Emission Tomography
PFA	ParaFormAldehyde
PI3K	PhosphatidylInositol 3-Kinase
PROM1	Prominin1
PTEN	Phosphatase and Tensin Homologue
qRT-PCR	Quantitative Reverse Transcription-Polymerase Chain Reaction
Rb	Retinoblastoma
RTK	Receptor Tyrosine Kinase
Sh	Short Harpain
Shh	Sonic Hedgehog
TBP	Tata Binding Protein

TCGA	Cancer Genome Atlas Research Network
VEGF(R)	Vascular Endothelial Growth Factor (Receptor)
WHO	World Health Organization

FIGURES INDEX

TABLES INDEX

ABSTRACT

Glioblastoma multiforme (GBM) is the most common and lethal type of brain tumor in adults. There are some evidences that it is maintained by a population of cells, namely cancer stem cells, able to self-renew and propagate the tumor. Despite recent advances in surgical and therapeutic treatment, no tangible improvements have been made to prolong the patients' survival.

The role of the cell surface CD133 as a cancer stem cell marker in brain tumors has been widely investigated, since it identifies cells within glioblastomas able to initiate neurosphere growth and form heterogeneous tumors when transplanted in immune-compromised mice. However, evidences of CD133-negative cells exhibiting similar properties have been reported, making definitive conclusions on the correlation between tumor-initiating capabilities of glioma stem cells and CD133 expression difficult to drawn. Moreover, the functional role of CD133 in cancer stem/progenitor cells is not known.

We analyzed the efficiency of CD133 in the identification and isolation of glioblastoma stem cells and we investigated its functional role, studying the biological effects of CD133 down-regulation in GBM-derived neurospheres *in vitro* and *in vivo*.

We observed that CD133 is homogenously expressed in the cytoplasm of the cells composing the neurospheres, while its expression on the cell surface is highly variable. Cloning of single CD133-positive and CD133-negative cells demonstrated that CD133 shuttles dynamically between the plasmamembrane and the cell cytoplasm and no hierarchical relation can be established.

Knockdown of CD133 by lentiviral-mediated short hairpin RNAs (shRNA) reduces the self-renewal and tumorigenic capacity of the GBM-derived neurosphere cells.

Taken together, our data suggest that cell surface CD133 is not useful for the isolation of glioblastoma stem cells, since a complex regulation of its expression in terms of protein levels and cellular localization exists. However, CD133 may contribute to the maintenance and the tumorigenic potential of glioblastoma stem cells. This implies that CD133 could be used as a therapeutic target in glioblastomas, regardless of its expression on cell surface.

1. INTRODUCTION

1.1 Brain tumors

Gliomas are a heterogeneous group of oncological diseases, characterized by complex cellular composition and diffuse invasiveness. These tumors diffusely infiltrate the surrounding normal tissue and have a strong tendency to progress into a malignant and then fatal outcome.

Over the last years our knowledge about brain tumors has increased significantly, especially important progresses have been made on glioblastoma, the most aggressive among brain tumors, and unfortunately the most common.

The demonstration of the existence of cancer stem cells has shed light on some issues such as the cell of origin of these tumors and the characteristics of cells resistant to conventional therapies. The development of new animal models and large-scale genomic analysis allowed the identification of mutations that drive tumor development. International organizations comprising several institutes around the world, such as The Cancer Genome Atlas (TCGA), were created with the mission of understanding 'the molecular basis of cancer through the application of genome analysis technologies' (TCGA, 2008) and especially selected glioblastoma as the first cancer type for study, based on its uniformly poor prognosis and limited treatment options. TCGA permitted the collection of a great amount of data relating to brain tumors and the creation of web-tools freely accessible by the entire scientific community.

With these advances in our understanding about the biology of glioblastoma, improvements have come in therapy. Sadly, despite some advances in treatment, the overall survival of GBM patients cases is still not substantially different compared to the last decade.

1.1.1 Epidemiology of gliomas

Gliomas are the most common primary tumors of the central nervous system. Every year approximately five of hundred thousand individuals are diagnosed with glioma; the 60-70% of them is represented by the glioblastoma multiforme. Individuals of all ages can be affected but they are most common among elderly people. The peak of onset of glioblastomas is around 50 - 55 years, with men slightly more prone to these neoplasms. Furthermore, the incidence is 2 - 3 times

higher in white than in black people (Wen & Kesari, 2008). Prognosis is poor and the median survival is 14.6 months (Stupp et al, 2007); only few patients survive for three or more years. Main risk factors are high dose radiation, hereditary syndromes and increasing age. Only 5% of patients have a family history of gliomas: in most cases they are affected by rare genetic syndromes, such as neurofibromatosis type 1 and 2, the Li-Fraumeni syndrome and Turcot's syndrome. However, the genetic bases of malignant gliomas have not been identified yet.

1.1.2 Morphological classification of gliomas

Gliomas are classified according to the World Health Organization (WHO) guidelines (Louis et al, 2007). This classification system is based mainly on histopathology, according to morphological similarities between tumor cells and normal glial cells, cytoarchitecture and immunohistological marker profile. The WHO divides the diffuse gliomas into three main categories: astrocytomas (related to astrocytes), oligodendrogliomas (related to oligodendrocytes) and oligoastrocytomas (related to a mixture of these two cell types), and a grading system was created as a scale of malignancy. Four grades (I, II, III, and IV) distinguish astrocytomas and two grades (II and III) oligodendrogliomas and oligoastrocytomas. Lower grade astrocytomas (grade I-II) are well differentiated, have increased cell density and some cellular anomalies or atypias, but in general they resemble the non-neoplastic tissue. Tumors of higher grade (grade III tumors) are anaplastic with nuclear atypia, increased vessels and cell density and elevated mitotic activity. The grade IV astrocytoma, also known as glioblastoma multiforme (GBM), exhibits the additional presence of microvascular proliferation, necrosis and diffuse infiltration throughout the brain parenchyma, which denote the fully malignant state. The moniker "multiforme" derives from the varied morphological features of this tumor, in which heterogeneous cell populations with high degree of cellular and nuclear polymorphism and numerous giant cells coexist with area of high cellular uniformity.

Glioblastoma can be separated into two main subtypes on the basis of clinical presentation and biological and genetic differences (Furnari et al, 2007; Ohgaki & Kleihues, 2007) (Figure 1).

Primary glioblastomas occur *de novo* with no previous lower grade pathology, typically in patients older than 50 years of age. On the contrary, secondary glioblastomas are quite rare and are

manifested in younger patients as low grade or anaplastic astrocytomas that worsen over a period of 5-10 years into glioblastoma. Late-stage mixed gliomas or oligodendrogliomas can also resemble glioblastoma (Miller & Perry, 2007). Primary and secondary glioblastomas present distinct genetic alterations affecting similar molecular pathway. Primary GBMs are characterized by EGFR amplification and mutations, loss of heterozygosity of chromosome 10q, deletions of PTEN and p16. Secondary GBMs are more frequently characterized by mutations in p53 tumor suppressor gene, over-expression of PDGFR, abnormalities in the p16 and Rb pathways, and loss of heterozigosity of chromosome 10q. Despite the genetic differences and their distinct clinical course, primary and secondary glioblastomas are morphologically indistinguishable and respond similarly to conventional therapy, but they may respond differently to targeted molecular therapy (Figure 1).

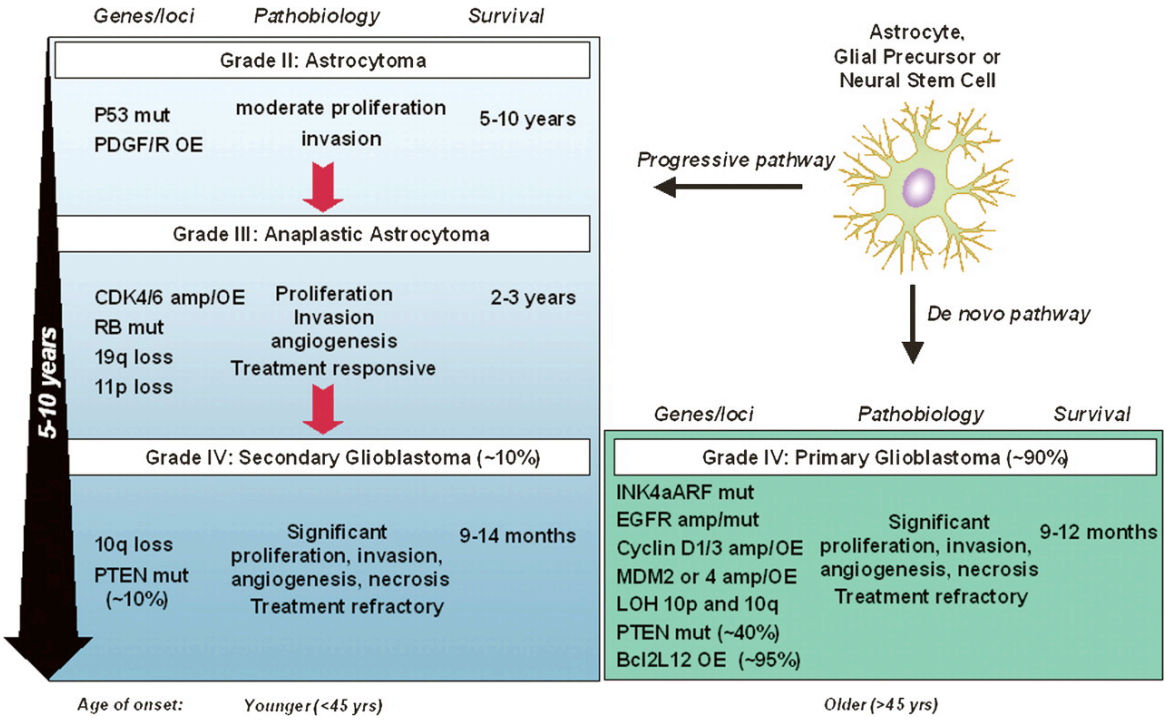

Figure 1. Chromosomal and genetic aberrations involved in the genesis of glioblastoma.
Pathobiologies, survival, genetic and chromosomal alterations involved in the development of primary and secondary glioblastomas are shown. Although histologically indistinguishable, these grade IV gliomas occur in different age groups and present distinct genetic alterations affecting similar molecular pathways. (OE) Overexpressed; (amp) amplified; (mut) mutated. Adapted from Furnari et al., 2007.

1.1.3 Genetic abnormalities in gliomas

Numerous molecular abnormalities are linked to the pathogenesis of different glioma variants. The comparative genomic hybridization analyses (CGH) and the large-scale integrated genomic analyses (Parsons et al, 2008; TCGA, 2008) have resulted in more comprehensive analyses of the molecular aberrations underlying gliomagenesis. The Cancer Genome Atlas (TCGA) has so far accumulated expression, copy number alterations and sequencing data from hundreds of histologically confirmed glioblastomas and has comprehensively catalogued the genomic anomalies associated with GBM. Furthermore, the biological relevance of many of these molecular abnormalities to the process of gliomagenesis has been confirmed by mouse modeling studies (Huse & Holland, 2009).

Genetic alterations characteristic of astrocytic glioma lead to aberrant activation of key signaling pathways mainly those involved in mitogenic signaling and cell cycle control.

1.1.3.1 Growth factor pathways

Alterations of the receptor tyrosine kinases (RTKs) and their associated downstream pathways occur in a large percentage of diffuse gliomas and appear to be critical to oncogenesis in these tumors. Genomic amplification and activating mutations in the EGFR locus occur almost exclusively in primary glioblastomas and represent the most prevalent RTK-associated molecular abnormality in malignant glioma (~45% of GBM). About half of the tumors with EGFR amplification express a constitutively autophosphorylated variant of EGFR, known as EGFRvIII, that lacks the extracellular ligand-binding domain (exon 2 through 7) (Frederick et al, 2000; Furnari et al, 2007; Pelloski et al, 2007).

Enhanced PDGF signaling, either through receptor (PDGFR) amplification/mutation or through ligand over-expression has been found to be a common feature of low grade gliomas along with a significant subset of glioblastomas (Westermark et al, 1995). Although activating mutations in PDGFRA are uncommon (Clarke & Dirks, 2003), frequent co-expression of both receptor and its ligand, most commonly PDGFB, indicates the potential for autocrine or paracrine loops boosting oncogenic signaling through the PDGF network.

Hepatocyte growth factor (HGF) and its RTK MET (also known as HGFR) appear to operate in a smaller subset of GBMs (Abounader & Laterra, 2005), as does the RTK ligand IGF2 (Soroceanu et al, 2007).

Common signal transduction pathway activated by growth factors is the MAPK pathway, which is involved in proliferation and cell cycle progression, and the PI3K-Akt-mTOR pathway, which is involved in the inhibition of apoptosis and cellular proliferation. Further dysregulation of the downstream PI3K-AKT-mTOR and Ras-MAPK signaling pathways also exists in the majority of malignant gliomas (Furnari et al, 2007). Mutations in the catalytic or regulatory domain of PI3K that are hypothesized to lead to its constitutive activation occur in 15% of GBMs. Notably, PTEN and NF1, important negative regulators of the PI3K-AKT-mTOR and Ras-MAPK networks, respectively, are frequently mutated or deleted in GBM (36% and 18%, respectively), and loss of PTEN at the protein level is found in more than 80% (TCGA, 2008).

1.1.3.2 Cell cycle regulators

p53 and RB functions are inhibited by mutations or copy number alterations in at least 87% and 78% of GBMs, respectively (TCGA, 2008). Additionally, mutations in the TP53 gene frequently characterize low-grade astrocytomas and the secondary glioblastomas into which they evolve (Furnari et al, 2007). The Rb tumor suppressor pathway has been shown to be defective in a significant number of high-grade gliomas of both astrocytic and oligodendroglial lineage, either by inactivating mutations in RB1 itself or by amplification of its negative regulators CDK4 and, less frequently, CDK6 (Costello et al, 1997; Henson et al, 1994). Analogously, amplification of the p53 antagonists MDM2 and MDM4 have also been found in distinct subsets of Tp53‐intact glioblastomas, as mutations and/or deletions in the CDKN2A locus that encodes both INK4A and ARF, which are crucial positive regulators of RB and p53, respectively.

1.1.3.3 Other genetic alterations

Integrated genomic analysis has facilitated the identification and characterization of additional genes involved in glioma pathogenesis. Missense mutations in IDH1 are found in a significant number of glioblastomas that tend to occur mostly in younger patients with more protracted clinical

courses (Parsons et al, 2008). These point mutations are restricted exclusively to the R132 residue in the active site region of the protein in which they disrupt hydrogen binding with its substrate (Parsons et al, 2008; Yan et al, 2009). Interestingly, a separate group of gliomas harbor mutations in the IDH1 homologue IDH2 at the analogous residue (R172). Further investigations have shown that mutations in IDH1 and IDH2 are present in a high proportions of grade II and III astrocytic and oligodendroglial tumors (72–100%) along with secondary glioblastomas (85%), but are largely absent in primary glioblastomas (5%) (Hartmann et al, 2009; Yan et al, 2009). Furthermore, across all histological types of diffuse glioma, IDH mutations tend to segregate with other low-grade glioma-associated genomic abnormalities, such as TP53 mutations and 1p/19q deletion, and are not associated with EGFR amplification and chromosome 10 loss, anomalies occurring frequently in primary GBM. These findings define an oncologic pathway for low-grade gliomas and the malignant tumors into which they evolve, which is distinct from the one used by *de novo* primary GBM. The IDH1 mutation is associated with longer survival (Hartmann et al, 2010) of patients with secondary glioblastoma and thus may be a highly valuable prognostic biomarker (von Deimling et al, 2011). IDH mutational status has also been linked with DNA methylation profiles in diffuse glioma. Recent analysis by TCGA has demonstrated a small subset of GBMs (8.8%), which exhibit a G-CIMP characterized by stereotyped hypermethylation of CpG islands in over 1,500 loci across the genome (Noushmehr et al, 2010). G-CIMP-positive GBMs exhibit increased frequency of characteristic copy number alterations (CNAs) in 8q and 10p and are highly enriched for IDH mutations. By report, approximately 87% of G-CIMP-positive versus 5% of G-CIMP-negative tumors was IDH-mutant, combining TCGA data with a validated tumor set. The striking correlation between G-CIMP and IDH mutation is common across all diffuse glioma variants, especially in lower-grade astrocytomas and oligodendrogliomas.

1.1.4 Molecular classification of gliomas.

The WHO glioma classification has shown a remarkable prognostic power, however considerable variability in clinical outcome among patients within each diagnostic category still exists. This is mainly due to the molecular complexity of gliomas and it has created the need of a more accurate

classification of gliomas. The identification of prognostically distinct molecular subtypes within otherwise morphologically homogeneous gliomas is also crucial.

Gene expression profiling studies have been used to identify subclasses of gliomas based on transcriptional signatures. Earliest studies identified gene expression differences among morphologically defined gliomas. Differentially expressed genes were found among GBM and lower grade gliomas (Fuller et al, 2002; Li et al, 2009; Nutt et al, 2003; Rickman et al, 2001; Shai et al, 2003; Shirahata et al, 2007) primary and secondary GBMs (Godard et al, 2003; Miraglia et al, 1997; Shai et al, 2003), adult and pediatric brain tumors, or a variety of morphologically defined glioma subtypes (van den Boom et al, 2003). These studies confirmed that morphological differences among gliomas are reflected at the mRNA level. In some cases gene expression profiles classify diagnostically challenging malignant gliomas in a manner that better correlates with clinical outcome than standard pathology does (Nutt et al, 2003; Shirahata et al, 2007).

Several schemes for classifying GBM subtypes based on expression signatures have been proposed in the past several years (Freije et al, 2004; Nigro et al, 2005; Phillips et al, 2006; Verhaak et al, 2010; Vital et al, 2010). The first relevant study carried out by Phillips and colleagues divides a cohort of malignant gliomas, comprised of both WHO grade III and IV, into three molecular subtypes named Proneural, Proliferative, and Mesenchymal based on the key features of the molecular signatures associated with each group. The Proneural subtype is defined by genes implicated in neurogenesis. It is associated with better outcome than either of the other two tumor subtypes. In contrast, the Proliferative and Mesenchymal gene signatures are defined by proliferation- and extracellular matrix/invasion-related genes respectively, and are both associated with poor outcome. GBMs with Proliferative signatures have an elevated MIB-1 index in tumor cells, whereas GBMs of the Mesenchymal subtype show evidence for increased angiogenesis. The authors speculated that poor outcome of Proliferative and Mesenchymal tumors may be differentially associated with a high rate of tumor cell proliferation or angiogenesis, respectively. Prognostic significance of molecular subtype was validated in an independent cohort of 184 gliomas of various histological types. Remarkably, nearly all WHO grade III tumors (65 out of 73 gliomas) fell into the Proneural subgroup, along with a subset of glioblastomas occurring in younger patients with prolonged disease courses. Moreover recurrent tumors, although mostly

retaining their initial transcriptional subclassification, seemed to significantly shift their mRNA signatures towards the Mesenchymal profile. Of note, a recent work has identified a set of master regulator transcription factors, the most important of which are STAT3 and C/EBP-β, which seem to mediate the expression of the Mesenchymal phenotype and so enhance glioblastoma aggressiveness (Carro et al, 2010).

An additional clustering analysis using transcriptional data obtained by the TGCA on 200 primary GBMs has established four distinctive GBM subtypes, namely Proneural, Neural, Classical, and Mesenchymal (Verhaak et al, 2010). Significant similarities, but not an entirely overlap, were found between the mesenchymal and proneural phenotypes described in Phillips' and Verhaak's works. Unlike previous studies, the TCGA proneural subtype is not associated with improved prognosis in the TCGA data set consisting solely of grade IV astrocytoms, but it is in the validation of the data sets, containing lower-grade gliomas. Conversely, re-analysis of the TCGA data using Phillips' molecular subtype designations confirmed a slightly more favorable prognosis of the "Phillips-proneural" relative to "Phillips-mesenchymal/proliferative" GBMs (Huse et al, 2011). Because of the tremendous amount of molecular data available for these tumors (TCGA, 2008) recurrent genomic aberrations in each molecular subtype were identified.

The proneural subtype is more diffused in younger patients, as found in previous studies (Lee et al, 2008; Phillips et al, 2006) and harbors frequent PDGFRA amplification and point mutations in IDH1, TP53 mutations and loss of heterozigosity and PIK3CA/PIK3R1 mutations. The proneural group shows high expression of oligodendrocytic development genes (such as PDGFRA, NKX2-2 and OLIG2) and this signature contained several proneural development genes as well as DCX, DLL3, ASCL1 and TCF4 (Phillips et al, 2006). The neuronal subtype was characterized by the expression of neuron markers such as NEFL, GABRA1, SYT1 and SLC12A5. The classical subtype was characterized by frequent EGFR amplification and EGFRvIII mutations and a distinct lack of TP53 mutations and CDKN2A deletion. The mesenchymal subtype was typified by deletion of NF1, TP53, and PTEN genes and displayed expression of mesenchymal markers, such as CHIL3 (also known as YKL40) and MET, as described elsewhere (Phillips et al, 2006). Moreover, higher overall necrosis, microvascular proliferation and inflammatory infiltrates are frequent in mesenchymal GBM, while necrosis typically lacks in the proneural subtype.

Using a proteomic analysis three proteomically-defined subclasses of GBM have been identified. These subclasses are characterized by protein- and phosphorylation-level signaling abnormalities in the EGFR, PDGFR, and NF1 pathways and correspond to classical, proneural, and mesenchymal subtypes of GBM, respectively (Brennan et al, 2009).

Analysis of epigenetic changes performed by TCGA on GBMs identified a distinct subset of samples with characteristic promoter methylation alterations, indicating the existence of a G-CIMP phenotype (Noushmehr et al, 2010). G-CIMP tumors were mainly secondary or recurrent GBMs and were tightly associated with IDH1 mutations and displayed distinct copy-number alterations. Patients with G-CIMP positive tumors were younger at the time of diagnosis and survived longer than G-CIMP negative GBM patients. The integration of DNA methylation and gene expression data showed that G-CIMP positive tumors represented a subset of proneural tumors. At the end, G-CIMP could be used to further refine the expression-defined groups into an additional subtype with clinical implications.

Several studies have been published on the identification of glioma subtypes based on gene expression profiles, but no consensus gene expression profile in malignant gliomas reproducibly associates with patient outcome across independent datasets.

However, the first gene expression profile based diagnostic test is currently being evaluated in two prospective, randomized clinical trials (Colman et al, 2010). A 9-gene profile (AQP1, CHI3L1, EMP3, GPNMB, IGFBP2, LGALS3, OLIG2, PDPN, and RTN1) predictive of clinical outcome was identified for the development of a qRT-PCR assay performed on FFPE samples. On the basis of the logistical difficulties in obtaining fresh frozen tumors for DNA microarray based assays, such an assay is absolutely critical for successful clinical implementation with FFPE GBMs, which constitute the vast majority of clinical samples. In summary, molecular sub-typing has now the potential to become a readily implemented clinical test that may guide future treatment decisions.

1.1.5 Brain tumor therapy

1.1.5.1 Glioma diagnosis

Patients with a malignant glioma may present a variety of symptoms including headache, confusion and loss of memory, neurological deficits and personality changes. The diagnosis of malignant

gliomas is usually made by magnetic resonance imaging (MRI), computer tomography (CT) or positron emission tomography (PET). The images typically show an enhancing mass surrounded by edema. Glioblastomas frequently have central areas of necrosis and more extensive peritumoral edema than that one associated with anaplastic gliomas.

1.1.5.2 Glioma prognosis

Despite decades of research and clinical trials, life expectancy for glioma patients has not improved considerably and is only about 2-3 years for anaplastic astrocytoma and 15 months for glioblastoma (Stupp et al, 2005). There are several reasons why it has been so difficult to find new effective therapies against glioma. First, drug delivery is limited by the blood-brain-barrier impediment and the distorted glioma vessels. Second, the invasive nature of gliomas makes the complete surgical resection of the tumor impossible. Third, tumor cells have also a strong inherent propensity for malignant progression and some cells, supposedly the cancer stem cells, are resistant to therapy (Bao et al, 2006). Lastly, over-expression of proteins involved in DNA repair machinery could cancel the effects of radio- and chemotherapy.

1.1.5.3 Treatment

The standard treatment for gliomas is the surgical resection, radiotherapy and chemotherapy using alkylating agents. The size and localization of the tumor is important for the possibility to perform optimal surgery. Due to their invasive growth, gliomas indeed are impossible to resect completely. Surgical elimination of the tumor reduces the symptoms caused by mass effect and seems to give a modest survival advantage to the patient.

For patients with glioblastoma, the median survival from time of diagnosis is about three months without treatment. After treatment with surgery and postoperative temozolomide and radiotherapy, the survival increases to 14.6 months (Stupp et al, 2007). MGMT is an important repair enzyme that contributes to resistance to temozolomide. MGMT methylation silences the gene, decreasing DNA repair activity and increasing the susceptibility of the tumor cells to temozolomide. Treatment with temozolomide in glioblastoma patients with MGMT promoter methylation prolonged the survival to 2 years (Hegi et al, 2005).

Several approaches have been used to target individual signaling molecules involved in gliomagenesis. Particular interest has focused on inhibitors of RTKs and their downstream effectors, and on inhibitors of angiogenesis.

EGFR is one of the most widely expressed RTK in human gliomas, so several EGFR inhibitors have been developed (Castillo et al, 2004). Gefitinib (ZD1839, Iressa™) (Rich et al, 2004) and erlotinib (Tarceva®) (Prados et al, 2006) have been investigated in recurrent gliomas with limited activity. An alternative approach has been developed based on a vaccination strategy against the constitutively activated EGFRvIII (Sampson et al, 2008). CDX-110™ is a peptide-based vaccine that targets the tumor specific mutated segment of EGFRvIII and it is currently in phase II/III randomized studies with radiation and temozolomide.

Therapies directed towards the PDGFR pathway include many different putative targets (Grossman et al, 2001; Kilic et al, 2000). Imatinib (Gleevec®), a tyrosine kinase inhibitor specific for Abl kinase, c-KIT and PDGFR, has been demonstrated to have only limited anti-tumor activity in patients with recurrent malignant glioma (Raymond et al, 2008). PDGF antagonists might target the pericytes to preferentially block angiogenesis in established tumors (Sennino et al, 2007).

Since angiogenesis is a hallmark of malignant glioma and affects drug delivery, anti-angiogenic treatment could be of value in combination with already existing treatment modalities. The VEGF signalling pathway is the cornerstone in angiogenesis, so most anti-angiogenic therapies towards target VEGF or VEGFR. Bevacizumab (Avastin®) is a humanised anti-VEGFA mAb. Promising results from a phase II study with bevacizumab in combination with irinotecan was reported in patients with recurrent high-grade glioma (Vredenburgh et al, 2007). However, there are emerging problems with both developing treatment-resistance and adverse effects associated with anti-VEGF therapy such as disturbance of VEGF-dependent physiological functions and homeostasis in the cardiovascular and renal systems, wound healing and tissue repair. This promoted the search for novel antiangiogenic therapies. VEGF-trap (aflibercept) is a soluble VEGF receptor binding VEGF-A, -B, and PDGF and has been shown to be effective in both initial and advanced phase of tumor development in a preclinical tumor model (Gomez-Manzano et al, 2008). This molecule is now in phase II trial in recurrent glioma that is not responding to temozolomide. Cediranib (AZD2171, Recentin™) is a RTK inhibitor of Pan-VEGFR 1-3, PDGFR and c-KIT. It is currently

in phase III clinical study in recurrent glioblastoma where patients are randomised between treatment with cediranib alone, cediranib in combination with lomustine (an alkylating agent) or lomustine with placebo. Using MRI, it is also shown that cediranib normalizes tumor vessels in glioblastoma patients and alleviates edema (Batchelor et al, 2007). Other VEGFR inhibitors that may be active against malignant glioma include the VEGFR/PDGFR inhibitors vatalanib (PTK 787), pazopanib (GW 786034), sorafenib, and sunitinib; the VEGFR/EGFR inhibitor vandetanib (ZD6474); the adnectin-based CT 322; and the VEGFR/c-Met kinase inhibitor XL 184 (Norden et al, 2008).

A great amount of signaling pathways and potential targets in malignant glioma has been described. Many clinical studies are ongoing. For summary of potential targets see figure 2.

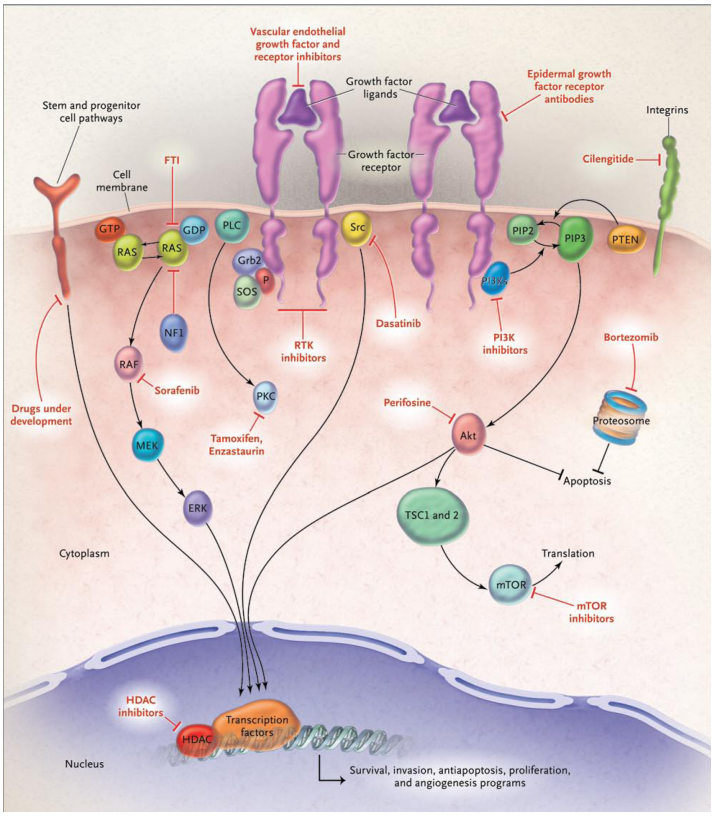

Figure 2. Major signaling pathways in malignant gliomas and the corresponding targeted agents in development for glioblastoma. Adapted from Wen and Kesari, 2008.

It is naive to believe that there will be one single treatment to cure all gliomas; rather the combination of multiple treatment strategies will have the best effect. Possibly, future patients will be given selected and individually targeted treatments based on the expression/mutation analysis of

that particular patient's tumor. Ideally, treatment could be tailored to achieve the highest possible efficacy depending on the expression of growth factors and mutated genes. Strong efforts are made to effectively target tumor stem cells that will be discussed in the next chapter. These cells are believed to survive both radiation and chemotherapy, and can generate new tumor cells during recurrence.

1.2 Cancer stem cells in solid tumors

Tumors are composed of a heterogeneous population of cells that exhibit different states of differentiation and proliferation capacity. At least two models have put forward to account for heterogeneity: the "cancer stem cell" (Bonnet & Dick, 1997; Reya et al, 2001) and the "clonal evolution" (Campbell & Polyak, 2007; Nowell, 1976) models (Figure 3).

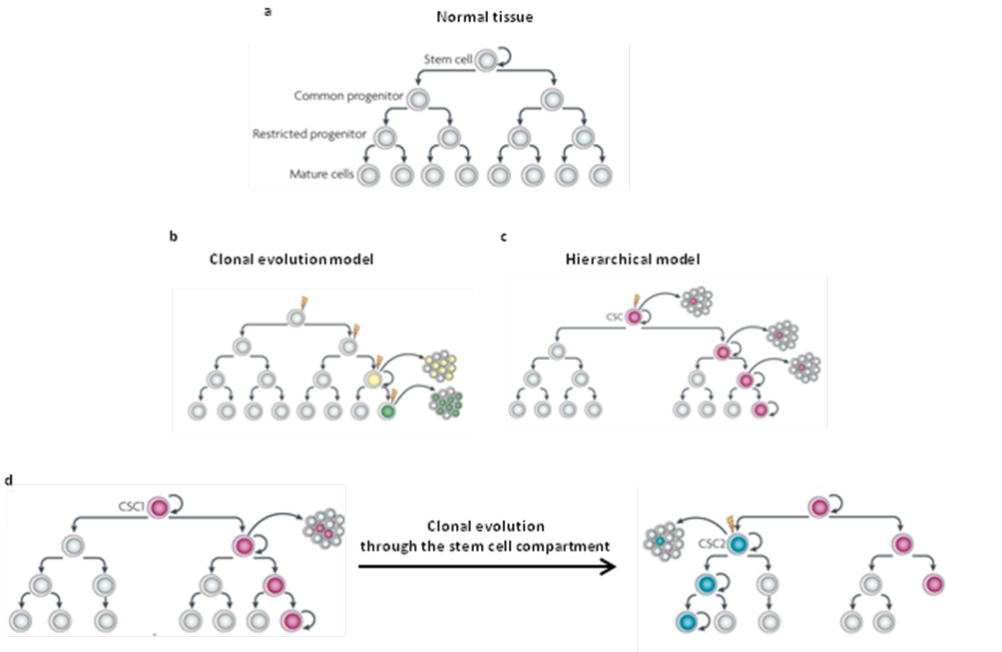

Figure 3. Cancer stem cells and clonal evolution models.
(a) In a normal tissue the cellular hierarchy comprising stem cells, which progressively generate more restricted progenitor cells and ultimately all the mature cell types that constitute the tissue. **(b)** In the clonal evolution model all undifferentiated cells have similar tumorigenic capacity. **(c)** In the cancer stem cell model, only the CSC can generate a tumor, based on its self-renewal properties and proliferative potential. **(d)** The two tumor models are not mutually exclusive- Initially, tumor growth is driven by a specific CSC (CSC1). With tumor progression, another distinct CSC (CSC2) may arise due to clonal evolution of CSC1. This may result from the acquisition of an additional mutation or epigenetic modification. This more aggressive CSC2 becomes dominant and drives tumor formation. Adapted from Visvader and Linderman, 2008.

The “cancer stem cell” hypothesis proposes that the growth and progression of many tumors are driven by a small subpopulation of cancer cells with stem-like features. These cells share important properties with normal tissue stem cells, including self-renewal (by symmetric and asymmetric division) and differentiation capacity, albeit aberrant. This implies that many cancers are hierarchically organized similarly to normal tissues. Just as normal stem cells differentiate into phenotypically diverse progeny with limited differentiation potential, CSCs also differentiate into phenotypically non-tumorigenic cells that compose the bulk of the cells within a tumor. The CSC model posits that differences in tumorigenic potential among cancer cells from the same patient are largely epigenetically determined, because it is unlikely that only rare cancer cells have a genotype permissive for extensive proliferation. However, there is no direct evidence that tumorigenic cells differ from non-tumorigenic cells as a result of epigenetic rather than genetic differences (Shackleton et al, 2009).

In the “clonal evolution” model all the cells have similar tumorigenic capacity. The mutated cells with a growth advantage are selected and expanded, with the cells in the dominant clone having a similar potential for generating tumor growth. The clonal evolution model postulates that genetic and epigenetic changes occur over time in individual cancer cells. If such changes confer a selective advantage they will allow individual clones of cancer cells to out-compete with other clones. Clonal evolution can lead to genetic heterogeneity, conferring phenotypic and functional differences among the cancer cells within a single patient (Shackleton et al, 2009).

It is important to note that the clonal evolution and the cancer stem cell model are not mutually exclusive in cancers that follow a stem cell model, as cancer stem cells would be expected to evolve by clonal evolution (Barabe et al, 2007). Thus, if a mutation conferring self-renewal or growth properties advantages occurs, a more dominant cancer stem cell may emerge among the others. For example, the leukemic stem cells that maintain chronic myeloid leukemia despite imatinib therapy would be selected by clonal evolution to develop imatinib resistance mutations over time (Shah et al, 2007).

The first evidence for the existence of CSCs came from acute myeloid leukemia (Bonnet & Dick, 1997; Lapidot et al, 1994), in which a rare subset of cells comprising 0.01-1% of the total population could induce leukemia when transplanted into immunodeficient mice. These concepts

and experimental approaches were then applied to solid tumors such as breast (Al-Hajj et al, 2003), brain (Singh et al, 2004) and colon (Ricci-Vitiani et al, 2007) cancers.

Most studies on cancer stem cells follow a common scenario: a marker or a combination of markers is found to be expressed in a heterogeneous fashion in a certain tumor type. On the basis of this marker heterogeneity or using markers of normal stem cells of the same organ, subpopulations of cells are sorted from primary tumors and transplanted into immunodeficient mice by limiting dilution; then, the tumor growth is evaluated some weeks or months later. Different capacity for tumor initiation between tumor cell subsets can be interpreted as evidence for the presence of CSCs in the primary tumor (Figure 4).

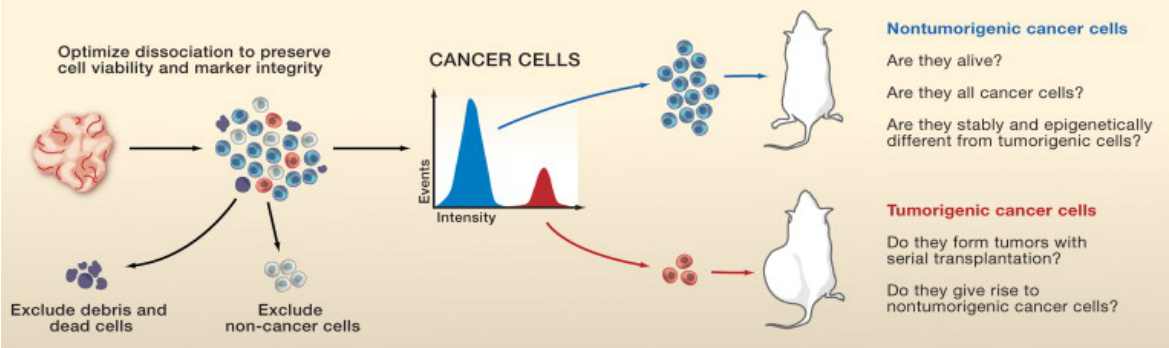

Figure 4. Testing the Cancer Stem Cell Model.
The tumor is dissociated into single cells using conditions optimized to maximize the preservation of cell viability and surface marker expression. The cells are sorted by flow cytometry using specific cell surface markers. The tumorigenicity of all cells is tested using xeno-transplantation assays. Adapted from Shackleton et al, 2009.

According to the CSC model only a specific subset of cancer cell population should be able to sustain *in vivo* tumor growth, whether all other subsets should not. The transplanted tumors contain mixed populations of tumorigenic and non-tumorigenic cancer cells, thus recapitulating at least some of the heterogeneity of the parental tumor. However, the most convincing demonstration of CSC identity comes from serial transplantation of a cellular population into the animal model, which is the only true demonstration of self-renewal ability of a cancer cell.

The frequency of cancer stem cells is highly variable between solid tumors of the same type. Recent mathematical analyses have further indicated that CSCs in advanced tumors may not occur

as a small fraction (Kern & Shibata, 2007). Extensive *in vivo* limiting dilution analyses are required to determine the frequency of CSCs within solid tumors and to prove enrichment (Bonnefoix et al, 1996). This may eventually allows correlation between CSCs frequency, tumor grade and clinical outcome. It is also important to note that the nature of the xenograft model used and the site of transplantation influence the determination of stem cell frequency. The efficiency of human cell engraftment can be significantly influenced by the presence of residual immune effector cells in recipient mice (Quintana et al, 2008). The xenogeneic immune response that mice mount against human cells can reduce the ability of human cancer cells to engraft in mice, underestimating the frequency of human cancer cell with tumorigenic potential. On the other hand it is also clear that immune cells have a role in the progression of many tumors and this highly artificial animal model may not represent the true *in vivo* niche. The activity of tumor cells can also be influenced by an altered vascular environment, which creates the stem cell niche. Thus, the development of orthotopic transplantation assays is crucial.

The concept that cancer growth can be sustained by cancer stem cells leads to the necessity of new and more effective antitumor treatments. According to the CSC model, therapeutic approaches that do not eradicate the CSC compartment are likely to achieve little success; they might kill the majority of tumor cells and induce temporary regression of gross tumor lesions but fail to prevent disease relapse and metastatic dissemination (Figure 5).

1.2.1 Neural Stem Cells

Neural stem cells (NSCs) are multipotent cells within the brain capable of self-renewal and differentiation into all major cell types of the central nervous system (neurons, astrocytes and oligodendrocytes) (Mayer-Proschel et al, 1997; Rao et al, 1998) (Figure 5). During development NSCs are found in the ventricular zone of the central nervous system. In the adult brain, NSCs are primarily restricted to two areas: the subependymal zone of the lateral ventricles and the subgranular zone of the dentate gyrus within the hippocampus. In the hippocampus, NSCs integrate functionally into the granule cell layer (Cameron & McKay, 2001). In the rodent brain, progeny from neural stem cells of the subventricular zone migrate along the rostral migratory stream to the olfactory bulb to differentiate into local interneuron (Lois et al, 1996; Luskin, 1993). In the human

brain, migration of neuroblasts toward the olfactory bulb may occur via alternate routes (Curtis et al, 2007; Sanai et al, 2004). Persistence of NSCs in the adult reflects their role in endogenous repair mechanisms and maintenance of normal brain functions. Adult neurogenesis is likely to have a crucial role in the neurobiological basis of learning and memory (Aimone et al, 2006).

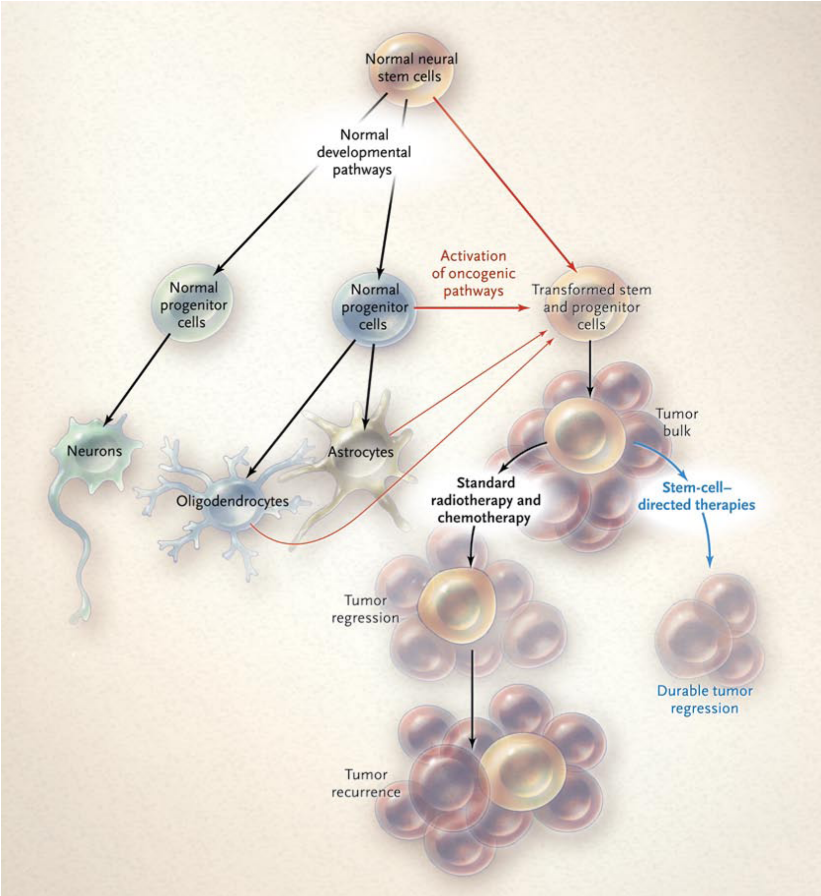

Figure 5. Resistance Mechanisms in Glioma Cells.
Normal neural stem cells self-renew and give rise to multipotential progenitor cells that form neurons, oligodendroglia, and astrocytes. Glioma stem cells arise from the transformation of either neural stem cells or progenitor cells (red) or, less likely, from differentiation of oligodendrocytes or astrocytes (thin red arrows) and lead to malignant gliomas. Glioma stem cells are relatively resistant to standard treatments such as radiation and chemotherapy and lead to re-growth of the tumor after treatment. Therapies directed at stem cells can deplete these cells and potentially lead to more durable tumor regression (blue).

1.2.3 Glioma stem cells (GSCs)

The presence of stem cells in brain tumors has been demonstrated in several studies (Galli et al, 2004; Hemmati et al, 2003; Ignatova et al, 2002; Singh et al, 2003; Singh et al, 2004; Yuan et al, 2004). However the isolation of brain tumor cells with tumorigenic capacity, tested *in vivo* using the xeno-transplantation assay, was initially reported independently by two groups (Galli et al,

2004; Singh et al, 2004). Although reaching at similar conclusions, they used different approaches for isolating brain tumor stem cells: the cell sorting based on selection for the cell surface marker CD133 (Singh et al, 2004) and the neurosphere assay (Galli et al, 2004).

1.2.3.1 Isolation of glioma stem cells using cell surface markers

The first prospective *in vitro* and *in vivo* identification and characterization of a putative CSC from human brain tumors was based on cell sorting for the neural stem cell surface marker CD133 (Singh et al, 2003; Singh et al, 2004). Uchida and colleagues sorted human fetal brain cells for CD133 expression highly enriching for stem cell properties *in vitro* and *in vivo* (Uchida et al, 2000). Then CD133 was used to sort fresh human brain tumors. *In vitro*, CD133-positive cells formed clonogenic neurosphere colonies, proliferated and could be induced to differentiate into mature neural cell lineages that were characteristic of the mature lineages seen in the patient's original tumor. Moreover CD133-positive brain tumor cells were highly enriched for tumor initiating activity in vivo. As few as 100 CD133-positive cells were able to initiate fatal infiltrative tumors in immunocompromised NOD/SCID mice after orthotopic transplantation. Injection of 100000 CD133-negative cells did not lead to tumor formation, although viable human tumor cells could be identified in the mouse brains four months after transplantation, suggesting that these cells were viable, but were no longer able to initiate tumor formation. Serial passage of CD133-positive cells re-isolated from the primary transplant and injected into secondary recipient was also shown. It is important to note that sorting for CD133 enriches for cancer stem cells but does not definitively identify them. Furthermore several studies have questioned the utility of CD133 in the isolation of glioma stem cells. Hence, a number of cell surface markers have been proved useful for the isolation of GSCs, including CD15 (Son et al, 2009), CD44 (Anido et al., 2010), Integrin-α6 (Lathia et al, 2010), ABCB5 as well as Hoechst33342 exclusion by the side population cells (Bleau et al, 2009; Harris et al, 2008). Notably, none of these markers are exclusively expressed by the CSCs and in all the tumor samples, highlighting the necessity of additional and more specific markers or the use of combinatorial markers.

1.2.3.2 Isolation of glioma stem cells using the neurosphere assay

In serum-free culture, in the presence of mitogens including epidermal growth factor (EGF) and fibroblast growth factor (FGF), human brain tumor stem cells can be grown as single cell–derived colonies, namely neurospheres (Galli et al, 2004; Hemmati et al, 2003; Ignatova et al, 2002; Singh et al, 2003; Yuan et al, 2004). The neurosphere assay was initially used by Reynolds and Weiss in 1992 to isolate neurospheres from the mouse striatum (Reynolds & Weiss, 1992) and was subsequently used to successfully enrich tumor-initiating cells from brain tumors. This assay is currently used as the standard *in vitro* method for identifying the presence of stem cells derived from both tumor and non-tumor tissues (Chaichana et al, 2006; Reynolds & Rietze, 2005; Vescovi et al, 2006). Similar sphere-forming assays are also used in other stem cell systems, including skin (Toma et al, 2001) and breast (Al-Hajj et al, 2003).

The selective serum-free conditions, in which the neurosphere assay is carried out, allow the stem-like cells to continually divide and form multipotent clonal spheres, while the more differentiated cells incapable of self-renewal and multipotency die off with serial passages (Chaichana et al, 2006; Reynolds & Rietze, 2005) (Figure 6).

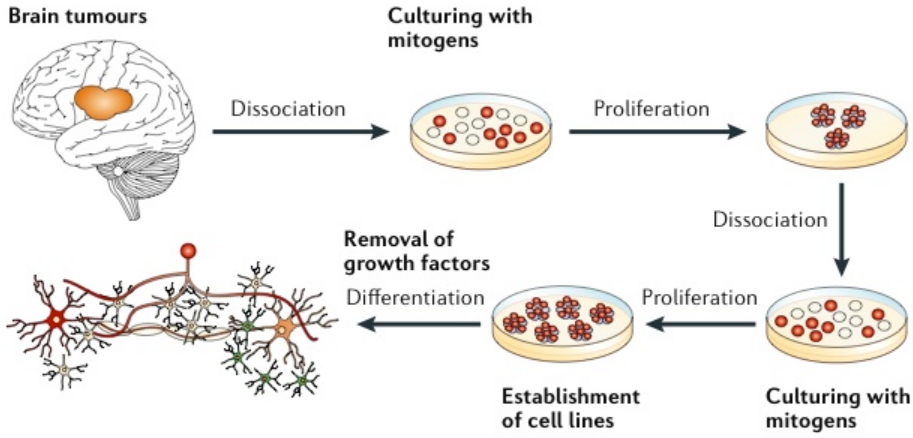

Figure 6. Isolation, perpetuation and differentiation of brain tumor stem cells in culture.
The neurosphere assay in a serum-free culture system that allows the isolation of stem cells based on their exclusive and extensive self-renewal potential. Adapted from Vescovi et al. 2006.

Notably, on mitogen removal and in addition of serum the cells can be differentiated into neurons, astrocytes and oligodendrocytes. The assay thus provides culture conditions allowing competent

cells to exhibit the cardinal stem cell property of self-renewal over an extended period of time, then generating a large number of progeny that can differentiate into the primary cell types of the tissue from which they were obtained (Louis et al, 2008). Neurosphere initiating cells isolated from human GBM have stem-cell characteristics: extensive self-renewal, multipotency and the capacity to initiate new tumors that recapitulate the histological features of the parental tumor, when transplanted into the brain of immunodeficient mice (Galli et al, 2004).

Most importantly, *in vivo* studies have shown that neurosphere formation is a significant predictor of clinical outcome in glioma patients, independent of Ki67 proliferation index, and is a robust, independent predictor of glioma tumor progression (Laks et al, 2009).

Hence the neurosphere assay has become the method of choice to study neural and brain tumor stem cell populations *in vitro*. However, it is associated with some limitations.

Neurospheres are composed by a heterogeneous cell population that consists of stem cells, together with progenitors and more differentiated cells (Reynolds & Weiss, 1996; Suslov et al, 2002). Only the stem cells can exhibit extended self-renewal over serial passages, while the progenitor cells may not be able to form neurospheres for more than six passages and the terminally differentiated cells are not able to form any sphere. A true separation of stem cells and progenitor cells in the neurosphere remains problematic. However, recent studies have found that spheres >2 mm in diameter show high proliferative potential and multilineage differentiation over time, whereas smaller spheres have limited proliferation potential and typically only differentiate into cells with an astrocytic phenotype (Liu et al, 2009; Louis et al, 2008). Thus, larger neurospheres (>2 mm) are more likely to be derived from stem cells, rather than from progenitor cells with limited proliferative and differentiating capacities (Louis et al, 2008).

Besides being used to enrich CSCs, neurosphere assays are also widely adopted to estimate stem cell frequency by counting secondary neurosphere formation, however an estimation of stem cell frequency based on the number of secondary neurospheres could significantly overestimate stem cell number because of the existence of confounding spheres derived from progenitors (Reynolds & Rietze, 2005). The *in vivo* limiting dilution assay made through injection of a progressive lower number of cells in the mouse brain, could be a more accurate assay to calculate the stem cell frequency in the neurosphere. Moreover, the transplantation of individual glioma spheres into

mouse brains, and the serial transfer of the xenograft tumors through mice for several passages could demonstrate the *in vivo* self-renewal ability of CSCs.

The ability to grow human brain tumor cells as neurospheres is variable. Glioblastoma cells are most easily grown in these conditions, but other types of brain tumors, such as medulloblastoma and ependymoma, can be grown only for short periods in neurosphere conditions (Taylor et al, 2005).

Nevertheless, application of serum-free growth conditions to glioblastoma-derived cells has enabled growth of cell lines that retain the same genotype of the patient's primary tumor (Vik-Mo et al, 2010), and which show stable stem cell properties *in vitro* and more faithful generation of models of the disease after xenotransplantation *in vivo* (Lee et al, 2006). These methods clearly show the advantages of serum-free based culture methods for studying human brain tumor cells, and suggest that serum-based cultures have limited utility.

1.2.4 Cell of origin of gliomas

The term cancer stem cell does not imply that this tumor cell derives from a normal stem cell. It is not yet clear whether cancer-initiating events occur in NSCs, progenitors or differentiated cells. However, NSCs are reasonable candidates as cell of origin of brain tumor stem cells, because their lifespan can easily induce the acquisition of multiple gene abnormalities necessary for tumorigenesis (Dalerba et al, 2007; Hanahan & Weinberg, 2000). Currently, in mouse brain tumors experimental evidences are indicating stem cells and progenitor cells as well as more differentiated cells as cell of origin (Bachoo et al, 2002; Holland et al, 2000; Liu et al, 2011; Stiles & Rowitch, 2008; Uhrbom et al, 2002) (Figure 5). It is also of relevant note that brain tumors of different phenotypes, in different locations and with different genetic mutations may have different cell of origin (Stiles & Rowitch, 2008). Identifying the cell of origin of brain tumor may be important for several reasons. The particular cell in which an oncogene is expressed may determine the subsequent phenotype and resulting aggressiveness of the tumor, suggesting that different treatments could depend on the cell of origin of the tumor.

1.2.5 Glioma stem cell niche

Stem cell biology is strongly supported by a specialized microenvironment or stem cell niche. Stem cell niches are complex dynamic entities that actively regulate stem cell function (Scadden, 2006), in particular their self-renewal and fate. Calabrese and colleagues demonstrated that stem cells from various brain tumors, including glioblastoma, are maintained within vasculature niches that mimic the neural stem cell niche (Calabrese et al, 2007). Notably, co-transplanting brain tumor stem cells and endothelial cells into immunocompromised mice, the initiation and growth of tumors in the brain were accelerated by the endothelial derived factors.

Brain tumor stem cells seem to have potent angiogenic properties and can recruit vessels during tumorigenesis. It was shown that CD133-positive human glioblastoma CSCs produced high level of VEGF and formed highly vascular and hemorrhagic tumors in the brains of immunocompromised mice. Furthermore, treating CD133-positive cells with bevacizumab blocked their ability to induce endothelial cell migration and tube formation in culture, and initiate tumors *in vivo* (Bao et al, 2006). Moreover it was observed that glioblastoma stem cells directly differentiate into endothelial cells lining tumor vessels (Ricci-Vitiani et al, 2010; Wang et al, 2010). As well as regulating stem cell proliferation and cell-fate decisions, niches also have a protective role defending stem cells from environmental insults (Moore & Lemischka, 2006).

1.2.6 Implications of glioma stem cells in the therapy

From a clinical perspective, the cancer stem cell concept has significant implications, as these cells need to be eradicated in order to provide long-term disease free survival (see Figure 5). Cancer stem cells are thought to be resistant to chemotherapy and targeted therapy, through active mechanisms. They often express higher level of drug-resistance proteins such as ABCG2 and ABCG5 and multidrug resistance protein 1 (MDR1) transporters. Human CD133-positive glioblastoma cells are resistant to a variety of chemotherapeutic agents and to radiotherapy (Eramo et al, 2006; Kang & Kang, 2007).

The gene profile of CD133-positive cells exhibits a high expression level of anti-apoptotic genes and chemotherapy resistance genes, such as breakpoint cluster region psuedogene 1 (BCRP1) and

O6-methylguanine-DNA-methyltransferase (MGMT), rendering these cells resistant to many commonly used chemotherapeutic agents (Liu et al, 2006; Salmaggi et al, 2006).

CD133-positive cells play a crucial role also in radiation therapy failure. In a study conducted by Bao et al., the CD133-positive cells showed a more potent activation of DNA damage checkpoint mechanisms. This repair mechanism has been shown to be targetable through pharmacologic inhibition of the checkpoint kinases Chk1 and Chk2, which renders the CD133 glioblastoma cells more radiosensitive (Bao et al, 2006).

Glioma stem cells might be further protected from conventional therapies by factors within the vascular niche. Treatments that disrupt aberrant vascular stem cell niches could therefore result efficient against gliomas, because they might also function to disrupt stem cell maintenance. Calabrese and colleagues showed that treating glioblastoma-bearing mice with bevacizumab depleted tumor blood vessels and caused a dramatic reduction in the number of glioblastoma stem cells and the growth rate of the tumor (Calabrese et al, 2007).

Also pathways regulating neural stem cell proliferation and differentiation might be targeted in brain tumor treatment. Promotion of tumor stem-cell differentiation may be an important strategy for treatment of brain tumor stem cells. Vescovi and collegues (Piccirillo et al, 2006) have shown that BMPs, which normally induce astrocyte differentiation from normal neural precursors, have been shown to promote glioblastoma cell differentiation in vitro and in vivo, reducing stem cell tumorigenicity in vivo. Another possibility is to target the process of CSC differentiation into endothelial cells in the tumor (Ricci-Vitiani et al, 2010; Wang et al, 2010).

Signaling pathways that regulate stem-cell self-renewal and proliferation, such as Notch, Shh, and Wingless pathways are potentially important targets in the therapy against glioma stem cells.

1.3 CD133

CD133 is considered a marker of stem cells in diverse normal tissues and cancer types. Several studies demonstrated the utility of CD133 in the enrichment of population of cells with stem-like properties in normal and tumor tissues, but there is also a large body of evidence narrowing down its use as a stem cell marker. In this section all the relevant findings concerning CD133 as structural component of the cell membrane and as stem cell marker in normal and cancer tissues are

described.

1.3.1 Structure of CD133

CD133 (also known as prominin-1) was the first identified member of the prominin family, composed of pentaspan membrane proteins. It is an 865 aminoacid protein that contains five transmembrane domains, an extracellular N-terminus, a cytoplasmic C-terminus, and two large extracellular loops with eight consensus sites for N-linked glycosylation (Figure 7).

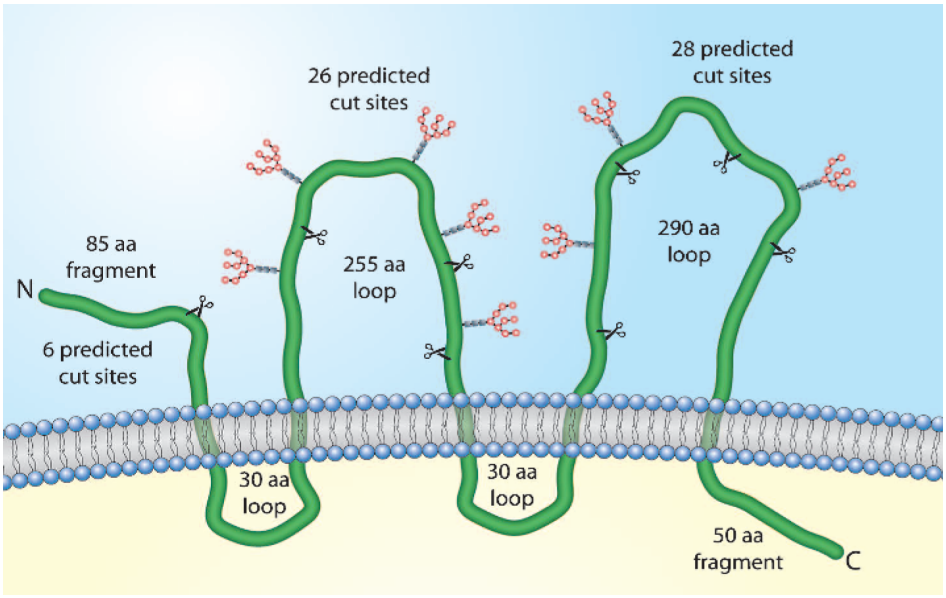

Figure 7. Schematic diagram of CD133 structure. The five transmembrane structure of the CD133 molecule including the aminoacid lengths of the intra- and extracellular loops and the number of predicted trypsin cleavage sites. The actual numbers and positions of glycosylation sites are as yet unknown. Adapted from (Sakariassen et al, 2007).

CD133 gene (PROM1) is conserved throughout the animal kingdom. The human PROM1 gene is mapped on chromosome 4p15 (Corbeil et al, 1998; Miraglia et al, 1997). In addition to the rodent and human, CD133 and predicted CD133-like molecules have been identified in worm, fly, fish and chicken (Fargeas et al, 2003; Roper et al, 2000; Weigmann et al, 1997). In humans, transcription of CD133 is driven by five tissue-specific alternative promoters resulting in the formation of differentially spliced mRNA isoforms which are further regulated by methylation status and result in CD133 variants with distinct cytoplasmic C-terminal domains (Fargeas et al, 2004; Kemper et al, 2010; Shmelkov et al, 2004).

1.3.2 Cellular localization of CD133

At subcellular level, CD133 selectively marks plasma membrane protrusions such as the microvilli and the primary cilia that are located in the apical domain of polarized epithelial cells (Corbeil et al, 2000; Dubreuil et al, 2007; Weigmann et al, 1997). Moreover, if the protein is expressed exogenously in non-epithelial cells such as CHO cells, CD133 preferentially localizes in lamellipodia and filopodia structures (Corbeil et al, 2001) In hematopoietic stem cells CD133 is localized on the protrusions of migratory polarized cells together with adhesion molecules (Bauer et al, 2008). Its specific localization on these plasma membrane domains is related to the presence of cholesterol directly bound by CD133 and specific membrane lipid domains named "Lubrol rafts" (Marzesco et al, 2009; Roper et al, 2000). This membrane micro-domains differ from that found in non-protruding area of the plasma membrane, as demonstrated biochemically using mild detergent and morphologically by co-localization with the ganglioside GM1 (Janich & Corbeil, 2007).

Recent studies have reported a cytoplasmic rather than an exclusive plasma membrane localization of CD133 (Corbeil et al, 2000; Immervoll et al, 2008). In particular Bauer et al demonstrated that human hematopoietic stem cells contain an important intracellular pool of CD133, primarily located in membrane vesicles within multivesicular bodies (Bauer et al, 2011). In human glioblastoma cell lines cultured in serum-free conditions or in presence of serum, CD133 is accumulated in intracellular structures such as the endoplasmic reticulum and the Golgi apparatus (Campos et al, 2011). Moreover, an asymmetric segregation of CD133 was observed in mitotic glioma stem cells, almost always associated with Numb asymmetry (Lathia et al, 2011).

1.3.3 The biological function of CD133

Little is known about the biological functions of CD133. The specific localization of CD133 in the apical membranous protrusions of the microvilli of epithelial cells may suggest that it is involved in the maintenance of apical–basal polarity and cell migration (Corbeil et al, 2001; Kosodo et al, 2004). A functional role as an “organizer” of plasma membrane topology can also been ascribed to CD133 (Corbeil et al, 2001; Zacchigna et al, 2009). Interactions between CD133 and cholesterol within such novel membrane microdomains suggest that CD133 might be important for maintaining an appropriate lipid composition within the plasma membrane (Roper et al, 2000).

Although tightly associated with plasma membrane, CD133 is released into numerous physiological body fluids including urine, saliva, seminal fluids and cerebrospinal fluids in association with small membrane vesicles (Huttner et al, 2005; Huttner et al, 2008; Marzesco et al, 2005). Remarkably, CD133-containing membrane vesicles appeared to be up-regulated in patients affected by epilepsy or glioblastoma, suggesting that neural stem cells and putative cancer stem cells might release them as well (Huttner et al, 2005; Huttner et al, 2008). Small CD133-containing membrane particles were also found in the ventricular fluid within the developing mouse neural tube, and their appearance coincided with the regression of microvilli and the formation of large pleomorphic protuberances on the embryonic neuro-epithelium (Marzesco et al, 2005). It is important to point out that such vesicles are budding from the tip of a microvillus or a primary cilium by a molecular mechanism involving cholesterol-dependent membrane microdomains (Corbeil et al, 2010; Marzesco et al, 2009). Interestingly such release occurs during and after the differentiation of Caco2 cells and human hematopoietic stem cells (Bauer et al, 2011) or, *in vivo*, of neural progenitor cells (Marzesco et al, 2005). These findings highlighted a potential functional role of CD133, supporting the hypothesis that its expression may sustain a stem cell phenotype. CD133-containing lipid rafts may host key determinants or players necessary to maintain stem cell properties; upon their release a cell might become committed to differentiation (Bauer et al, 2008; Bauer et al, 2011). In agreement with this, it has been demonstrated that neurogenic cell divisions of neural progenitors and asymmetric division of glioblastoma stem cells, involve an asymmetric distribution of CD133 (Kosodo et al, 2004; Lathia et al, 2011).

Notably, loss of CD133 due to a frameshift mutation in the PROM1 gene results in a truncated protein that is no longer transported to the cell surface, and is associated with retinal degeneration (Maw et al, 2000). This is possible because of impaired generation of the invaginations and/or impaired conversion of the invaginations to disks, suggesting a role of CD133 in the formation of plasma membrane protrusions.

1.3.4. CD133 as normal stem cell marker

CD133 alone or in combination with other markers, has been used to identify stem cells from a variety of tissues. However, to determine whether CD133 is a valid marker for stem cells in a

tissue, it is crucial to understand the biology of the cells expressing the protein and distribution pattern of the cells within the tissue.

On human bone marrow cells, the CD133 antibody recognizes a CD34-bright subset of hematopoietic stem cells and early progenitor cells that engraft successfully in a fetal sheep transplantation model and exhibit long-term repopulating potential (Miraglia et al, 1997; Yin et al, 1997). CD133 appears to be a reliable marker for the isolation of neural stem cells (as described in the paragraph "Isolation of glioma stem cells using cell surface markers"). In single cells derived from fresh human fetal brain tissue, CD133(+) CD34(−) CD45(−)-sorted cells initiated neurosphere cultures, which could differentiate into both neurons and glial cells and exhibited self-renewal potential. Upon transplantation into brains of immunodeficient neonatal mice, the cells showed potent engraftment, proliferation, migration, and neural differentiation (Uchida et al, 2000). In adult human prostate, CD133 identifies stem cells able to reconstitute prostatic-like acini when grafted into immunocompromised mice (Richardson et al, 2004). In the stomach, duodenum, and colon, cells at the basis of the crypts - where stem cells are likely to reside - expressed CD133 at their apical/endoluminal surface, suggesting that stem cells may be among the CD133(+) cells in these organs (Immervoll et al, 2008). CD133 also marks the bone marrow-derived circulating endothelial progenitors that participate in tumor angiogenesis (Shaked et al, 2006). On the other hand, it appears clear that not all CD133-expressing cells are stem cells. Several studies indicate that CD133 is expressed in differentiated epithelial cells in a variety of organs such as the pancreas (Immervoll et al, 2008; Lardon et al, 2008), liver, salivary gland and lachrymal glands, colon, stomach and duodenum, sweat glands, and uterus (Immervoll et al, 2008; Karbanova et al, 2008) and kidneys (Sagrinati et al, 2006). Furthermore using a knock-in LacZ reporter mouse (CD133lacZ/+) model, in which the endogenous CD133 promoters drive the expression of LacZ, the reporter gene LacZ was found expressed in differentiated epithelia in colon and other tissues (Shmelkov et al, 2008). These findings are consistent with a more recent study demonstrating that CD133 is expressed in a variety of developing and adult tissues in a mouse model with an inducible Cre, nuclear LacZ reporter allele knocked into the Prominin1 locus (Zhu et al, 2009). Taken together, these studies indicate that the overall expression of human CD133 is beyond the stem cells and it appears to be a general marker of apical or apico-lateral membrane of glandular

epithelia. Furthermore to date, no stem cell population from any tissue type can be prospectively isolated to clonal purity on the basis of a single marker.

Furthermore it is of significance to consider that the expression of glycosylated epitopes of CD133 (such as AC133 and AC141) have been used to define and isolate the various stem cell populations. Therefore it is possible that the expression of AC133 and AC141 antigens may not be synonymous of CD133 expression. Florek *et al* defined an antibody that recognized human CD133 independently of glycosylation (**α**hE2), and found that CD133 antigen expression was retained in differentiated Caco2 cells and was present on the apical membrane of the proximal tubules of the adult kidney. A multiple tissue expression array showed that human CD133 mRNA was strongly expressed in several tissues including adult kidney, mammary gland, trachea, salivary gland, placenta, pancreas, digestive tract, and testes (Florek et al, 2005).

1.3.5 CD133 as cancer stem cell marker

Evidences for the existence of CD133-expressing cancer stem cell populations have been provided in numerous tumor types including leukemia (Bhatia, 2001), prostate cancer (Collins et al, 2005), colon cancer(O'Brien et al, 2007; Zhu et al, 2009), lung cancer (Eramo et al, 2008), hepatocellular carcinoma (Suetsugu et al, 2006), ependymoma (Taylor et al, 2005), melanoma (Monzani et al, 2007), ovarian cancer (Ferrandina et al, 2009), medulloblastoma and glioblastoma (Singh et al, 2004). These CD133 expressing cancer cells all exhibited features of stem cells such as self-renewal, potency in proliferation and capacity to initiate tumors after transplantation into immunodeficient mice.

1.3.6 CD133 as marker of glioma stem cells

With regard to brain tumors, Singh et al (Singh et al, 2003; Singh et al, 2004) were the first to describe a CD133-positive tumor cell population, with stem cells characteristics, that is capable of self-renewal and exact recapitulation of the original tumor when transplanted into immunodeficient mouse brains (as described above).

Quantitative analysis of CD133 positive cells by flow cytometry has generally found them to be present at low, and sometimes barely detectable, levels in human gliomas, glioma sphere cultures

and established glioma cell lines (Clement et al, 2009; Joo et al, 2008; Shu et al, 2008; Singh et al, 2004; Wang et al, 2008), consistent with the assumption that CSCs are a rare cell population in solid tumors. However, some studies have reported exceptionally high CD133 positive (20%–60%) fractions in some human GBMs and/or glioma cell lines (Joo et al, 2008; Singh et al, 2004; Son et al, 2009), according to immunohistochemical findings demonstrating that many GBMs contain more than 25% CD133 positive cells (Zeppernick et al, 2008).

1.3.6.1 Prognostic value of CD133 in glioblastoma

Studies investigating the distribution and the prognostic value of CD133 have reported inconsistent findings (Beier et al, 2008; Christensen et al, 2008; Immervoll et al, 2008; Pallini et al, 2008; Rebetz et al, 2008; Thon et al, 2010; Zeppernick et al, 2008; Zhang et al, 2008). On one hand, a quantitative correlation of glioma grade with the presence of CD133 positive cells within tumors and a negative association between CD133 expression and patient survival, have been demonstrated in large cohorts of glioma patients. Opposite results were obtained by Christensen et al (Christensen et al, 2008) demonstrating no correlation between the presence of tumor cells expressing CD133, and both tumor grade and clinical outcome.

It is noteworthy that CD133 antigen has been used to enrich for cancer stem cells using flow cytometry, but whether or not CD133 expression measured by mRNA and/or protein on immunoblotting or immunofluorescence identifies cancer stem cells is not yet clearly established. However, the association of CD133 mRNA and protein with poor prognosis has been reported in several studies (Metellus et al, 2011; Raso et al, 2011; Yu et al, 2010), including a very recent one that analyses the prognostic impact of CD133 mRNA in 48 glioblastomas (Metellus et al, 2011).

To address the issue of the clinical relevance of CD133, we interrogated the *in silico* GBM patient databases, REMBRANDT and TCGA, and we found that CD133 mRNA does not correlate with patient survival, contrary to what was previously shown (Figure 8). This analysis made in hundreds of GBM specimens confirms that CD133 has no value as a prognostic marker in glioblastomas (Brescia et al, 2011).

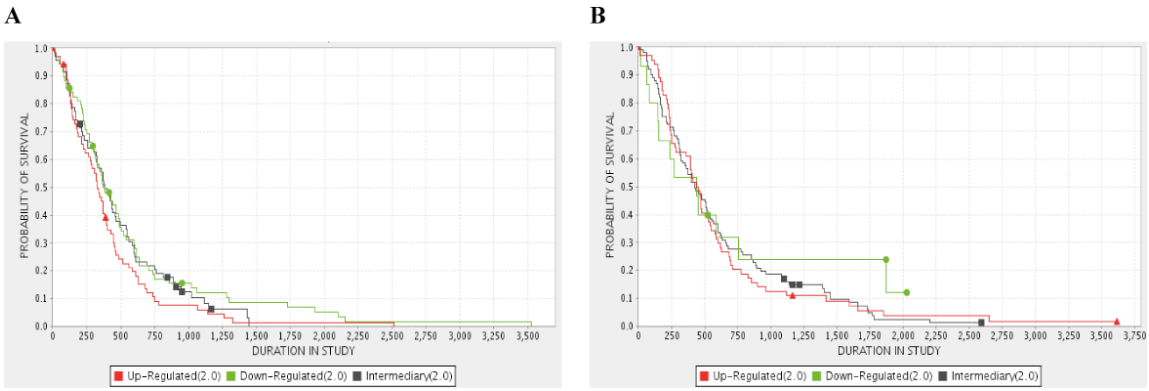

Figure 8. CD133 in GBMs is not predictive of patient survival
Kaplan-Meier survival plot for glioblastoma patients with differential tumor CD133 expression calculated by TGCA (A) and REMBRANDT (B) database. The log-rank P-value for significance of difference of survival between groups was calculated as >0.05 in all cases.

1.3.6.2 Limitations in the use of CD133 as glioblastoma stem cell marker

A great source of inconsistency in experimental results may derive from the use of alternative antibodies recognizing different CD133 protein epitopes. The most widely used antibodies in CD133-related experiments are the CD133/1, directed against the AC133 epitope, and the CD133/2, directed against AC141 epitope. The AC133 and AC141 epitopes are both glycosylated and have distinct spatial locations (Miraglia et al, 1997; Yin et al, 1997), but their molecular nature and their locations on the CD133 protein have not been determined. Several reports have documented an overlap of the AC133 and AC141 positive cell populations (Corbeil et al, 2000; Florek et al, 2005; Yin et al, 1997), although currently there are no specific studies on the comparability of antibodies recognizing these two different epitopes. Indeed, immunohistochemical staining of AC133 and AC141 epitopes poses a special challenge leading some researchers to use alternative antibodies recognizing the CD133 protein. A recent study demonstrated the inconsistent CD133 detection when using different primary CD133 antibody clones in immunohistochemistry (Bidlingmaier et al, 2008; Hermansen et al, 2011).

In addition, the glycosylated nature of the AC133 epitope has been questioned since CD133/1 antibody can effectively detect bacterially expressed, unglycosylated CD133 (Kemper et al, 2010). Moreover, the exclusive detection of glycosylation-dependent epitopes does not exclude the expression of differentially or non-glycosylated CD133. Several studies have demonstrated that the AC133 and AC141 epitopes can be down-regulated independently on the CD133 mRNA (Corbeil

et al, 2000; Florek et al, 2005) and that the tissue distribution of CD133 mRNA is more widespread than expression of the AC133 epitope. CD133 is expressed in differentiated epithelial cells in a variety of tissues, though it has been used to identify normal stem cells and cancer stem cells in many of these organs (Shmelkov et al, 2008).

Another matter of debate is the fact that the expression of CD133 is subjected to changes in the microenvironment cues. Indeed it has been demonstrated that CD133 expression is up-regulated by hypoxia (Griguer et al, 2008) and that it is finely regulated during the cell cycle progression of neural and embryonic stem cells (Sun et al, 2009).

1.3.6.3 CD133-negative GSCs

There are several lines of evidence to suggest the existence of CD133-negative glioma stem cells. First, CD133 is not detectable in many fresh GBM specimens (Beier et al, 2007; Joo et al, 2008; Son et al, 2009) and in established glioma cell lines, which can nonetheless form tumors *in vivo* (Son et al, 2009; Wang et al, 2008).

Second, cells with stem cell characteristics and tumorigenic potential can be isolated from CD133-negative gliomas as well as from CD133 positive tumors. Stem cells isolated from CD133-positive and -negative tumors may differ in terms of other phenotypic features, such as proliferation, invasiveness and expression profiles (Lottaz et al, 2010). A recent study based on gene expression profile analysis of CSC isolated from CD133-positive and CD133-negative gliomas, have led to the definition of two different types of glioma stem cells: Type 1 CSCs that are CD133 positive and grow as floating neurospheres and Type 2 CSCs which are CD133 negative and grow adherently. Interestingly, Type 1 cells were reminiscent of fetal neural stem cells and Type 2 cells genetically resemble adult neural stem cells (Lottaz et al, 2010).

Third, both CD133-positive and CD133-negative cells isolated from the same tumor specimen can be cultured as neurospheres under serum free conditions, and both populations of cells are able to self-renew and to initiate and propagate tumors upon xenotransplantation. Indeed, CD133-negative cells are able to generate CD133 positive progeny *in vitro* and *in vivo* (Chen et al, 2010; Wang et al, 2008). Chen *et al.* recently demonstrated the existence of three different, but coexisting types of glioma stem cells, which differ in CD133 expression: Type 1 (CD133-negative cells able to

generate CD133-positive and CD133-negative progeny), Type 2 (CD133-positive cells able to generate CD133-negative and CD133-positve cells) and Type 3 (CD133-negative which generate only CD133-negative progeny) (Figure 9).

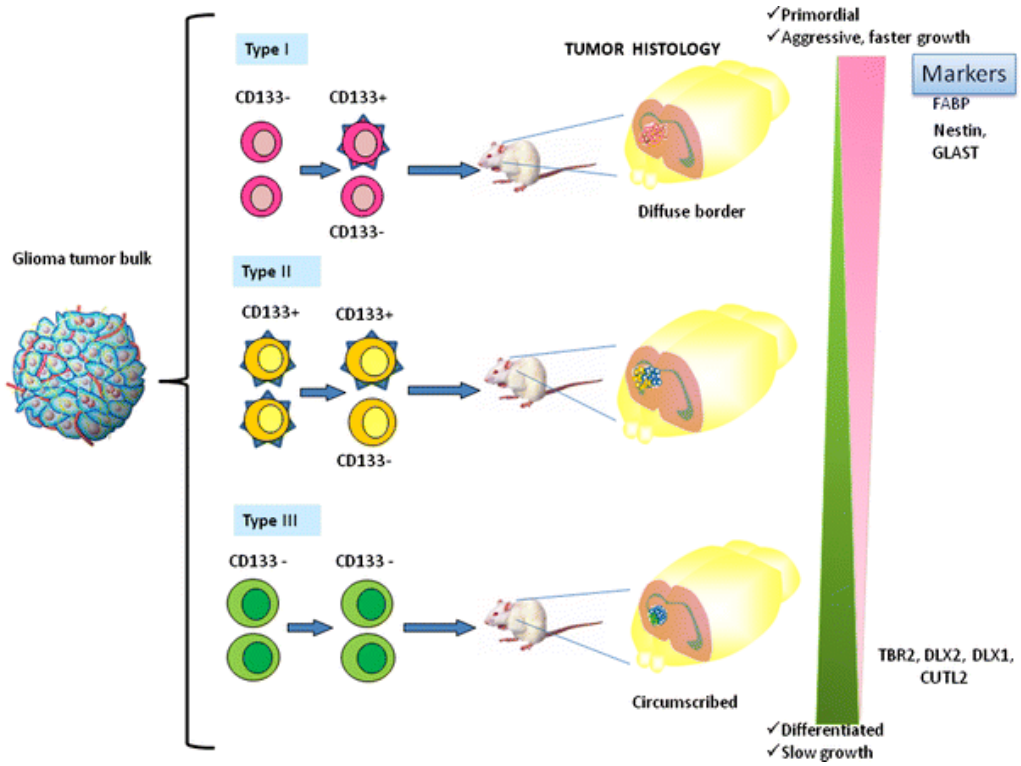

Figure 9. GBM cells classified into three clonogenic neurosphere cell types that produce different patterns of cells. All cell types can generate grafts in nude mice, but each cell type has distinct growth kinetics, histological features, and molecular signatures. Grafts of type I cells generate aggressive and faster-growing tumors, compared to type III cells that generate slow-growing and circumscribed lesion. Furthermore, type II cells form grafts with intermediate features between type I and III. Type I and II cells express radial glial markers, including FABP or BLBP and other neural stem cell markers such as nestin and GLAST at a much higher level than in type III cells. Indeed, type III cell cultures expressed markers of intermediate progenitor cells, including TBR2, DLX2, DLX1 and CUTL2.

All these cell type are capable of self-renewal, initiation of neurosphere growth and generation of highly malignant tumors. However these cell types have distinct growth kinetics and form tumors with distinct histological features, and molecular signatures.

A hierarchical lineage has been established between these three types of cells, suggesting that type I (CD133-negative) cells are the most primordial, whereas type III cells represent the most differentiated state, and type II clones are intermediate between the type I and III cells.

2. MATERIALS AND METHODS

2.1 Preparation of cell suspensions from patient tumors

This study was approved by the Ethical Committee for human experimentation of IEO (European Institute of Oncology) and all patients signed an approved consent document prior to surgery. Surgical specimens of tumors were collected at the Neurosurgery Dpt. at IRCCS Istituto Clinico Humanitas and examined by a neuropathologist to verify that each case met criteria for GBM and to select a tissue fragment with high content of viable tumor tissue. Each tissue specimen was minced in to small pieces and maintained in sterile saline at room temperature. One piece of the mincate was fixed in formaldehyde solution (38%) and successively paraffin-embedded; the remaining tissue was dissociated into single cell suspension in warmed EBSS (Earle's Balanced Salt Solution) containing papain (2 mg/ml) (Worthington Biochemical), EDTA (0.8 mg/ml) and L-Cystein (0.8 mg/ml) at 37C for 1-2 hours. The dissociated tumor was filtered through a 70 micron filter and washed a minimum of three times prior to culturing or FACS analyses.

2.2 Neurosphere culture

Neurosphere cultures were maintained in neurosphere culture medium consisting of DMEM-F12 1:1 (Dulbecco's Modified Eagle Medium – Ham's F12 Nutrient Mixture) medium (Invitrogen) supplemented with B27 Supplement (Invitrogen), EGF (20 ng/ml), b-FGF (10 ng/ml) (PeproTech) and 2 ug/ml Heparin (Sigma), at 37°C in a 5% CO2 humidified incubator. All cultures were passaged by mechanically dissociation when spheres reached approximately 300-500 microns in diameter, and cell counts were performed at the time of passage. For cultures passaged at intervals longer than one week, media containing fresh growth factors was added twice weekly.

To established neurosphere cultures, dissociated tumor cells were seeded at an initial density of 1-2 x 10^5 cells/ml. Sorted populations from each tumor case were matched for plating density.

2.3 Cytotoxic Ab-mediated assay

The cytotoxicity of anti-CD133 monoclonal antibodies (mAbs) was measured as follows: 3.000 cells/well were plated in 96-well plates in a volume of 100 μl of complete medium. Twenty-four

hours later, the unconjugated mAb directed against epitope 1 of CD133 (AC133 Miltenyi) and the Ab directed against HA (Sigma) as control were added at different concentrations. Seventy-two hours later, the Ab-containing medium was removed, and the cytotoxic effect of anti-CD133 Ab was determined using the MTS/PMS (3-(4,5-dimethylthiazol-2-yl)-5-(3-carboxymethoxyphenyl)-2/phenazine methosulfate) microtiter plate assay (Promega).

2.4 FACS analysis and sorting

CD133 expression was monitored by use of CD133/1 Ab-PE (Miltenyi,). For FACS analysis, all patient samples were analyzed within 24 hr of surgery and all cultures were analyzed at 6 days (±1 day) after passaging. For staining of neurospheres, cultured cells were mechanically dissociated, washed with PBS and suspended in cold FACS buffer (PBS with 0.5% BSA and 2mM EDTA) at a density of $2x10^6$ cells/ml. For CD133 extracellular staining, CD133/1 Ab-PE (mouse 1:10) was added to the cells; for each sample analyzed, a duplicate sample was stained with mouse Ig2a-PE (Miltenyi) as an isotype control. Following incubation at 4^oC in the dark for 10 minutes, cells were washed twice in FACS buffer and fixed in paraformaldehyde 20 minutes on ice. For CD133 intracellular staining, 10^6 cells were pre-incubated with a five-fold excess of biotin-conjugated CD133/1 Ab to saturate extracellular binding sites. Cells were then permeabilized for intracellular staining with the Inside Stain Kit (Miltenyi) for 20 minutes at room temperature, washed once in FACS buffer and stained with CD133/1 Ab-PE resuspended in Inside Perm buffer for 10 minutes at room temperature. Finally the cells were washed once in Inside Perm buffer and resuspended in FACS buffer. Gating for single cells was established using forward scatter in the isotype control sample. The isotype control sample was utilized to establish a gate in the PE channel. Cells showing signal for CD133 above the gate established by the isotype control were deemed to be CD133-positve cells.

Analysis of patient samples was performed using the CD133/1 Ab-PE. Gating for single viable cells was established using forward scatter, side scatter and DAPI staining in the isotype control sample. The isotype control sample was utilized to establish a gate in the PE channel. Cells showing signal for CD133 above the gate established by the isotype control were deemed to be CD133-positve cells.

For FACS sorting, cells were dissociated into single-cell suspensions and labeled with anti-CD133-PE Ab (Miltenyi). These labeled cells were then physically sorted using the FACS Vantage SE flow cytometer (BD). For magnetic cell sorting, single-cell suspensions were incubated with CD133 microbeads and FcR-blocking reagent (Miltenyi), and then separated by using MACS separation system (Miltenyi). We have followed the manufacturer's protocol in these steps. In order to ensure high purity of sorted populations, we have used two separation columns consecutively. We confirmed the purity of cells by FACS analysis of tumor cells after cytofluorimetric or magnetic sorting. Purities of sorted CD133-positive and CD133-negative cells from a series of freshly dissociated tumors or neurosphere lines were determined to be about 95.8% and 97.2%, respectively.

2.5 Lentiviral mediated CD133 silencing

The vector pLentiLox3.7-Puro-GFP (pll) was used to generate lentiviral plasmids that express short hairpin RNAs (shRNAs) based on the cDNA of CD133; sh1 corresponds to nucleotides 949–967 (exon 7) (GACCCAACATCATCCCTGT) (Rappa et al, 2008), sh2 corresponds to nucleotides 885-905 exon 6 (AAGGCGTTCACAGATCTGAAC); Genbank accession no. NM006017. BLAST research ensured that the sequences have no significant homology with other human genes. As control vectors, we used the same lentiviral vector carrying a shRNA sequence nonspecific to any human gene (CGTACGCGGAATACTTCGA).

Sequences encoding short hairpin RNAs were cloned into the XhoI and HpaI sites of a modified pLentilox 3.7 vector, in which the NheI/EcoRI fragment encoding GFP was replaced by a NheI/EcoRI fragment containing the PUROMYCIN resistance gene fused to GFP sequence.

To generate lentiviral particles, pll-sh1, pll-sh2 and pll-NT as control were transfected into 293T packaging cell line together with the packaging plasmids pMDLg/pRRE, pRSV-REV and pMD2G by calcium phosphate transfection method. Viral particle-containing supernatants were collected at 48 hours after transfection and filtered through 45 microns filter. One volume of PEG-*it* Virus Precipitation Solution (System Bioscience SBI) was added to every four volumes of lentiviral supernatant. The supernatant/PEG-*it* mixture was incubated at least for 12 hours at +4^{o}C and centrifuged at 1500xg for 30 minutes. The lentiviral pellet was resuspended in PBS and stored at -

80°C. Viral titer was measured by serial dilution of virus on 293T cells followed by FACS analysis of GFP-positive cells 48h after infection.

For infection, 5 x 10^7 viral particles were added to 10^5 cells in the presence of 8 µg/mL polybrene (Sigma-Aldrich). Three days after infection, cells were selected in puromycin (Sigma-Aldrich) for three days and then used for experiments.

2.6 Western blotting

Cells were lysed in ice-cold lysis buffer (50 mM Tris-Cl pH8, 150 mM NaCl, 5 mM EGTA pH8, 1,5 mM $MgCl_2$, 10% glycerol, 1% Triton, 50 nM NaF, 10 mM NaPP, 10 mM $NaVO_4$, 10 mM PMSF, 10 µM leupeptin and 10 µM aprotinin) for 15 minutes on ice. Lysates were centrifuged at 12000 rpm, supernatant collected and protein concentration was measured by the Bradford assay (Biorad). Equal amounts of total proteins were loaded onto 1.5 mm thick polyacrylamide gels for electrophoresis. The proteins were transferred in western transfer tanks (Biorad) to nitrocellulose in 1x transfer buffer (20% methanol). Filters were blocked in 5% milk in TBS (125 mM NaCl, 25 mM Tris pH8, 0,1% Tween) for 1 hour at room temperature. Primary antibodies and dilutions used were: CD133/1 (W6B3C1, mouse monoclonal, Miltenyi, 1:100) and actin (mouse monoclonal, Sigma-Aldrich, 1:1000) used to normalize the amount of lysate loaded on the gel. The bound primary antibody was detected with horseradish peroxidase-conjugated (HRP) secondary antibody (Sigma-Aldrich) using ECL (Enhanced ChemioLuminescence) Western Blotting detection reagent (Amersham Bioscences).

2.7 Quantitative RT-PCR analysis

Total RNA from neurosphere cultures was isolated with RNeasy Mini kit (Quiagen), while total RNA from FFPE paraffin embedded brain slides was isolated with FFPE RNeasy FFPE kit (Quiagen). Polymerase chain reaction with reverse transcription (RT–PCR) was performed using the M-MuLV reverse transcriptase (Finnzymes). Quantitative PCR (qRT-PCR) was performed using the Syber Green PCR Master Mix (Applied Biosystems) and signals were detected using a 7,500 Fast Real-Time PCR System (Applied Biosystems). Data were analyzed with the AB Sequence Detection Software, Version 1.4 (Applied Biosystems) using TBP in neurospheres and

HPRT1 in xenotrasplanted mouse brains, amplified with human specific primers, as housekeeping genes. All samples were run in triplicate in each experiment and results were expressed as mean ± standard deviation. Q-PCR primer sequences used:

CD133 forward 5' - ACCAGGTAAGAACCCGGATCAA - 3'

reverse 5' - CAAGAATTCCGCCTCCTAGCACT - 3'

ACTIN forward 5' - AGAAAATCTGGCACCACACC - 3'

reverse 5' - AGAGGCGTACAGGGATAGCA - 3'

HPRT1 forward 5' - TGACCTTGATTTATTTTGCATACC - 3'

reverse 5' - CGAGCAAGACGTTCAGTCCT - 3'

2.8 Clonogenic assay

The colony forming cell assay, or methylcellulose assay, is based on the ability of progenitor cells to proliferate and differentiate into colonies in a semi-solid media, in response to growth factors stimulation. The colonies formed can be enumerated and characterized according to their unique morphology.

The standard protocol was used with minor modifications. The cells were resuspended in D-MEM/F12 medium with growth factors and an equal volume of Methylcellulose (StemCell Technologies) was added; the methylcellulose concentration in the final cell mixture was approximately 1.27%. 1.5 mL (3000 cells) of the final cell mixture was added to a 35 mm culture plate with grid (at least three plates were prepared for each condition). The medium was spread evenly by gently rotating the plate. Three sample plates and an uncovered plate containing 3 - 4 mL sterile water, necessary to maintain the humidity necessary for colony development, were placed in a 100 mm culture plate and covered.

The cells were incubated for 14 - 16 days at 37° C and 5% CO_2, avoiding disturbing the plate during the incubation period to prevent shifting of the colonies. The colonies were scored at the end of the incubation period. Individual colonies were identified and counted using an inverted microscope and the scoring grid. Colonies consisting of at least 40 cells were counted.

2.9 Analysis of apoptosis

For apoptosis analysis, infected cells (GFP+) were first fixed in 1% formaldehyde for 20 minutes on ice, washed once in PBS and fixed again in ethanol 75% for 30 minutes on ice. Fixed cells were incubated in Propidium Iodide (2.5 µg/ml) and RNAse (250 µg/ml) for 12 - 16 hours at +4^{o}C and analyzed by flow cytometry.

2.10 Animal experiments

An intracranial orthotopic model was utilized for evaluation of cell tumorigenicity. Cells from dissociated neurospheres were resuspended in 2 µl of PBS and stereotaxically injected into the nucleus caudatus (coordinates: 0.7 - 1 mm posterior, 3 mm left lateral, 3.5 mm in depth from the dura) of 5-weeks-old female CD-1 nude mice. The mice were maintained until development of neurologic signs and then killed for the analysis of tumor histology and immunohistochemistry.

CD-1 nu/nu mice were housed in plastic cages and were kept in a regulated environment (22 ± 1°C; 55 ± 5% humidity), with a 12 h light/dark cycle (lights on at 7:00 A.M.). Food and water were available *ad libitum*.

T2-weighted MR images were obtained using a 9.4-T magnet (Varian) and tumor areas were calculated from resulting images on a single scan in 3 mice per group using ImageJ software.

Experiments involving animals were performed in accordance with the Italian Laws (D.L.vo 116/92 and following additions), which enforces EU 86/609 Directive (Council Directive 86/609/EEC of 24 November 1986 on the approximation of laws, regulations and administrative provisions of the Member States regarding the protection of animals used for experimental and other scientific purposes).

2.11 Immunohistochemistry and immunofluorescence

For Hematoxylin and Eosin staining, sections were deparaffinized in xylene, rehydrated in a graded alcohol series and stained in Mayer hematoxylin. After counterstain in eosin-phloxine B solution the sections were dehydrated in alcohol and cleared in xylene. For immunohistochemistry, mouse brains and human surgical samples were formalin fixed and paraffin-embedded. 5 µm sections were cut and placed onto Polysine slides (Thermo Scientific), deparaffinized with xylene and

rehydrated in a graded alcohol series. Tissue endogenous peroxidases were blocked with 3% hydrogen peroxide and antigen retrieval was carried out in EDTA (0.01 M, 0.05% Tween pH6) or sodium citrate (0.01 M, pH 6.0) in a waterbath (at 98 °C for 40 min). Paraffin embedded sections were blocked with 5% goat serum in PBS for 60 minutes, and incubated overnight with primary antibodies: GFP (mouse monoclonal, SantaCruz, 1:200), CD133 (AC133 clone mouse monoclonal, Miltenyi, 1:100). Tissue sections were washed in PBS and incubated with a secondary biotinylated antibody (Vector Lab, 1:200) for 1 hour. Antibody binding was detected using a Vectastain Elite Avidin-Biotin-Complex-Peroxidase kit following manufacturer's instructions. All sections were counterstained with Mayer's haematoxylin and visualized using a bright field microscope.

Immunofluorescence staining of neurosphere cells was carried out by fixing cells with 4% paraformaldehyde (PFA) for 10 minutes and then permeabilized with 0.2% saponin in blocking buffer (PBS containing 2% foetal calf serum; FCS). Cells were sequentially incubated for 1 hour with CD133 antibody (W6B3C1 mouse monoclonal, Miltenyi, 1:100), Ki67 (mouse monoclonal, BD Pharmingen, 1:50), Cleaved Caspase-3 (rabbit polyclonal, Cell Signaling, 1:100) at room temperature followed by 1 hour incubation with Cy3-conjugated AffiniPure donkey-α-mouse IgG (H+L) Fab fragment (Jackson ImmunoResearch Laboratories) at room temperature.

In the case of cell surface versus intracellular labeling, cells were first cell surface labeled with mAb CD133/1 (W6B3C1 clone) diluted in blocking buffer for 30 minutes in the cold, followed by 30 minutes incubation with Cy3-conjugated AffiniPure donkey-α-mouse IgG (H+L) Fab fragment (Jackson ImmunoResearch Laboratories) at +4^{o}C. Then the cells were fixed in Inside Fix Buffer (Miltenyi) 30 minutes RT and quenched with 0.1 mM glycine. Remaining mouse epitopes were saturated by incubation with unconjugated AffiniPure rabbit- α-mouse IgG (H+L) Fab fragment (Jackson ImmunoResearch). Afterward, cells were post-fixed with 0.2% PFA, permeabilized with Inside Perm Buffer (Miltenyi) and finally labeled with mAb CD133 for 30 minutes RT, followed by 30 minutes incubation with FITC-conjugated sheep-α-mouse IgG (H+L) Fab fragment (Sigma). As controls, no signal was observed when anti-CD133 primary antibody was omitted or only the CD133 immunoreactivity was detected when the second primary antibody was omitted, indicating that the first mouse primary antibody was fully saturated.

In all cases, nuclei were labeled with DAPI (Molecular Probes). The cells were mounted in glycerol. Confocal analysis was performed using Leica TCS SP2 microscope driven by Leica software. A 63x oil immersion objective (NA 1.4) was used. The same optical section thickness was set for all channels. Individual sections (0.5/1.0 μm interval) and their lateral projections are shown. The images shown were prepared from the confocal data files using ImageJ free software (rsbweb.nih.gov/ij/).

2.12 Microarray Analysis

Neurospheres derived from four different patients with different expression levels of CD133 were infected with NT and sh2 shRNAs and collected 72 hours after infection. Total RNA was isolated using with RNeasy Mini kit (Quiagen). Quantity and quality of total RNA samples was determinated using ND-8000 spectrophotometer (Nanodrop Technologies) and Agilent's Bioanalyzer 2100 (Agilent Technologies), respectively. The gene profile analysis was performed using the Affymetrix Microarray technology, available at Cogentech, within the IFOM-IEO-Campus.

Gene expression data were generated using Affymetrix exon expression chips HuGene-1_0-st-v1. Cel files were loaded into Genespring 11.0 software and expression values were obtained using RMA16 as summarization algorithm in conjunction with the core algorithm for transcript level selection. Each shCD133-treated sample was normalized to its NT-vector treated counterpart and ANOVA ($P<=0.05$) was performed to identify significant changes in shCD133-treated samples. Alternatively, genes were filtered on fold change with cutoffs varying between 1.2 and 1.5. The resulting gene lists were analyzed using Ingenuity Pathway Analysis software to identify significant overlaps with canonical pathways.

2.13 Statistical Analysis

Statistical analyses were performed using Prism 5.0 software. Data graphed with error bars represent mean $\pm$ standard deviation. Two-tailed Student's t test or one-way analysis of variance (ANOVA), corrected for multiple comparisons as appropriate, were used to determine the significance of any differences between experimental groups. In Kaplan Meyer curves, the

survivals were compared with log-rank analysis. Differences were considered “statistically significant” when $p < 0.05$ (*) and highly significant when $p < 0.01$ (**).

3. STUDY OBJECTIVES

Several evidences have been reported about the existence of cells with stem-like properties in human glioblastoma. These cells have been identified on the basis of the expression of the cell surface marker CD133 and showed self-renewal potential and the capacity to recapitulate the human tumor characteristics when transplanted into the brain of immunodeficient mice. On the other hand, CD133 have been proved not to be an informative marker in some human GBM cases for several reasons:

- CD133 expression is variable in glioblastomas (1% - 60%);
- GBMs with undetectable levels of CD133 exist. Neurospheres have been isolated from these tumors and they have tumorigenic potential *in vivo* (Beier et al, 2007; Son et al, 2009);
- CD133- negative cells isolated from CD133 expressing neurospheres are tumorigenic in nude rats (Wang et al, 2008) and nude mice (Joo et al, 2008).

Considering the aforementioned notions a definitive conclusion about the usefulness of CD133 as glioblastoma stem cell marker is difficult to drawn.

Moreover very little is known about the structure and the biological functions of this protein.

The aims of this study are mainly:

1) to study the role of CD133 in the identification of cancer stem cells derived from human glioblastomas and their derived neurospheres. Using the FACS sorting, the CD133-positive and CD133-negative cell fractions were compared for the self-renewal capacity *in vitro*, measured with the methylcellulose assay, and for their tumorigenic potential, transplanting the cells into the brain of nude mice;

2) to study the biological function of CD133 in glioblastoma stem cells. CD133 was knocked-down in GBM derived neurospheres, isolated from different patients, using lentivirus mediated shRNAs. The stem-like properties were analyzed in the CD133-silenced cells using the *in vitro* clonogenic assay and the *in vivo* xeno-transplantation.

4. RESULTS

4.1. CD133 is variably expressed in human glioblastomas and their derivative neurospheres.

We examined a series of newly diagnosed and recurrent glioblastoma cases, classified as grade IV according to the WHO system, to investigate the expression level of CD133 in acutely dissociated tumors and in established neurospheres cultures.

We screened for the plasma-membrane expression of the stem cell-associated epitope AC133 (CD133/1), widely used to identify and isolate stem cells from brain tumors (Singh et al, 2004). However, its nature and specific characteristics are still not clear: multiple results show that it was generated by post-translational modifications (like glycosylation) (Bidlingmaier et al, 2008) or specific folding of the protein, lost upon stem cell differentiation (Kemper et al, 2010).

We have established neurosphere cultures from GBM patient specimens by culturing freshly dissociated cells in serum-free media in the presence of FGF and EGF; these conditions are commonly used to culture neural stem cells (Lee et al, 2006). In order to be defined as cancer stem/progenitor cell populations, these cells are required to be clonogenic *in vitro*, express stem cell markers (like Olig2 or Sox2) (Ligon et al, 2007; Yuan et al, 1995), be capable of neuronal and/or glial differentiation and be tumorigenic *in vivo*, generating xenograft tumors that recapitulate the biological features of the parental GBM (Figure 10 and Table 1).

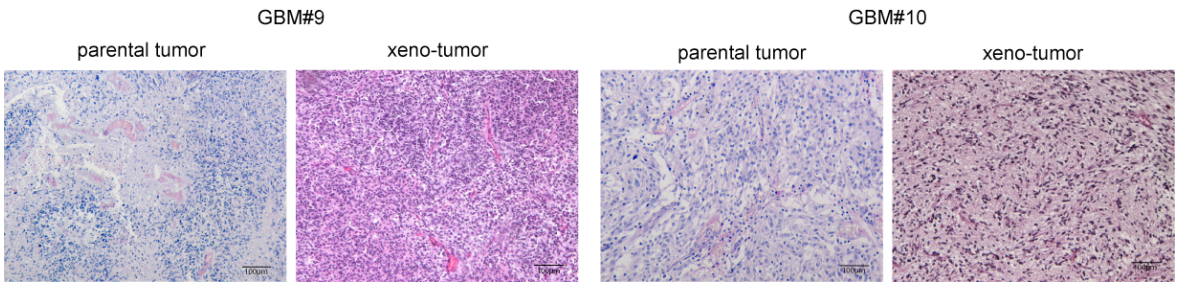

Figure 10. Representative images of Hematoxylin and Eosin staining of parental and xeno- tumors. Scale bar 100 microns.

Name	Survival time
GBM#7	53.3 ± 6.15
GBM#8	87.3 ± 8.3
GBM#9	92.33 ± 10.6
GBM#10	110 ± 3.05
GBM#11	76.3 ± 15.5
GBM#18	67.8 ± 4.9
GBM#20	70.8 ± 5.8
GBM#21	65.1 ± 2.5
GBM#23	135.6 ± 29.19
GBM#24	96.3 ± 5.1
GBM#25	142.5 ± 0.7

Table 1 Tumorigenic capacity of GBM-derived neurosphere cells. GBM-derived neurospheres were dissociated into single cells and 10^5 cells were injected into the brain of immunocompromised mice. Animals were monitored since neurological signs became evident and then sacrified. The presence of tumors was analyzed by Haematoxilin and Eosin staining on FFPE brain slides. Average ± standard deviation of the survival time (in days) of xeno-transplanted mice is reported.

We determined the expression of CD133 in different GBM-derived neurospheres by fluorescence activated cell sorting (FACS) analysis. Our screening revealed that the neurospheres analyzed had a wide range of cells expressing CD133 varying from 1.0% to 84.8% (Figure 11).

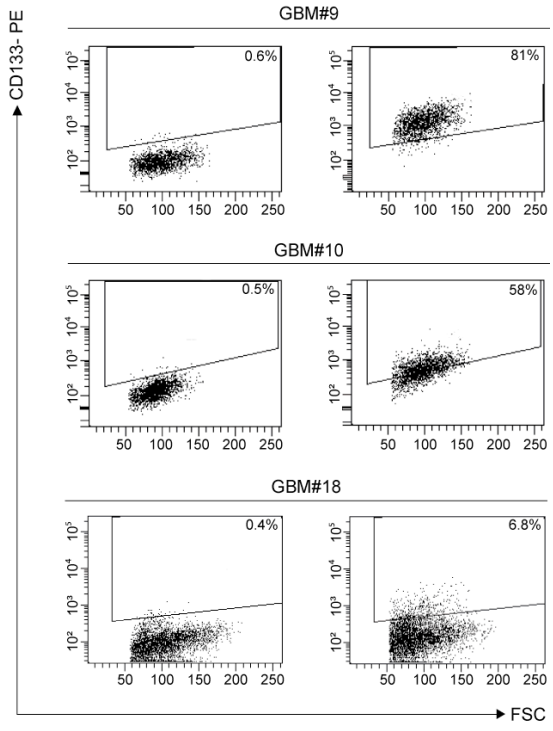

Figure 11. Representative FACS plots of extracellular CD133 expression in neurosphere lines. GBM#9 (with an abundance of CD133+ cells), GBM#10 (with an intermediate number of CD133+ cells) and

GBM#18 (with a paucity of CD133+ cells) neurospheres were dissociated and analyzed by FACS for the CD133 expression. In cells stained with the antibody against CD133 (right panels), CD133+ and CD133- cells are identified by a FACS gate (black line) established in corresponding isotype control plots (left panels).

Four of 11 neurosphere lines included in the study had an abundance of CD133-positive cells (from 84.8%- to 58.1%), (called CD133-high cells), similar to what has been previously reported (Piccirillo et al, 2006; Singh et al, 2004). The other seven neurospheres contained smaller populations of CD133-positive cells (called CD133-low cells) ranged from 8.4% to 1.0%. No GBM-derived neurospheres with undetectable levels of CD133 expression were found, in contrast with other reports (Beier et al, 2007; Joo et al, 2008; Ogden et al, 2008; Wang et al, 2008) (Table 2).

	Name	Tumor Stage	% CD133+ cells	Passage in culture	% CD133+ cells 2nd FACS of NS	Passage in culture
Neurospheres	**GBM#7**	Recurrent	3.7	p6	2.8±1.0	p8-15
	GBM#8	Newly Diagnosed	4.4	p6	3.1±0.9	p9-14
	GBM#9	Recurrent	81.3	p2	78.7±17.3	p5-13
	GBM#10	Recurrent	58	p3	47.1±6.4	p6-13
	GBM#11	Newly Diagnosed	84.8	p2	ND	ND
	GBM#18	Recurrent	6.8	p2	6.3±2.2	p4-10
	GBM#20	Newly Diagnosed	2.4	p2	4.6±2.2	p4-8
	GBM#21	Newly Diagnosed	1.0	p2	4.1±4.1	p3-7
	GBM#23	Newly Diagnosed	53.1	p3	34.9±12.5	p6-14
	GBM#24	Newly Diagnosed	4.36	p6	ND	ND
	GBM#25	Newly Diagnosed	8.4	p2	9.3±1.2	p4-6
Freshly isolated tumor cells	GBM#26	Newly Diagnosed	0.27	p0	ND	ND
	GBM#29	Newly Diagnosed	0.6	p0	ND	ND
	GBM#30	Newly Diagnosed	0.37	p0	ND	ND
	GBM#31	Newly Diagnosed	8.0	p0	ND	ND
	GBM#33	Recurrent	3.6	p0	ND	ND
	GBM#34	Recurrent	13.9	p0	ND	ND

Table 2. CD133 expression in GBM-derived neurospheres and in freshly dissociated tumors. Percentage of CD133+ cells (detected with the CD133/1 antibody) in dissociated neurospheres and in freshly isolated tumor cells was analyzed by FACS at two different *in vitro* passages. CD133-high cells are in red, CD133-low cells are in blue. ND (Not Determinated). Average ± standard deviation is indicated in the % CD133+ cells.

We have also studied CD133 expression in acutely dissociated tumors. Using flow cytometry, we found that 3 out of 6 tumors had less than 1% of CD133-positive cells, while the other 3 cases

displayed higher CD133 positivity, ranging from 3.6% to 13.9% positive cells (Figure 12 and Table 2), confirming then the high variability in the expression of CD133 in this type of brain tumor.

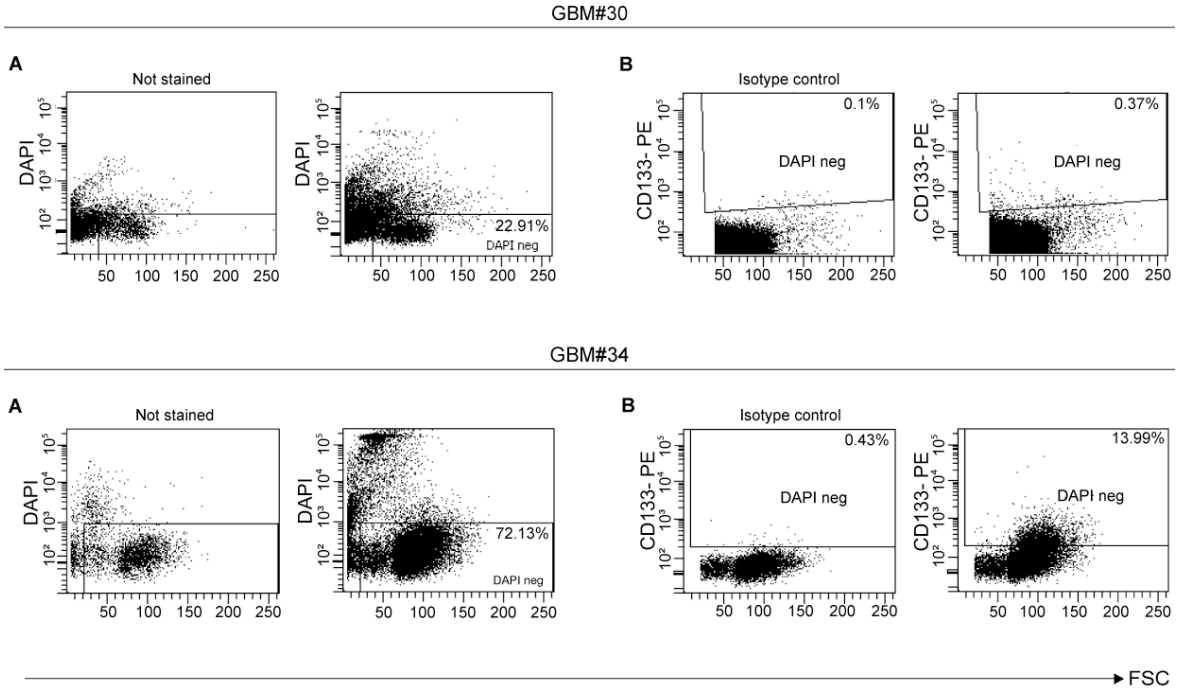

Figure 12. FACS plots of extracellular CD133 expression in freshly isolated surgical biopsies. Patient GBM#30, with a paucity of CD133+ cells, and patient GBM#34, with more CD133+ cells, are represented. In not PFA fixed samples DAPI is used to identify not viable cells. In the left plots (A) DAPI signal (y-axis) is plotted against the forward scatter (FSC) (x-axis). In cells stained with DAPI (left panels), the DAPI+ and DAPI – cells are identified in a FACS gate (black line) established in corresponding unstained plots. In the right panels CD133/1-PEsignal (y-axis) is plotted against the forward scatter (FSC) (x-axis). In DAPI negative cells (viable cells) stained with antibody to CD133 (right panels), CD133+ and CD133- cells are identified by a FACS gate (black line) established in corresponding isotype control plots.

No significant differences in the capacity to grow as neurospheres and in the tumorigenic potential were observed between CD133-high and CD133-low neurospheres, although different neurospheres varied in the frequency of clonogenic cells.

Analysis of the different neurosphere lines revealed substantial variation in the percentage of CD133-positive cells that remained constant for individual cell line over several *in vitro* passages (Table 2).

In order to determine whether these CD133-positive cells identified in the neurospheres exist in the corresponding human GBMs *in situ*, we performed immunohistochemical analysis of patient-derived GBM paraffin sections. A subpopulation of cells with distinct cell membrane-associated

CD133 was detected in GBM patients, revealing the consistency between *in vitro* data and qualitative immunohistochemical evaluation (Figure 13). Interestingly, we noticed a cytoplasmic localization of CD133 rather than exclusive plasma membrane associated expression, in accordance to previous results (Campos et al, 2011; Ferrandina et al, 2009; Immervoll et al, 2008; Sasaki et al, 2010). In some cases, such as GBM#20, the neurospheres contained few CD133-positive cells while the corresponding tumor sample presented high CD133 expression, with a clear cytoplasmic localization. This result suggested an exclusive cytoplasmic localization of CD133 in some cases, not detected in not permeabilized cells, as those analyzed by FACS in our screening.

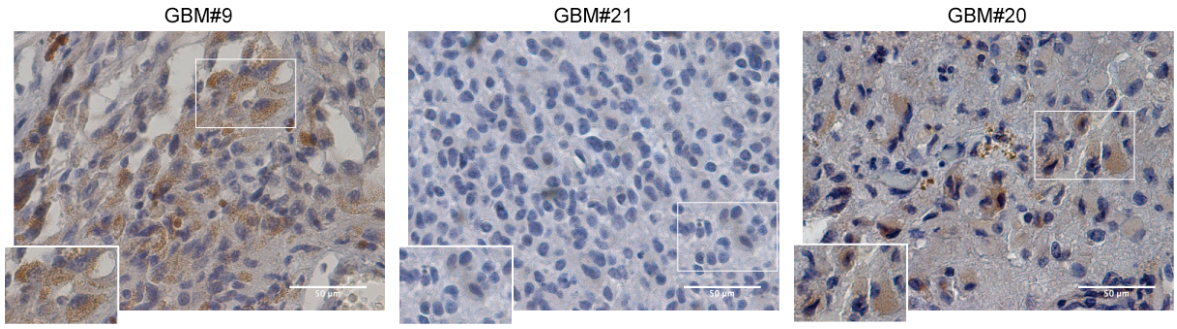

Figure 13. Immunohistochemical staining of CD133. Representative human GBM specimens: the corresponding neurospheres have been found by FACS to contain either high (GBM#9) or low (GBM#21 and GBM#20) percentages of CD133+ cells. In some cases the expression pattern of CD133 in the neurospheres and in the corresponding tumor are comparable; in others CD133 is expressed at higher levels in the tumor compared to the derived neurospheres. In all cases the localization of the protein is clearly cytoplasmic. Scale bar, 50 μm; in boxed areas CD133+ cells at higher magnification are represented.

4.2. Cytoplasmic localization of CD133 in GBM-derived neurospheres

In an attempt to further characterize the GBM-derived neurospheres for the expression of CD133, we analyzed CD133 mRNA expression levels by qRT-PCR. We found that in the majority of the samples analyzed, CD133 mRNA expression levels were consistent with the percentages of CD133+ cells measured by FACS: CD133-high neurospheres showed the highest CD133 mRNA levels. However, in 5 out of 7 CD133-low cells, CD133 transcript levels were only slightly lower than those of CD133-high cells (Figure 14) suggesting that mRNA levels not always reflect the CD133 levels in the membrane. The heterogeneous expression of CD133 mRNA in the

neurospheres induced us to study the expression of CD133 protein independently of the cell-membrane-associated protein.

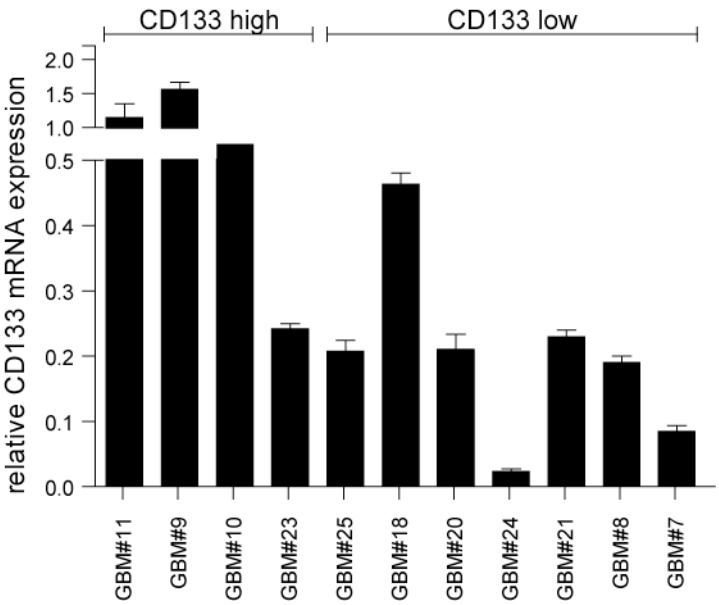

Figure 14. CD133 mRNA expression in GBM-derived neurospheres. Total RNA extracted from cultured neurospheres was analyzed for CD133 expression using qRT-PCR. TBP is used as reference gene for normalization of CD133 expression levels. The CD133 expression levels varied higly among different neurospheres lines. Bars show mean values and corresponding standard deviation of two independent experiments.

Analysis of total cell lysates showed comparable expression levels of CD133 in some CD133–low and CD133-high cells (Figure 15) further suggesting a cytoplasmic localization of CD133 protein. .

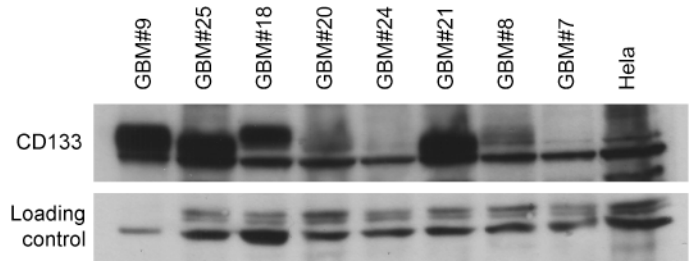

Figure 15. Expression of CD133 in CD133-low GBM-derived neurospheres analyzed by Western blotting. 30 micrograms of total cell lysate were loaded on an 8% polyacrylamide gel. 5 micrograms of total cell lysate of GBM#9 were used as positive control. To identify a potential negative cell line to use as negative control, we analyzed several cell lines by qRT-PCR and Western blotting. To our surprise, we found all cell lines to be positive for CD133 (Shmelkov et al, 2004). We than decided to use the Hela cell line that expresses CD133 at very low level, showing a faint band by Western blotting. Actin was used as loading control.

We investigated the CD133 localization within the neurosphere cells by immunofluorescence microscopy. The cell surface labeling revealed that CD133 is uniformly distributed in the plasmamembrane (Figure 16, red). Remarkably, a second labeling performed upon cell permeabilization revealed an additional, intracellular staining of CD133 (Figure 16, green). Thus, two distinct pools of CD133 molecules co-exist in GBM-derived neurosphere cells. Of note, the majority of cells showed both an extra- and intra-cellular localization CD133 in GBM#9 and GBM#10 neurospheres, while CD133 had an exclusive intracellular localization in GBM#18 cells. Note that in rare cells only an extracellular staining of CD133 could be detected.

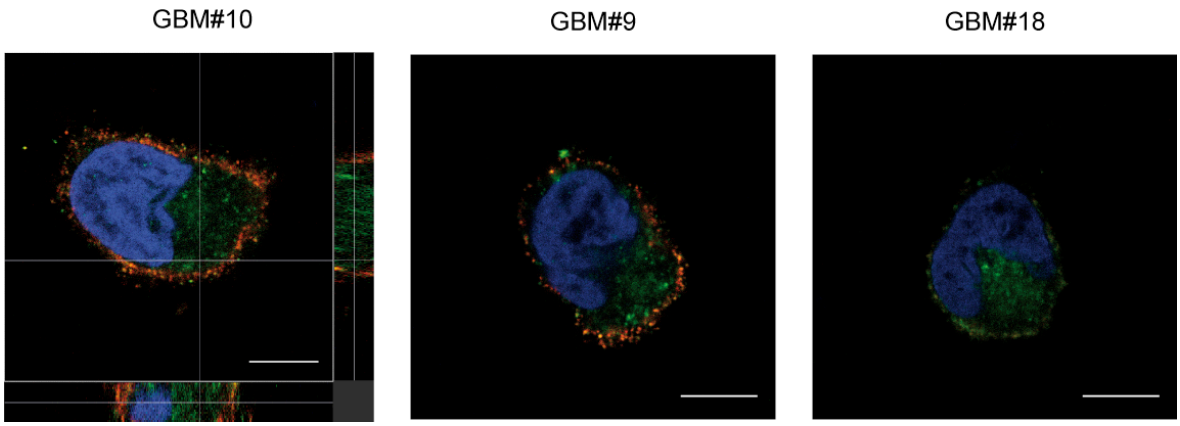

Figure 16. Two pools of CD133 co-exist in GBM-derived neurosphere cells.
GBM-derived neurosphere cells were first cell surface-labeled for CD133 (red) prior to PFA fixation and saponin permeabilization followed by a second round of CD133 labeling (green). The nuclei were stained with DAPI (blue). The labeled cells were analyzed using confocal laser scanning microscopy. A single optical x-y-plane section is shown. Scale bar, 10 µm

In addition, we performed a flow cytometry analysis of intracellular CD133 and we found a cytoplasmic localization of CD133 in almost all the neurospheres analyzed; in particular the CD133-low neurospheres had a discrete amount of intracellular CD133 (Figure 17). Notably, not all CD133-low cells had cytoplasmic expression of CD133, suggesting that a population of cells that does not express CD133 at all exist in the neurosphere.

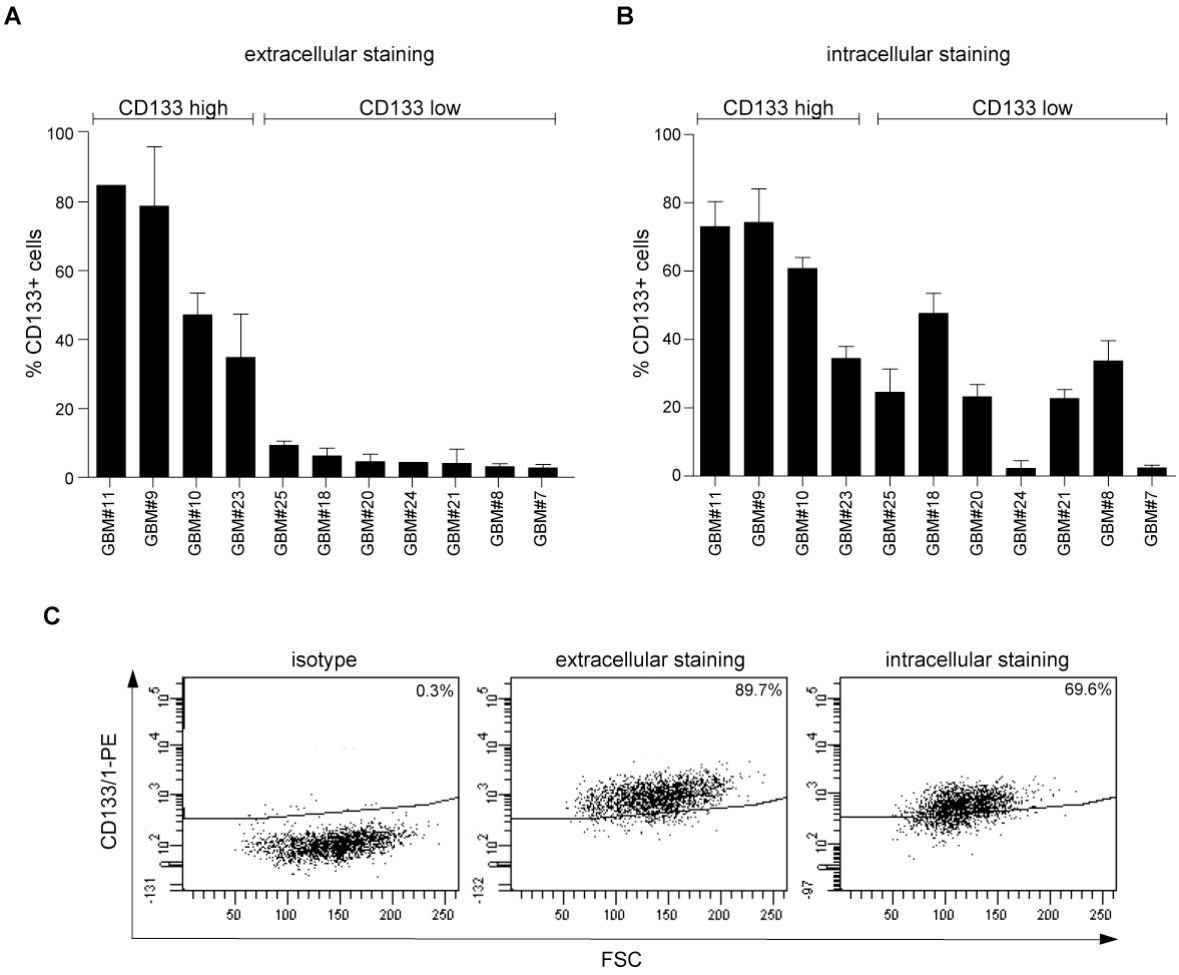

Figure 17. Flow cytometry analysis of extracellular and intracellular CD133 protein expression. CD133 expression on the cell surface or in the cytoplasm was analyzed in CD133-high and CD1333-low neurospheres using FACS analysis. Graphs show mean values and corresponding standard deviation of percentage of CD133+ cells calculated in two independent experiments. (C) Representative dot plots showing a flow cytometry analysis of extracellular and intracellular CD133 protein expression and a corresponding isotype control for the GBM#9 neurospheres. CD133/1-PE signal (y axis) is plotted against the forward scatter (FSC) (x axis).

4.3. Characterization of CD133-positive and CD133-negative cells

4.3.1 CD133 is localized in cytoplasm of CD133-negative cell fraction

The previous results suggested us the existence of at least two populations of cells within the neurosphere: 1. CD133 plasma-membrane associated cells, 2. CD133 cytoplasmic localized cells (with or without CD133 on the plasma-membrane). In order to further investigate in the phenotype of GBM-derived cells with respect to CD133 expression and sub-cellular localization, we sorted the cells into CD133-positive and CD133-negative fractions. We analyzed the sub-cellular localization and the expression levels of CD133 protein and mRNA in the two cell fractions. Then

we moved to analyze the capacity of these fractions to initiate neurosphere growth, the cloning efficiency and the tumorigenic potential.

We used fluorescence activated cell sorting (FACS) and magnetic beads separation to sort CD133-positive and CD133-negative cell fractions (Figure 18).

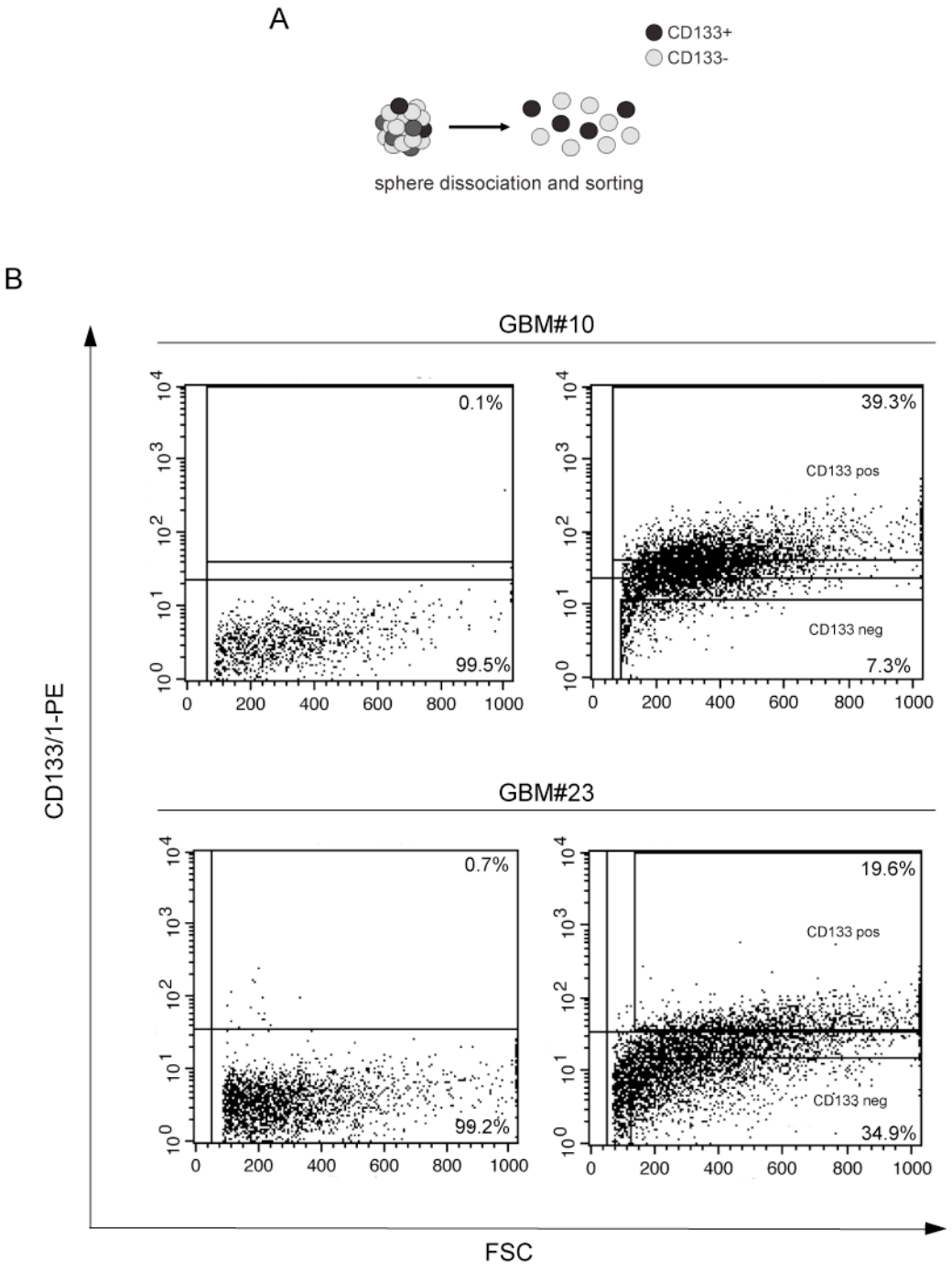

Figure 18. Sorting of GBM-derived neurospheres using CD133. (A) Scheme of the method. (B) Representative examples of sorting windows of GBM-derived neurospheres. For each FACS plot, a gate (black box) established on the base of the isotype control plot (left panels) separates cells quantified as CD133+ or CD133-. Cells in positive and negative sort windows were sorted. FSC (forward scatter).

Surprisingly the CD133-positive and CD133-negative cell fractions showed comparable expression levels of CD133 protein and mRNA when total cell lysates were analyzed by Western blotting and qRT-PCR (Figure 19 A and B). The total CD133 expression levels didn't change after culturing the cells *in vitro* for 15 days (Figure 19).

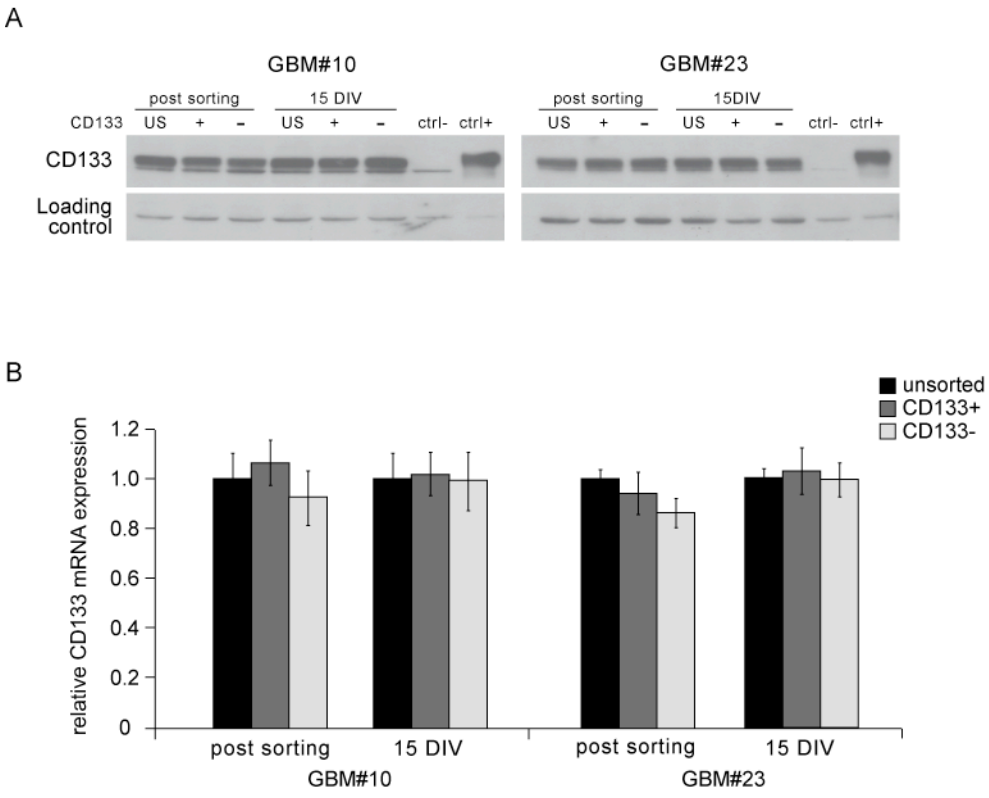

Figure 19. Analysis of CD133 expression in cell fractions sorted on the bases of CD133 cell surface expression. Total lysates of unsorted (US), CD133+ and CD133- cells were collected immediately after sorting (post sorting), and after 15 days of *in vitro* culture in methylcellulose (DIV days *in vitro*). The overall levels of CD133 expression do not vary in the three cell fractions. (A) Western blotting with AC133 mAb. 10 micrograms of total cell lysate were loaded on a 10% polyacrylamide gel. 2 micrograms total cell lysate of Caco2 are used as positive control. 10 micrograms of Hela total cell lysate are used as negative control. Actin is used as loading control. (B) CD133 mRNA expression is assessed by qRT-PCR. TBP is used as reference gene for normalization of CD133 expression levels. Bars show mean values and corresponding standard error of three independent experiments.

These findings induced us to look at the sub-cellular distribution of CD133 in the sorted CD133-positive and CD133-negative cell fractions. As expected we found that CD133 was not expressed on the plasma-membrane in almost all CD133-negative cells, however it was exclusively diffused in the cell cytoplasm (Figure 20). This observation is in accordance with other recent studies that reported a cytoplasmic localization of CD133 in tumor cells. After 15 days in culture, the CD133-

positive and CD133-negative cells had the same sub-cellular distribution of CD133, with the CD133-negative cells re-expressing the protein on the plasma-membrane (Figure 20).

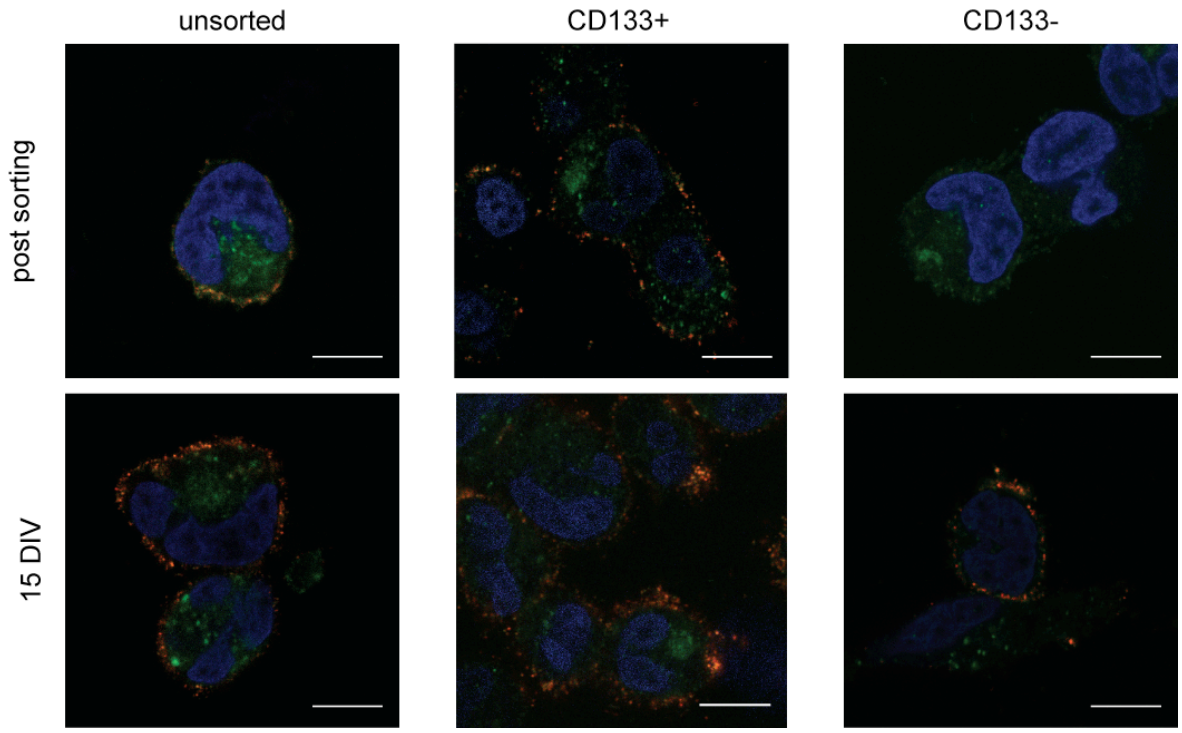

Figure 20. Subcellular localization of CD133 in CD133+ and CD133- sorted cell fractions. Neurosphere cells sorted for CD133 were first cell surface-labeled for CD133 (red) prior PFA fixation and saponin permeabilization, followed by a second round of CD133 labeling (green). CD133 is localized on the cell surface (not permeabilized cells) and in the cytoplasm of CD133-positive, while is localized exclusively in the cytoplasm of CD133-negative cells, when labeled immediately after sorting. After 15 DIV (days of *in vitro*) the two cell fractions have the same sub-cellular distribution of CD133. The nuclei were stained with DAPI (blue). The labeled cells were analyzed using confocal laser scanning microscopy. A single optical x-y-plane section is shown. Scale bar, 10 µm

Flow cytometry analysis of intracellular CD133 in GBM#10 and GBM#23 neurospheres showed cytoplasmic expression of CD133 in the unsorted, CD133-positive and CD133-negative cells (Figure 21). Moreover, almost all CD133-membrane positive cells have intracellular CD133, while only the 40% and 25% of CD133-membrane negative cells of GBM#10 and GBM#23 respectively were positive to the intracellular staining (Figure 21). This result suggests that a discrete amount of cells not expressing any CD133 composes the neurosphere. Of note, after 15 days in culture the three cell fractions had similar extracellular and intracellular CD133 localization (Figure 21). This is a strong indication of a dynamic plasma-membrane localization of CD133 in the cell, probably subjected to a re-cycling from the plasma-membrane to cytoplasm and *viceversa.* Nevertheless the

possible existence of a hierarchical organization between the CD133-positive and CD133-negative (cytoplasmic or not) cannot be excluded.

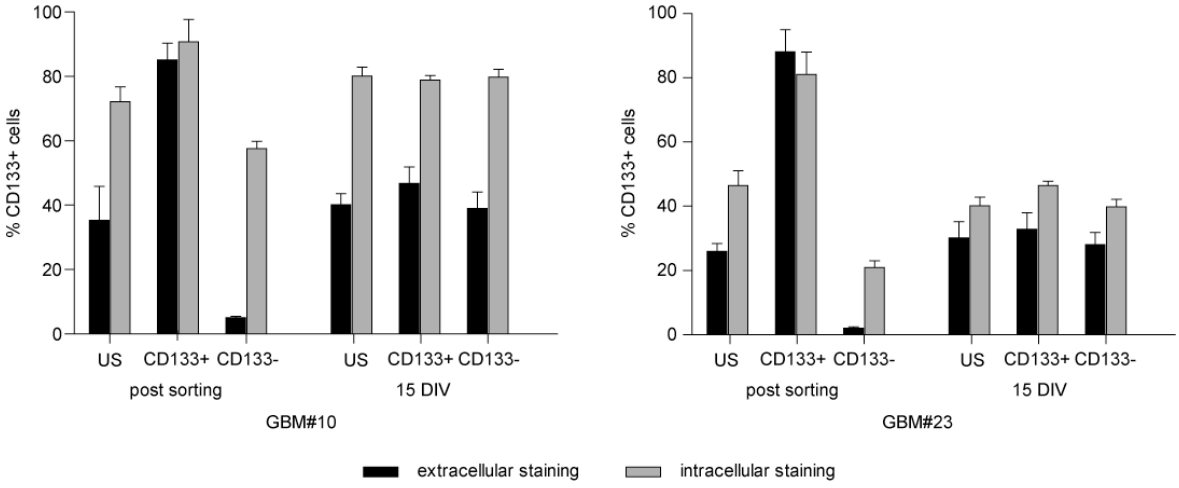

Figure 21. Extracellular and intracellular staining of CD133. Extracellular (black) and intracellular (grey) CD133 expression were analyzed in unsorted (US), CD133+ and CD133- cell fractions (GBM#10 and GBM#23) using FACS, immediately after sorting (post sorting) and after 15 days in culture (DIV days *in vitro*). Bars show mean values and corresponding standard deviation of two independent experiments

4.3.2 CD133-membrane negative cells have reduced clonogenic capacity

The CD133-positive and CD133-negative cell fractions sorted from GBM#10 and GBM#23 neurospheres displayed qualitative similar results for neurosphere growth in the sense that both fractions generated expandable neurospheres, although CD133-negative cells formed spheres slightly smaller in size than the CD133-positive cells (Figure 22 A).

The clonogenic efficiency was analyzed seeding the cells at low density in methylcellulose whose viscous composition does not allow the cells to aggregate. Single clones were counted after 15 days and the clonogenic cells were calculated as percent on the total seeded cells. The two GBM-derived neurosphere lines varied in their frequency of clonogenic cells: in both cases was observed a difference in the clonogenicity of CD133-positive and CD133-negative cells (Figure 22 B) and in the appearance of the neurospheres derived from them. However, CD133-positive cells formed more and larger colonies in methylcellulose than the CD133-negative cells (Figure 22 A), suggesting an increased self-renewal capacity. Interestingly, when the spheres formed in methylcellulose were dissociated and re-plated in the same conditions, there was no difference in

clonogenic capacity and sphere size between the two cell fractions (Figures 22 A and B). Intriguingly, the changes in sub-cellular localization of CD133 could correspond to the acquisition by CD133 negative cells of increased self-renewal capacity, feature of CD133 positive cells.

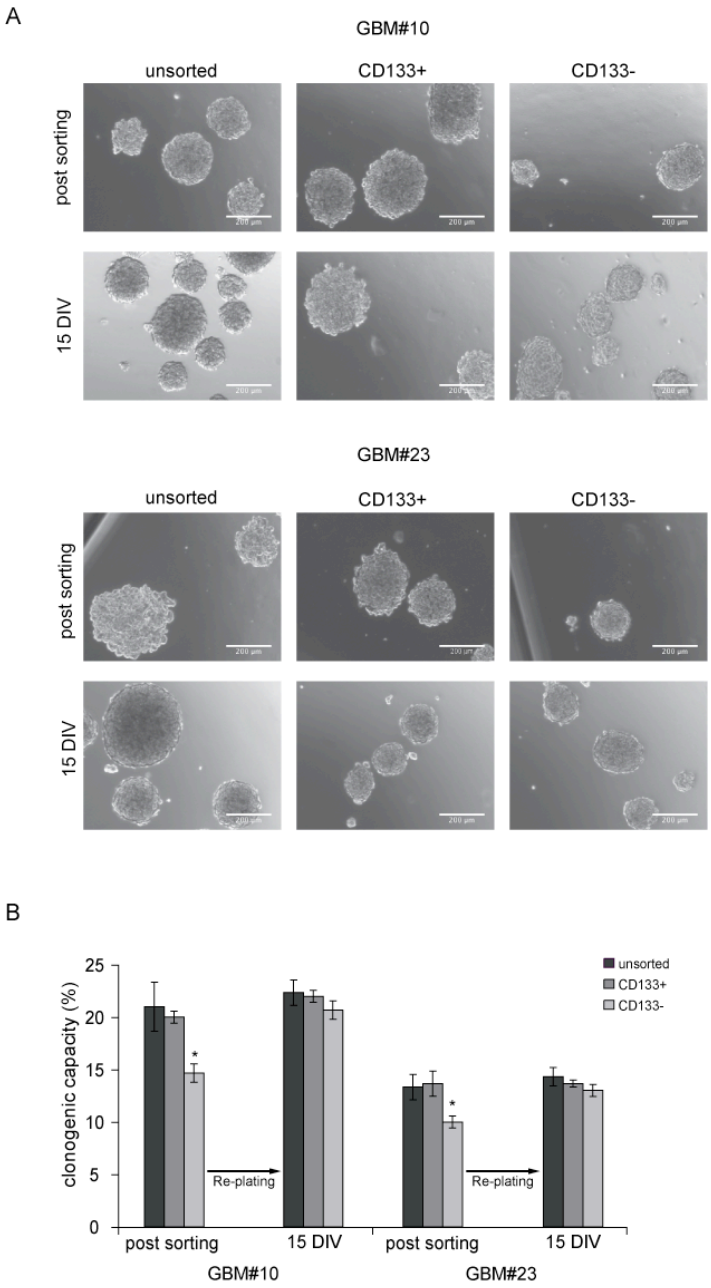

Figure 22. Clonogenic capacity of CD133-positive and CD133-negative cells. (A) Representative microphotographs of GBM#10 and GBM#23 spheres formed in methylcellulose by unsorted cells and CD133+ and CD133- fractions immediately after sorting and after 15 days in culture (DIV days *in vitro*) Scale bar, 200 µm. (B) Quantification of cloning efficiency of unsorted and sorted cells. CD133- cells are less clonogenic than CD133+ cells post sorting. After re-plating (at day 15 after sorting) the clonogenic capacity becomes equal between CD133+ and CD133- cells. Bars represent means and corresponding standard deviation of two independent experiments. (*) $p \leq 0.05$ calculated with Student's t test.

To further investigate the self-renewal capacity of these cells and to understand if a hierarchy could be established between CD133-positive and negative cells, we cloned single cells of each fraction and analyzed the plasmamembrane-associated-CD133 expression for each secondary population. Every clone examined was found to contain cells that initiate growth of secondary clones similar to the initial clone for appearance, growth and CD133 expression (Figure 23). Secondary clones from CD133-positive cells invariably contained a mixture of CD133-positive and CD133-negative cells and the percentage of CD133-positive cells in these expanded clonal cultures did not differ from the unsorted population. In addition all the secondary clones derived from CD133-negative cells contained a mixture of CD133-positive and CD133-negative cells, although there was a great variability in the content of CD133-positive cells among clones.

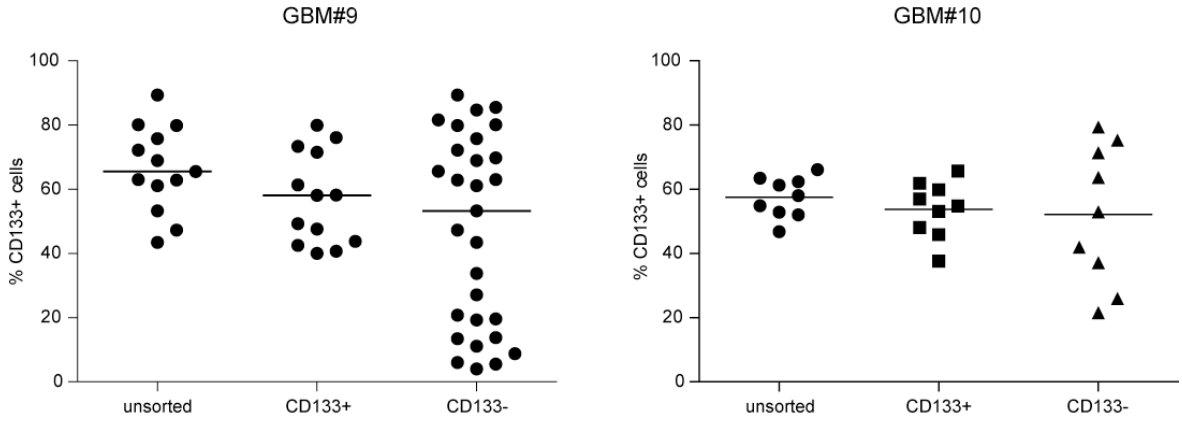

Figure 23. Clonal analysis of CD133+ and CD133- cells. Percentage of CD133+ cells, analyzed by FACS, in secondary clones formed by unsorted, CD133+ and CD133- single cells (GBM#9 and GBM#10) collected immediately after sorting. 30 and 10 clones per group were analyzed for GBM#9 and GBM#10 respectively. T-tests with Bonferroni's correction for multiple comparisons reveal no difference among groups. Bars represent median values.

We were not able to identify clones not re-expressing CD133 on the plasma-membrane or not expressing any CD133. These findings are consistent with a dynamic regulation sub-cellular localization of CD133 suggesting a shuttle of the protein between cytoplasm and plasma membrane, mediated by undetermined stimuli. In addition these results are in contrast with the lineage hierarchy model established between CD133-positive and CD133-negative cells by Chen et al. that implicates the existence of CD133-negative cells originating only negative cells (Chen et al, 2010).

4.3.3 Cytotoxic effect of Anti-CD133 mAb

Since the clonogenic potential of cells that do not express CD133 on the plasma-membrane is reduced, even if only transiently, it seems plausible that the plasma membrane localization of CD133 is important for the stem properties of the cell.

To investigate whether the block of plasma-membrane CD133 results in any effect on the cells, we exposed the GBM-derived neurospheres to an anti-CD133 antibody. We treated cells expressing different levels of CD133 with different doses of AC133 mAb and measured the percentage of viable cells after 72 hours. A dose dependent cytotoxic effect of AC133 mAb on neurosphere cells was observed (Figure 24). The growth of cells treated with the anti-HA antibody was not inhibited. The cytotoxic effect was observed only at the highest doses tested (5 – 10 μg/ml) in GBM#7 and GBM#18 cells, which express lower levels of cell surface CD133. The major effect in GBM#9 and GBM#10 cells can be explained by the fact that they express higher levels of cell surface-associated CD133. These results suggest that the cell surface associated CD133 is essential for the maintenance of glioma stem/progenitor cells at least in tumors expressing high CD133 levels on the plasmamembrane.

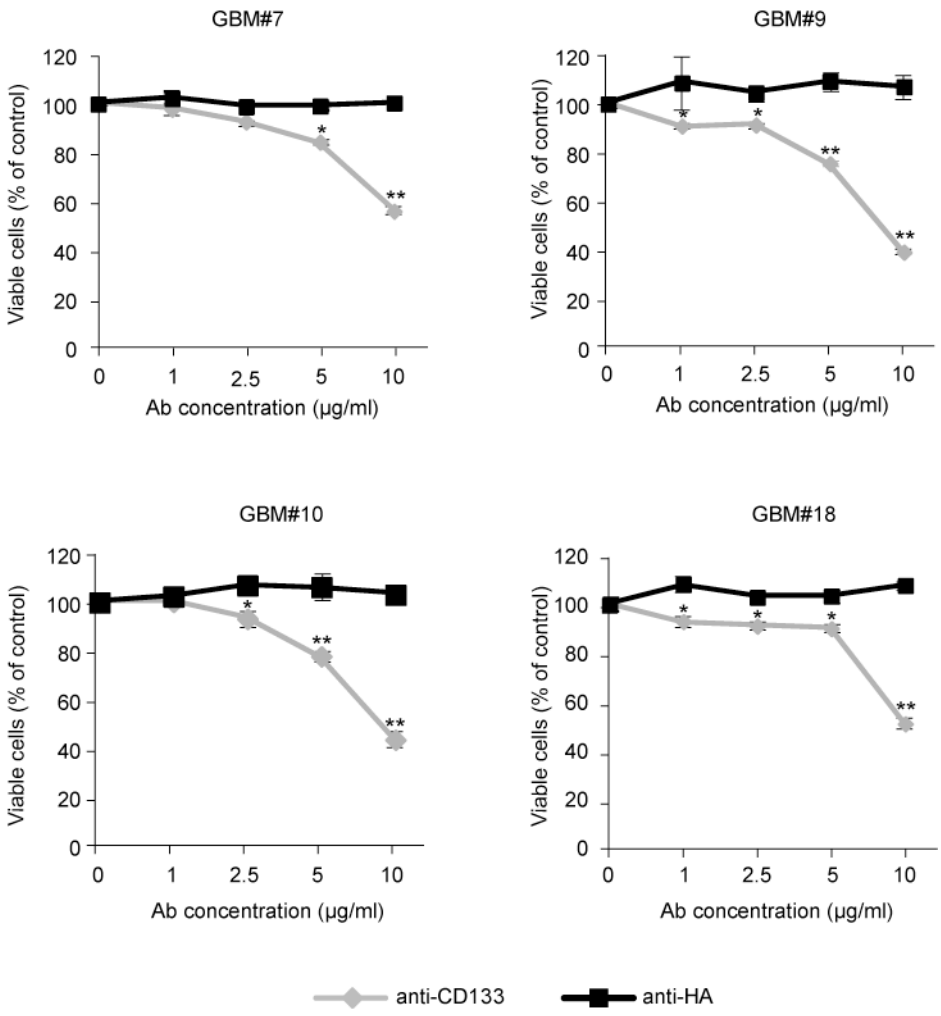

Figure 24. Cytotoxic effect of CD133/1 mAb in GBM-derived neurospheres. Cells were plated in complete medium and exposed to different concentrations of CD133/1 mAb for 72 hours. Cells treated with anti-HA Ab were used as control for cross-reactivity. Cytotoxicity was assessed by an MTS/PMS (3-(4,5-dimethylthiazol-2-yl)-5-(3-carboxymethoxyphenyl)-2/phenazine methosulfate) assay. SE (standard error) bars are presented at each measurement. (*) $p \leq 0.05$ and (**) $p \leq 0.01$ with one-way ANOVA comparison of the control group (anti-HA treated cells) to the corresponding anti-CD133 treated groups on the same day.

4.4 Both CD133-positive and CD133-negative cell fractions are tumorigenic *in vivo*

We examined the ability of progeny from CD133-positive and CD133-negative cells to generate orthotopic tumors in nude mice. For these studies, we inoculated sorted cells (n = 100000 per mouse) into the forebrain of 5 weeks old nude mice. Unsorted cells were injected as controls. All the three population of cells (unsorted, CD133+ and CD133-) formed tumors in mice, although the overall survival of tumor-bearing animals was significantly shorter in CD133-positive cell-injected mice than in mice injected with CD133-negative cells (Figure 25).

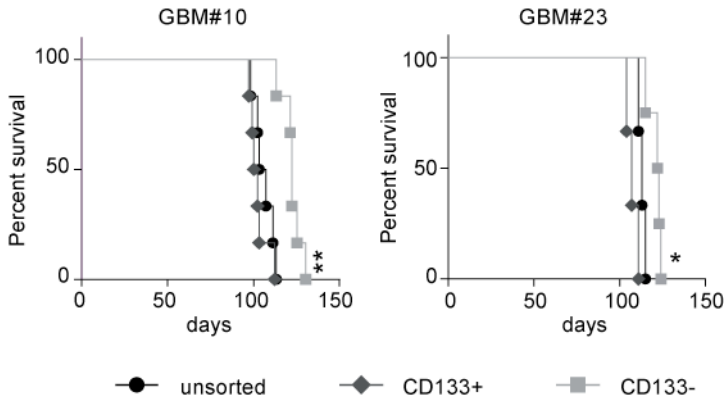

		Tumor incidence	Survival Average ± SD (days)
GBM#10	Unsorted	6/6	105.6 ± 5.7
	CD133+	6/6	102.1 ± 5.2
	CD133-	6/6	122.1 ± 5.5
GBM#23	Unsorted	3/3	113 ± 2
	CD133+	3/3	107.3 ± 2.6
	CD133-	4/4	121 ± 4.1

Figure 25. Kaplan-Maier survival graphs of mice injected with CD133 sorted cells. The animals were injected with unsorted, CD133+, or CD133- cells immediately after sorting. 100000 cells were orthotopically transplanted into the brain of each mouse. P value was calculated with log rank test: (*) $p \leq 0.05$; (**) $p \leq 0.01$

A series of mice, each inoculated with GBM#10 neurosphere cells, were monitored by magnetic resonance imaging (MRI) 4 weeks after implantation. Although all the mice inoculated with unsorted and CD133-positive cells harbored sizeable lesions at this time point, most mice implanted with CD133-negative cells showed no evidence of tumor (Figure 26).

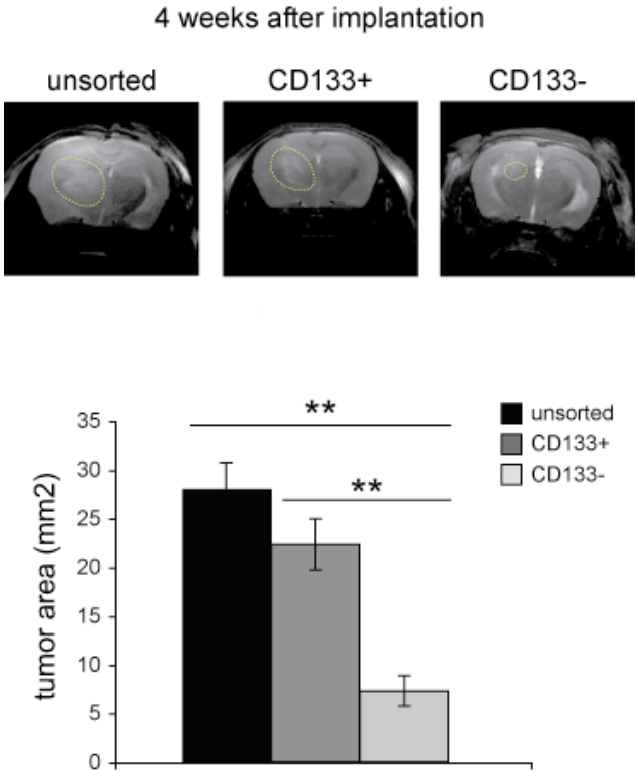

Figure 26. Representative T2 MRI images of grafts formed by unsorted, CD133+ and CD133- cells. Grafts formed by unsorted and CD133+ cells are visible at 4 weeks after implantation, whereas lesions from CD133- cells are typically not apparent or small at 4 weeks. These images are representative of the results from a total of 3 mice. Yellow line highlights tumor area. Bars represent the mean value of tumor area and standard deviation. (**) $p \leq 0.01$ calculated with two sided Student's t test.

However, histological analysis of mice, killed when showed neurological defects associated with signs of suffering and pain, demonstrated that tumors arose in all mice inoculated with the three cell populations (Figure 27 A). The cells showed similar diffuse growth, causing enlargement of the brain and hyperemia (in particular the GBM#10-derived cells), and infiltrated in the brain diffusely including the corpus callosum and the controlateral hemisphere (in particular the GBM#23-derived cells). The tumors were similar in cytoarchitecture, vascularization and invasiveness at the tumor center and periphery. Consistent with the *in vitro* data, immunohistochemical detection of CD133 in the xeno-tumors revealed that CD133 expression was similar within the tumors formed by CD133-positive and CD133-negative cells (Figure 27 B). The mRNA expression level of CD133 in the xeno-tumors formed by CD133-positive and CD133-negative cells sorted from GBM#10 and GBM#23 neurospheres were comparable, as shown by qRT-PCR analysis. The percentage of cells stained with the proliferation index Ki67 was similar in xeno-tumors formed by CD133-positive

and CD133-negative cells (Figure 27 A).

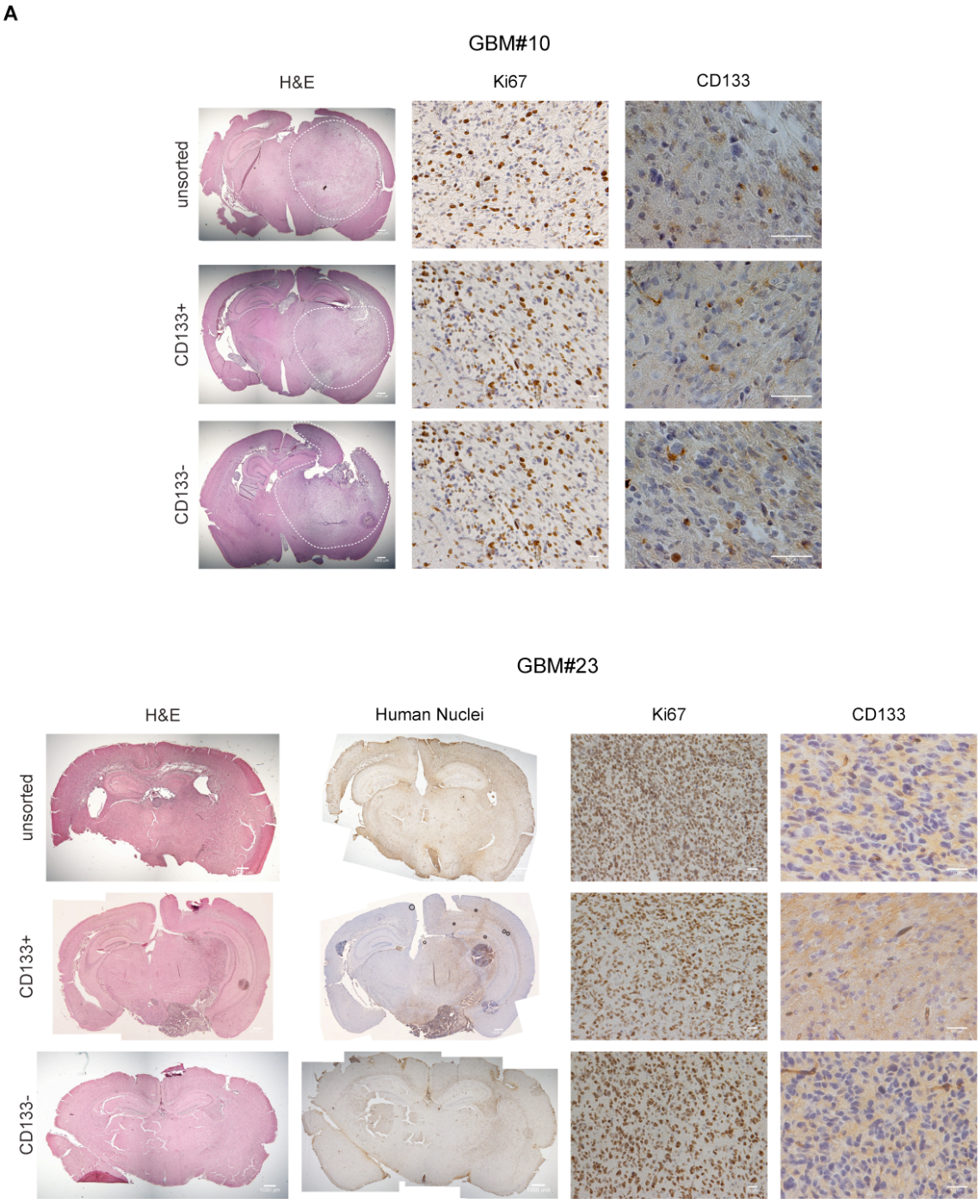

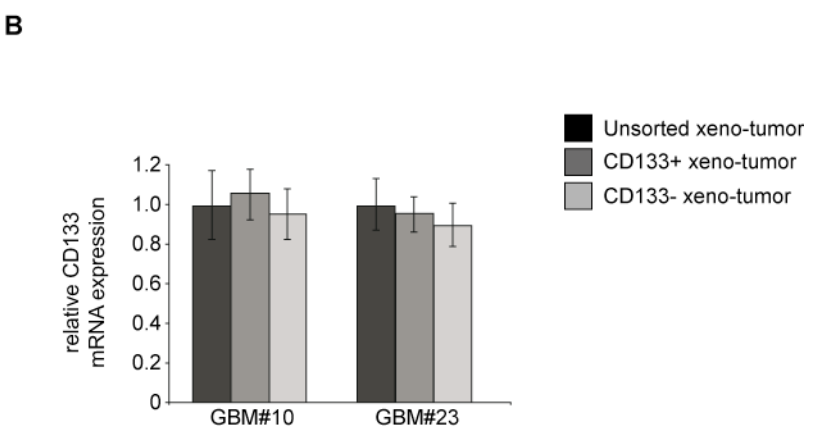

Figure 27. Immunohistochemistry of xenograft tumors derived from GBM-derived neurospheres. (A) Representative images of brains of immunocompromised mice implanted with unsorted, CD133+ and CD133- cells. After sorting identical numbers of viable cells (10^5 cells/mouse) were implanted and brains examined when mice showed neurological signs. Gross images for H&E staining and coronal sections from representative brains bearing glioma xenografts are displayed. White line highlights tumor area. Ki67 and CD133 staining showed that there is no difference among tumors formed by different cell fractions. Human Nuclei staining was shown in xenografts derived from GBM#23 neurospheres, since these cells formed more invasive tumors with no visible mass with H&E staining. Scale bar, 1000 μm (H&E and Human Nuclei) 50 μm (Ki67 and CD133). (B) CD133 mRNA levels are assessed by qRT-PCR in total RNA extracted from FFPE tissue samples (n=2 mice per group). HPRT1 (human specific) is used as reference gene for normalization of human CD133 expression levels. Bars show mean values and corresponding standard deviation of two mice.

4.4. Study of the functional role of CD133 in GBM-derived neurospheres

4.4.1 Silencing of CD133 in GBM-derived neurospheres

A direct role of CD133 in maintaining the tumorigenic potential of glioblastoma stem/progenitor cells remains to be defined. To investigate the function of CD133 we silenced CD133 gene expression in GBM-derived neurospheres. Given the expression of CD133 in the cell cytoplasm in most of our neurosphere lines (only GBM#7 and GBM#24 express low levels of CD133 both on the plasmamembrane and in the cytoplasm), and given the capacity of the plasma membrane-associated CD133-negative cells to re-express CD133 at plasmamembrane level and to form tumors in xeno-transplantation model, we targeted CD133 in all the cells that compose the neurosphere. To achieve a stable knock-down of CD133 in these cells, we cloned shRNAs directed against human CD133 within a lentiviral vector, which contains GFP and Puromycin resistance gene as reporters. Two different shRNAs where designed to silence CD133 targeting different mRNA regions, conserved in all the different splice variants (see Material and Methods).

One of them (sh2) gave a nearly complete knock-down of CD133 and was therefore used for all

subsequent experiments, together with the less efficient oligonucleotide sh1, as shown by Western blotting and qRT-PCR in figure 28.

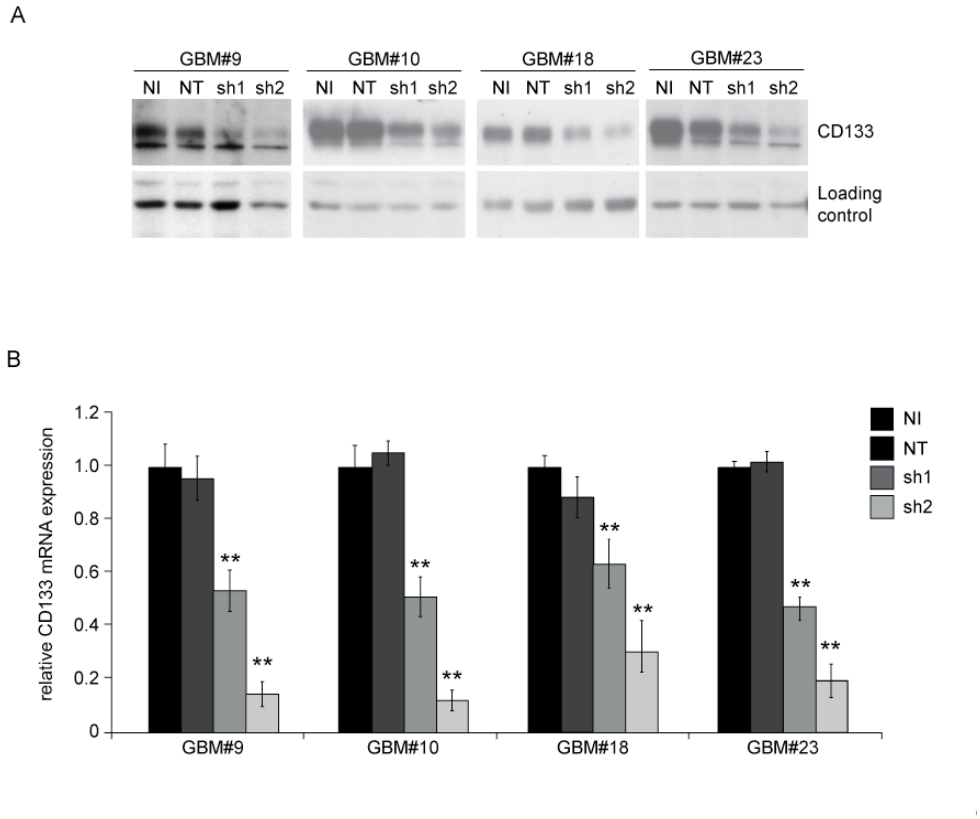

Figure 28. Knock-down efficiency of different shRNAs targeting CD133.
(A) Analysis of CD133 expression by Western blotting on different GBM-derived neurospheres infected with lentivirus directing against either non-targeting shRNA (NT) or CD133 specific shRNAs (sh1, sh2). NI is the not infected control. 20 micrograms of total cell lysate were loaded on a 10% polyacrylamide gel. Actin is used as loading control.
(B) The CD133 mRNA levels are assessed by qRT-PCR in cells collected 3 days after infection. TBP is used as reference gene for normalization of CD133 expression levels. Bars show mean values and corresponding standard deviation of three independent experiments. (**) $p \leq 0.01$ calculated with two sided Student's t test.

The same vector containing a shRNA targeting the luciferase mRNA sequence was used as control (NT, Non Targeting). Similar results were obtained in different GBM-derived neurospheres (GBM#9, GBM#10, GBM #18 and GBM #23).

Immunostaining of the cells with anti-CD133 antibody, 3 days after infection and puromycin treatment to select infected cells, showed that the virus was indeed able to knockdown CD133 expression in all the cells of the neurosphere, although the level of down-modulation varied among them (Figure 29). The silencing rate was fairly high, as only about 15% of GFP-positive cells were still CD133-positive, probably because they failed to correctly express the silencing shRNA.

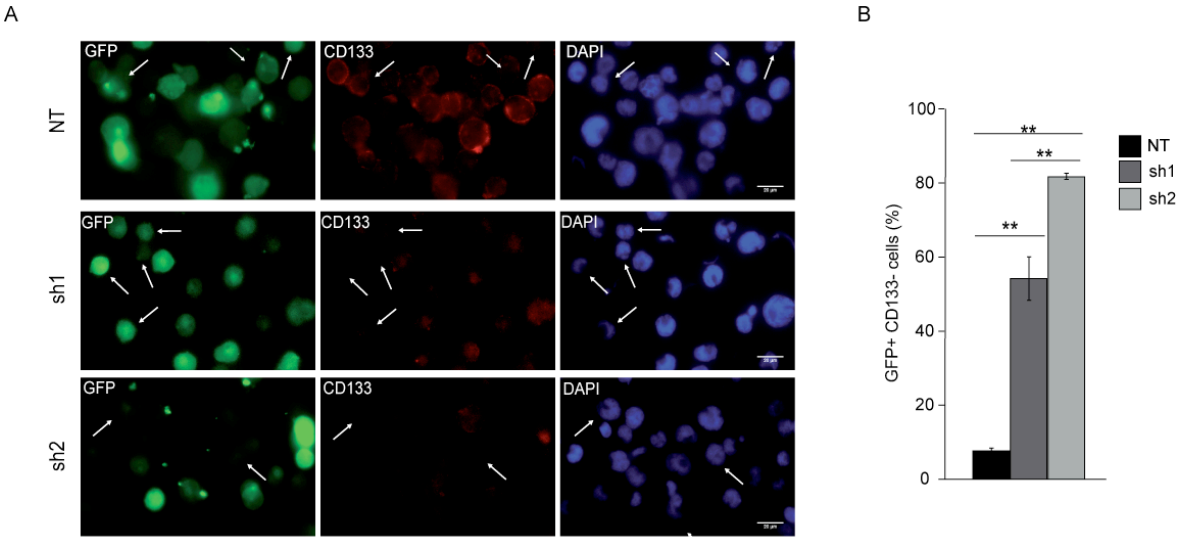

Figure 29. Knock-down efficiency of different shRNAs targeting CD133.
(A) Representative images of GFP (green) and CD133 (red) immunofluorescence staining in GBM#9 dissociated neurospheres infected and selected for 3 days with puromycin. DAPI (blue) is used to stain nuclei. Scale bar, 20 µm. (B) Percentage of GFP+ CD133- cells on the total number of nuclei is calculated. Bars show mean values and corresponding standard deviation of three independent fields counted. (**) $p \leq 0.01$ calculated with two sided Student's t test between groups.

4.4.2 Silencing of CD133 reduces the proliferation of GBM-derived neurosphere cells

When the infected cells where cultured under non-differentiating conditions and the cell viability was assessed by MTS/PMS assay, we found that CD133 knock-down was followed by a decrease in cell growth (Figure 30). The magnitude of the reduction in cell growth was proportional to the efficacy of the two shRNA constructs. These dose-dependent effects strongly suggest that the decreased growth we observed was a specific effect caused by reduction of CD133 expression. The reduction in cell proliferation caused by CD133 knock-down is a robust response common to stem/progenitor cells derived different GBM patients.

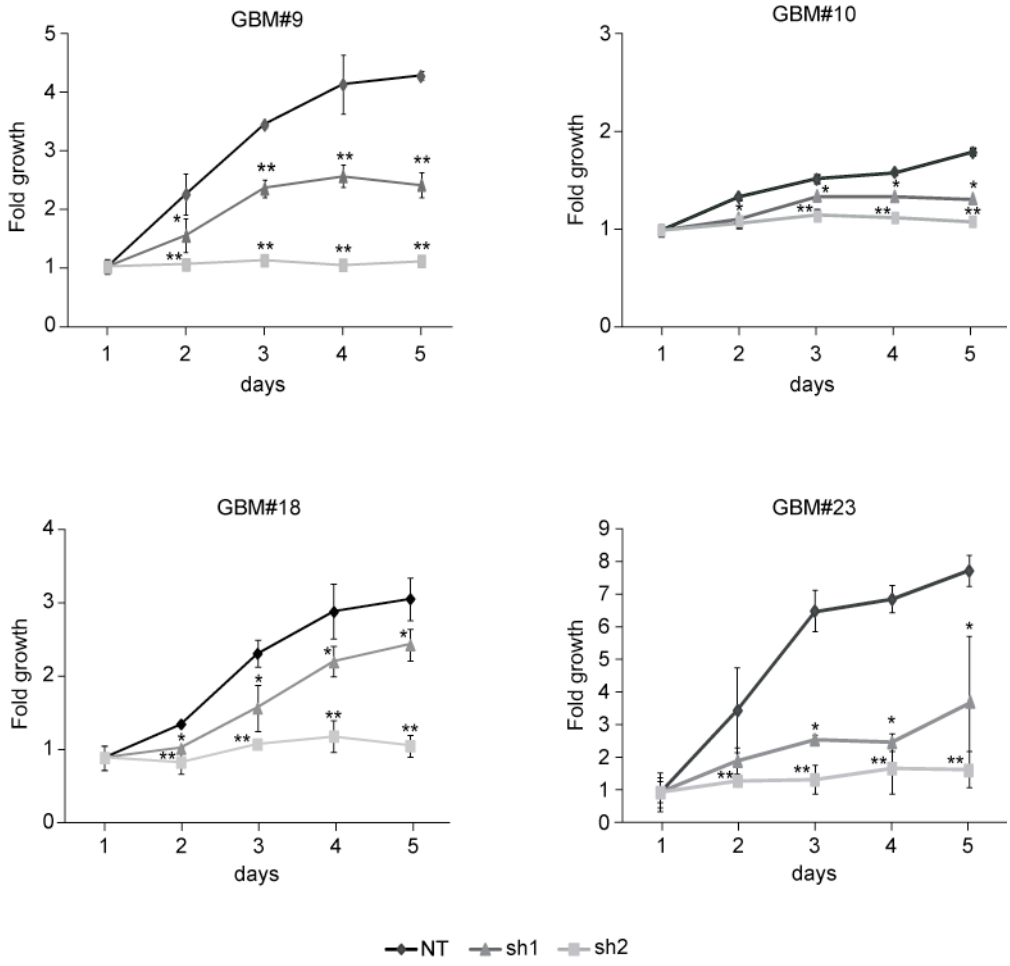

Figure 30. CD133 silencing inhibits growth of GBM-derived neurospheres.
Analysis of cell growth of both CD133-silenced and control cells using MTS/PMS assay. GBM-derived neurospheres were dissociated, infected and selected in puromycin for 3 days. Then they were plated at 3000 cells per well in quintuplicate. SE (standard error) bars are presented at each measurement (*) $p < 0.05$, (**) $p < 0.01$ with one-way ANOVA comparison of the control group (NT not targeting) to the corresponding CD133 silenced cells on the same day.

Analysis of the proliferative index ki67 performed by immunofluorescence confirmed the reduction in cell proliferation, since CD133-silenced cells have significantly less ki67 stained cells, compared to the control (Figure 31). Any alteration in the distribution into the cell cycle phases of CD133 silenced cells compared to the NT control was evident.

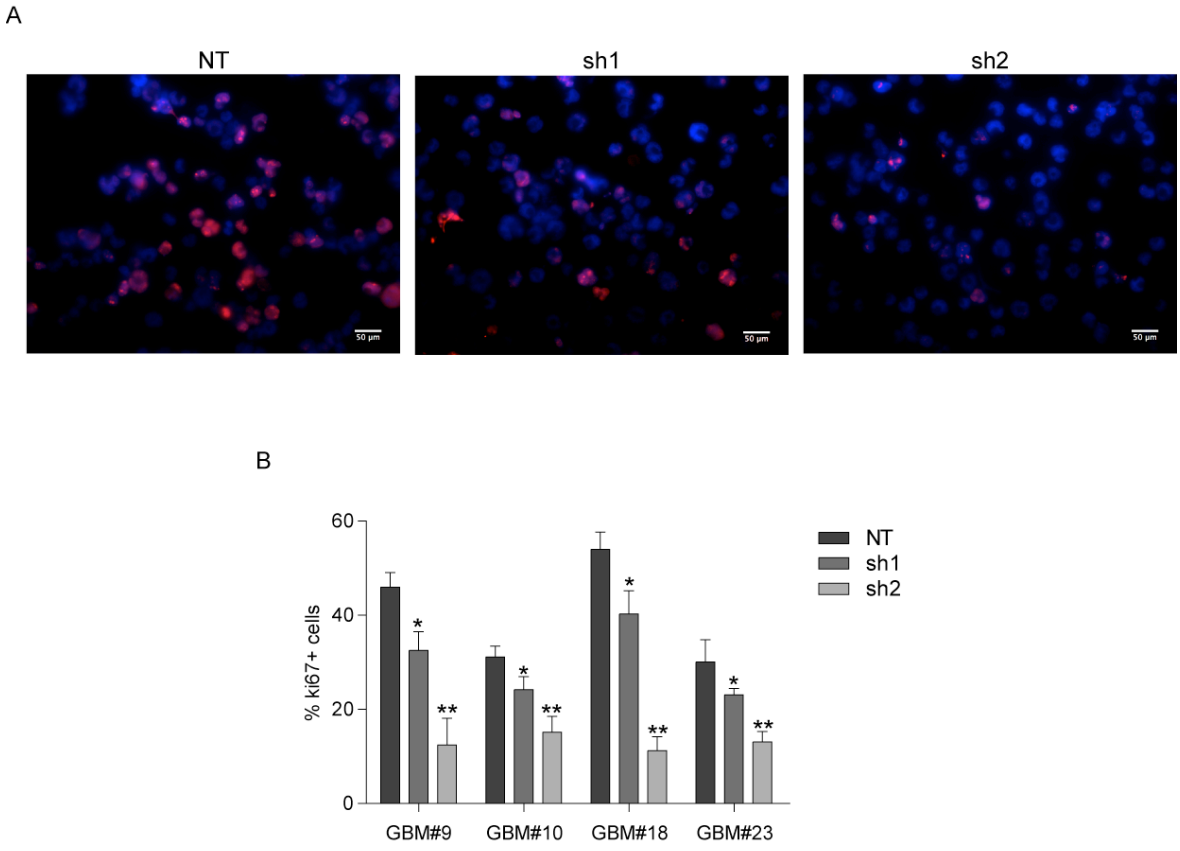

Figure 31. CD133 silencing reduced the proliferation of GBM-derived neurospheres. (A) Representative images of immunofluorescence staining of ki67 (red) in GBM#9 dissociated neurospheres infected and selected for 3 days with puromycin. DAPI (blue) is used to stain nuclei. Scale bar, 50 µm. (B) Percentage of Ki67+ cells on the total number of nuclei is calculated. Bars show mean values and corresponding standard deviation of five independent fields counted. (*) $p \leq 0.05$and (**) $p \leq 0.01$ calculated with two sided Student's t test between groups.

The rate of apoptosis was studied using PI staining (Figure 32) and measure of the cleavage of caspase 3 (Figure 33) by FACS and immunofluorescence staining respectively.

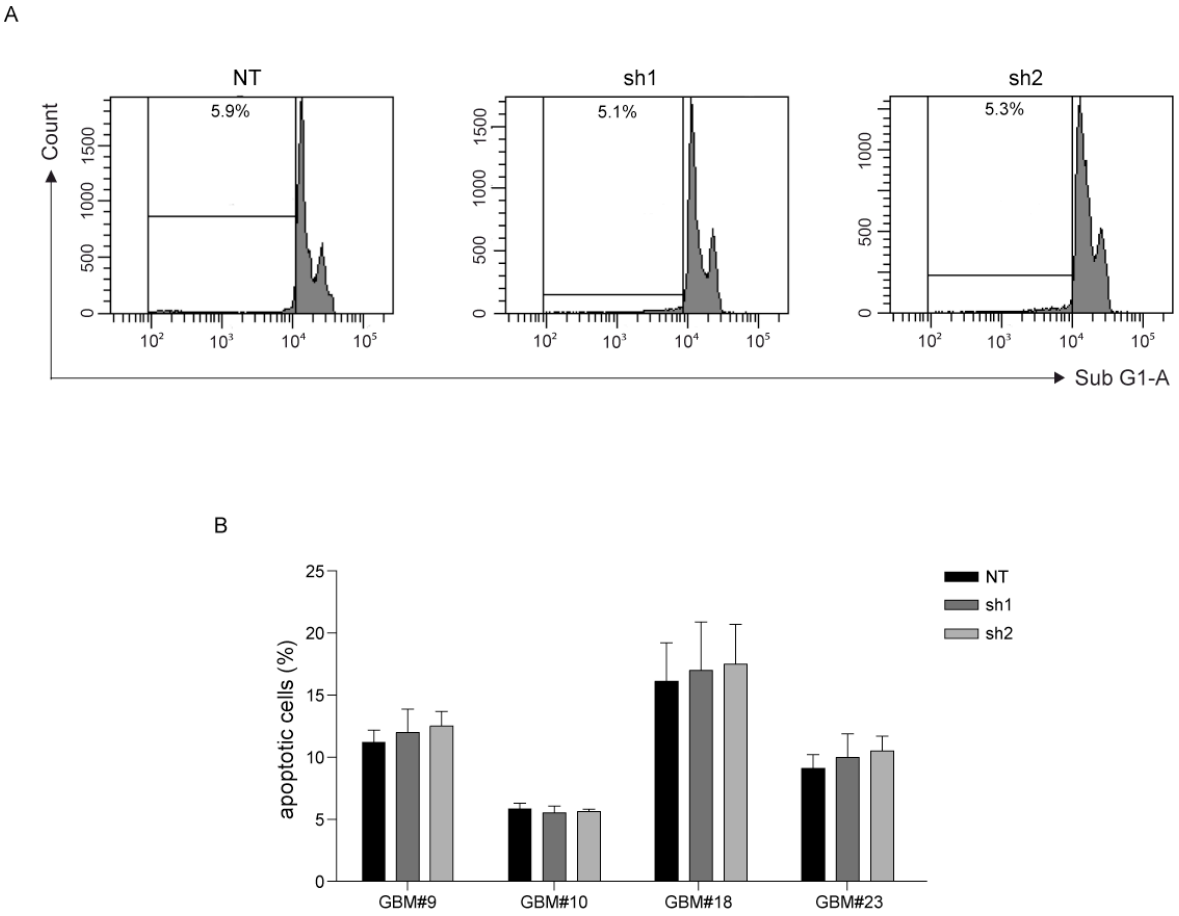

Figure 32. Apoptosis of CD133 interfered cells. (A) Representative plots of PI stained cells (GBM#10 NT, sh1, sh2). (B) Percentage of apoptotic cells in infected neurospheres derived from different patients. Bars represent means and standard deviation of two independent experiments.

No differences in the percentage of apoptotic cells between CD133 knocked-down cells and the control cells were detected, as confirmed by the analysis of another molecular event associated with apoptosis: the cleavage of caspase 3 (Figure 33).

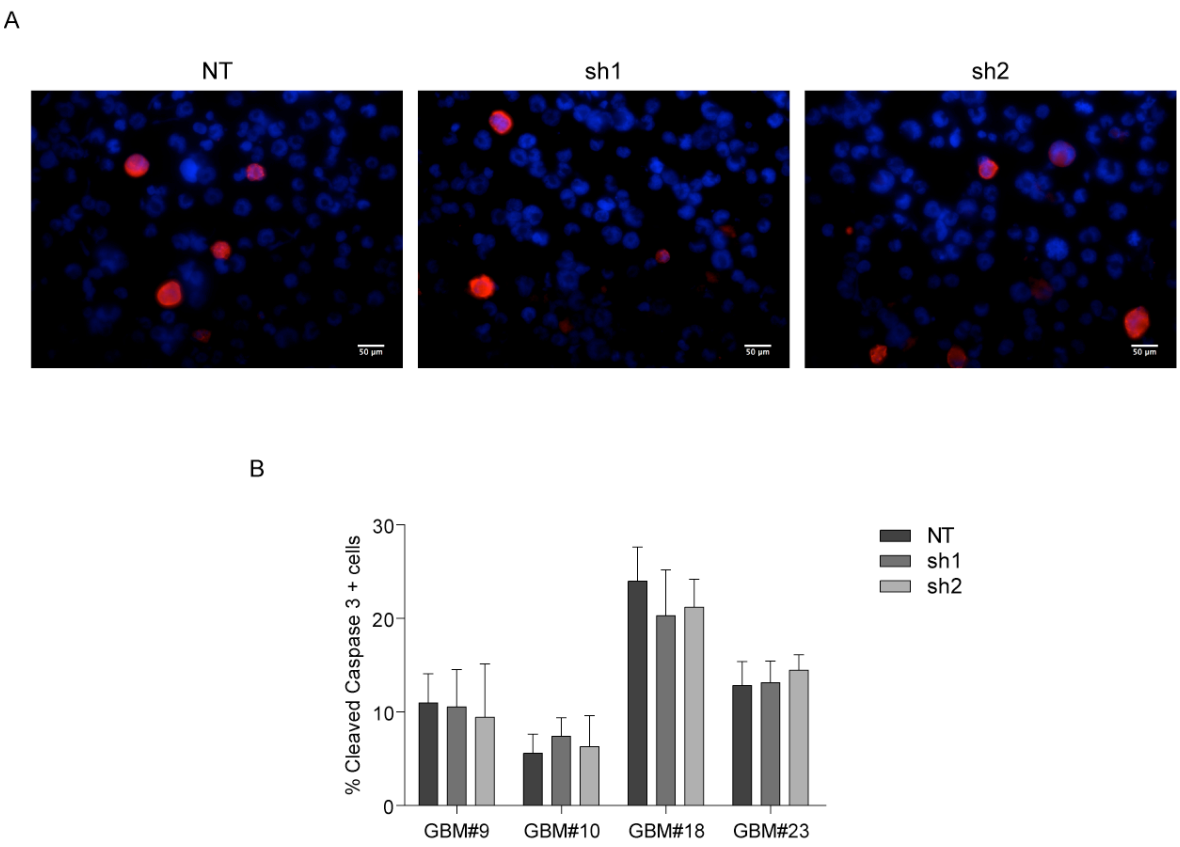

Figure 33. Apoptosis of CD133 interfered cells. (A) Representative images of immunoflurescence staining of Cleaved caspase 3 (red) in GBM#10 dissociated neurospheres infected and selected for 3 days with puromycin. DAPI (blue) is used to stain nuclei. Scale bar, 50 µm. (B) Percentage of Cleaved caspasese 3+ cells on the total number of nuclei is calculated. Bars show mean values and corresponding standard deviation of five independent fields counted.

These results indicate that CD133 regulates cellular proliferation and is not a survival factor for GBM-derived neurospheres.

4.4.3 Silencing of CD133 reduces clonogenicity and self-renewal capacity of GBM-derived neurospheres

Since a key characteristic of the cancer stem cells is the self-renewal capacity, we studied the clonogenicity of CD133 knock-down cells comparing the CD133-silenced cells to the control cells. Single cell suspensions were seeded on methylcellulose-coated coverslips and allowed to form colonies for 2 weeks. CD133 knocked-down cells formed fewer colonies than the control cells (Figure 34 A). Notably, CD133 knock-down decreased the clonogenic and the self-renewal capacities in a dose-dependent manner, consistent with the level of knockdown produced by each oligonucleotide.

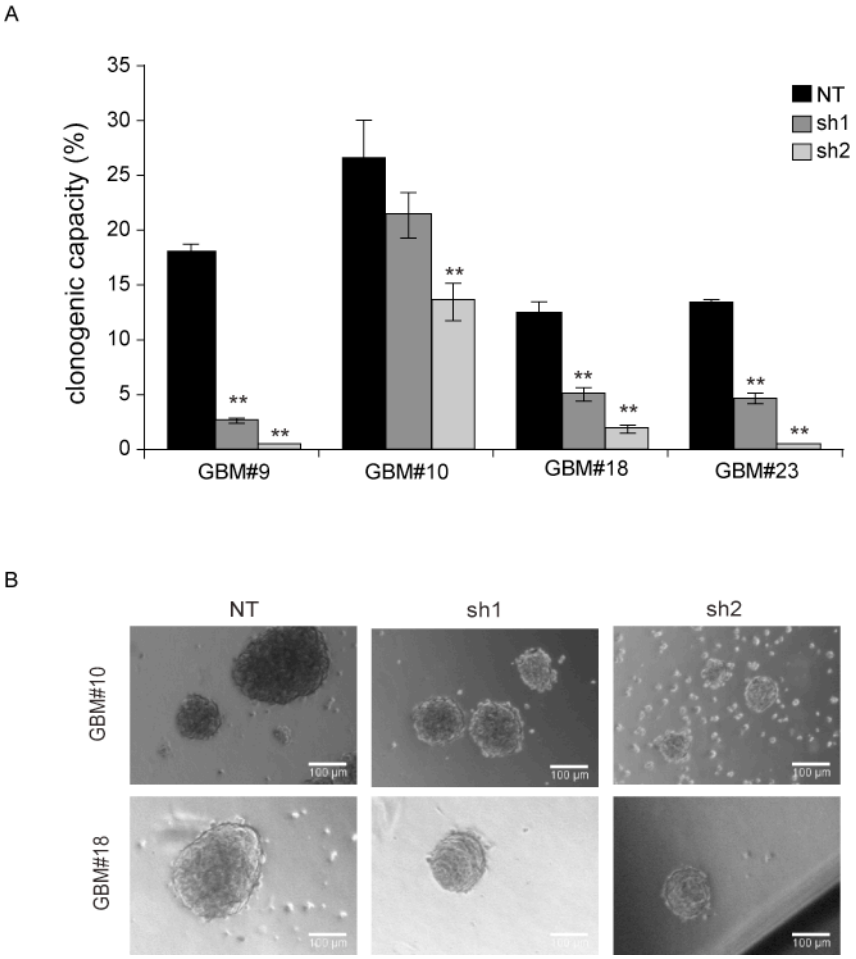

Figure 34. Analysis of cloning efficiency of CD133 interfered cells. (A) Quantification of cloning efficiency of silenced cells (sh1 and sh2) compared to the control cells (NT not targeting). Bars represent means and corresponding standard deviation of two independent experiments. (**) $p \leq 0.01$ calculated with Student's t test between sh1 or sh2 and NT. (B) Representative microphotographs of GBM#10 and GBM#18 spheres formed in methylcellulose by silenced and control cells. Scale bar, 100 µm.

The neurospheres formed by cells with reduced CD133 expression were markedly smaller than the spheres formed by the control cells (Figure 34 B). When the single spheres were dissociated and single cells were placed in a 96-well plate, the CD133-silenced cells reformed less spheres, additionally suggesting reduced self-renewal capacity (Figure 34).

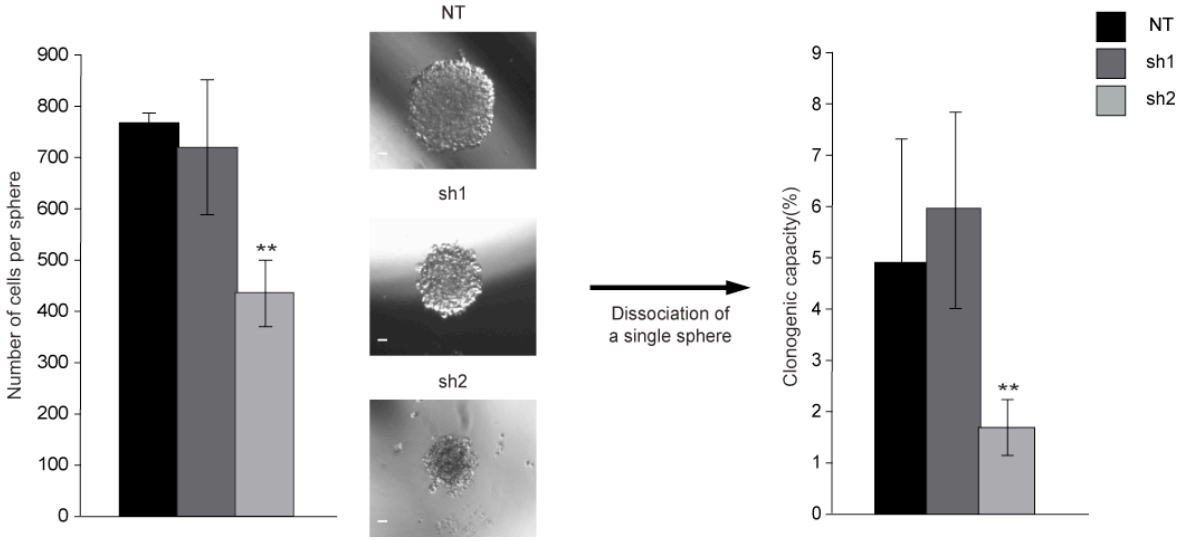

Figure 35. **CD133 knock-down reduces the clonogenic capacity of GBM-derived neurosphere cells.** In the GBM#10-derived neurospheres the number of cells within each single sphere is counted and reported as average number of cells (6 spheres of each group were counted). The cells are plated into 96-well plates at the density of 1 cell per well and the percentage of sphere formation is calculated after 2 weeks. Bars represent means and corresponding standard deviation of two independent experiments. (**), $p \leq 0.01$ calculated with Student's t test between sh2 and NT. Representative microphotographs of spheres are presented. Scale bar, 50 μm.

Together, these data indicate that CD133 has a function for the self-renewal potential of GBM-neurosphere cells, although its expression is not associated with the expression of other putative stem cell markers. Indeed, the expression of other putative stem cell markers in glioblastoma, such as Olig2 and Nestin, were not modified by CD133 knock-down (Figure 36).

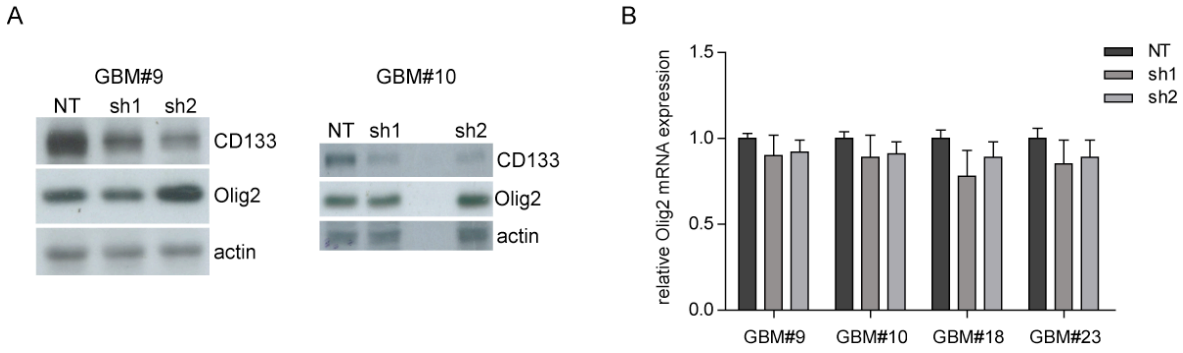

Figure 36. CD133 knock-down does not modify the expression of other CSCs markers. (A) Analysis of Olig2 expression by Western blotting on different GBM-derived neurospheres infected with lentivirus directing against either non-targeting shRNA (NT) or CD133 specific shRNAs (sh1, sh2). 20 micrograms of total cell lysate were loaded on a 10% polyacrylamide gel. Actin is used as loading control.
(B) The Olig2 mRNA levels are assessed by qRT-PCR in cells collected 3 days after infection. TBP is used as reference gene for normalization of Olig2 expression levels. Bars show mean values and corresponding standard deviation of two independent experiments.

4.4.4 Silencing of CD133 reduces the tumorigenic potential of the GBM neurospheres

In order to determine the tumorigenic potential of CD133 knocked-down cells *in vivo*, 100000 infected cells were injected into the brain of 5 weeks old nude mice. The animals were sacrificed at the first appearance of neurological signs. Almost all the mice died because of brain tumor formation, although a longer survival of mice injected with CD133 silenced cells occurred in all cases studied (injection of neurospheres derived from four different patients). Of note the fact that only the mice injected with cells interfered with the short hairpin 2, which was the more efficient in knocking down CD133, had a significant prolonged survival (Figure 37).

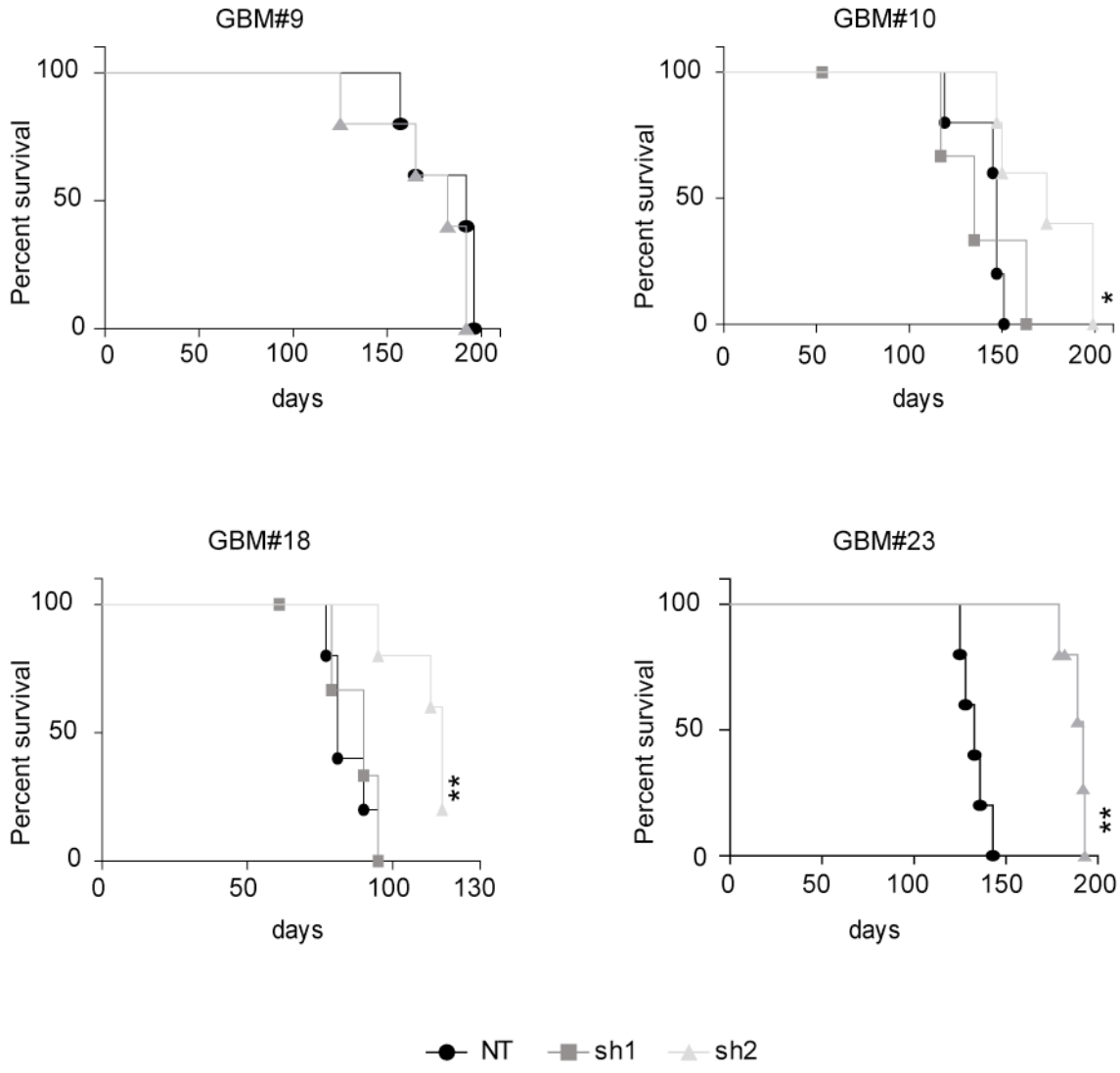

		Tumor incidence	Survival Average ± SD (days)
GBM#9	NT	5/5	181.2 ± 18.7
	sh2	5/5	171.2 ± 28.1
GBM#10	NT	5/5	141.8 ± 12.9
	sh1	5/5	155.8 ± 7.1
	sh2	5/5	180.5 ± 23.5
GBM#18	NT	5/5	84.8 ± 7.4
	sh1	3/5	88 ± 8.1
	sh2	4/5	110.5 ± 10.5
GBM#23	NT	5/5	133 ± 7
	sh2	4/5	187 ± 6.2

Figure 37. Kaplan-Maier survival graphs of animals injected with NT, sh1 and sh2 infected cells. CD133 silenced and control cells (100000 cells in each mouse) were orthotopically transplanted in nude mice (n = 5 animals per group). The sh2 tumor bearing mice showed a prolonged survival in GBM#10, GBM#18 and GBM#23 cases compared to the sh1 and NT tumor bearing animals. P-value was calculated by log rank test: (*) $p < 0.05$; (**) $p < 0.01$

Almost all tumors had similar cytoarchitecture and vascularization features (Figure 38). The cells formed an extensive tumor that invaded the brain and completely altered its structures. Immunohistochemistry showed that the tumor cells expressed GFP, confirming their origin from infected cells. Note that, xeno-tumors derived from GBM#23 invaded dramatically the brain without forming a tumor visible with the hematoxilin and eosin staining. To identify human cells in this case we stained the tumor with the human specific anti-nuclei antibody (Figure 38).

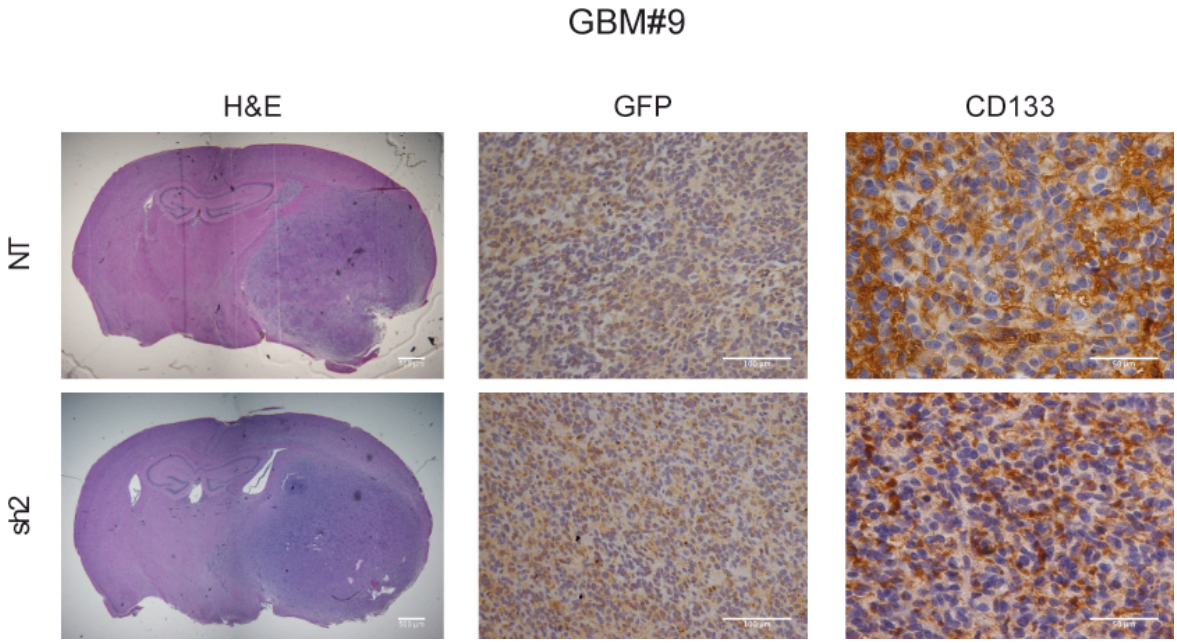

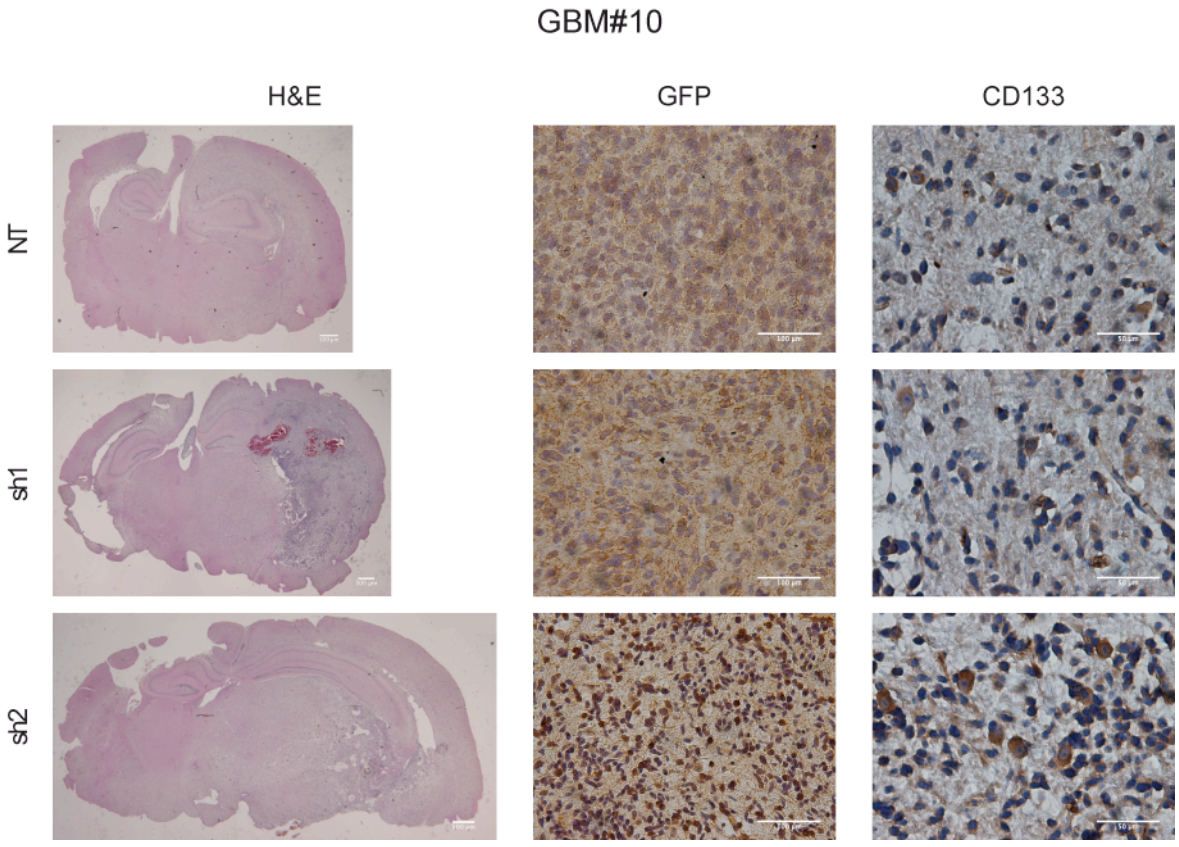
GBM#10
H&E
GFP
CD133
NT
sh1
sh2

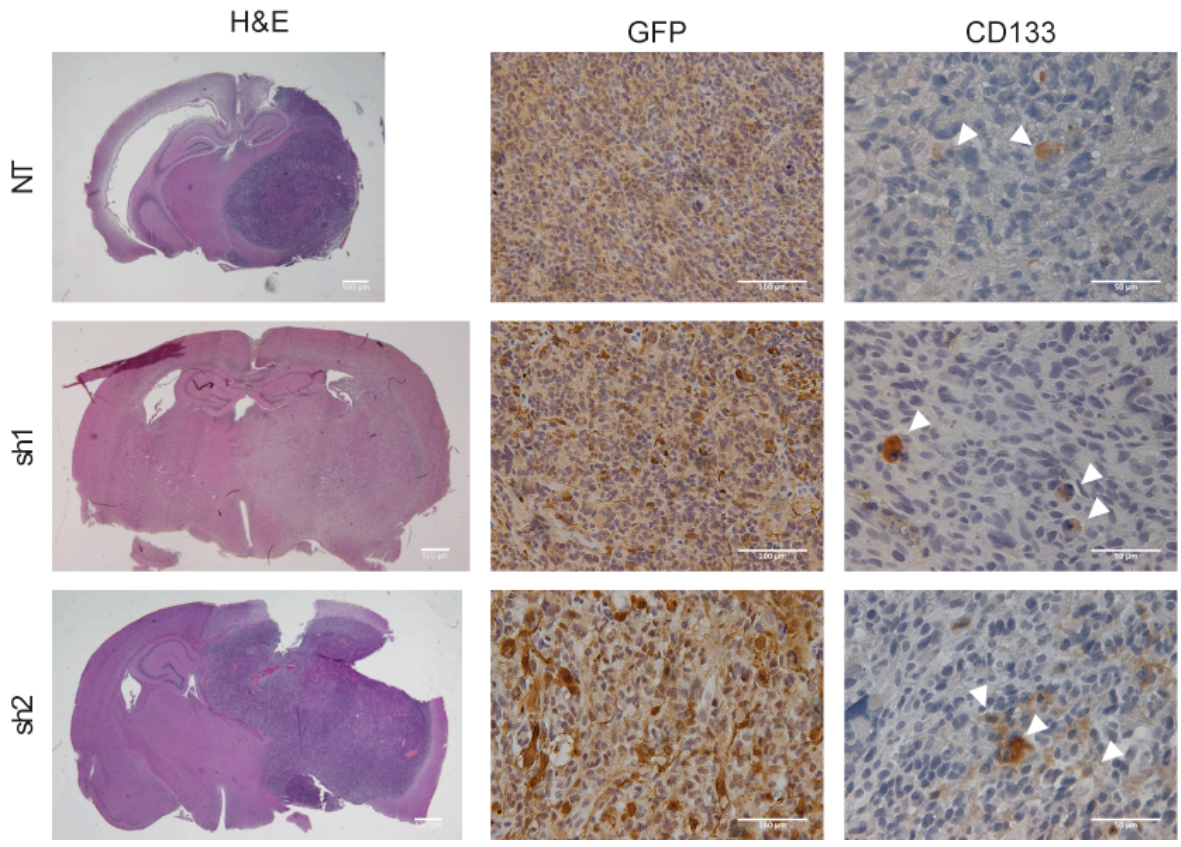
GBM#18
H&E
GFP
CD133
NT
sh1
sh2

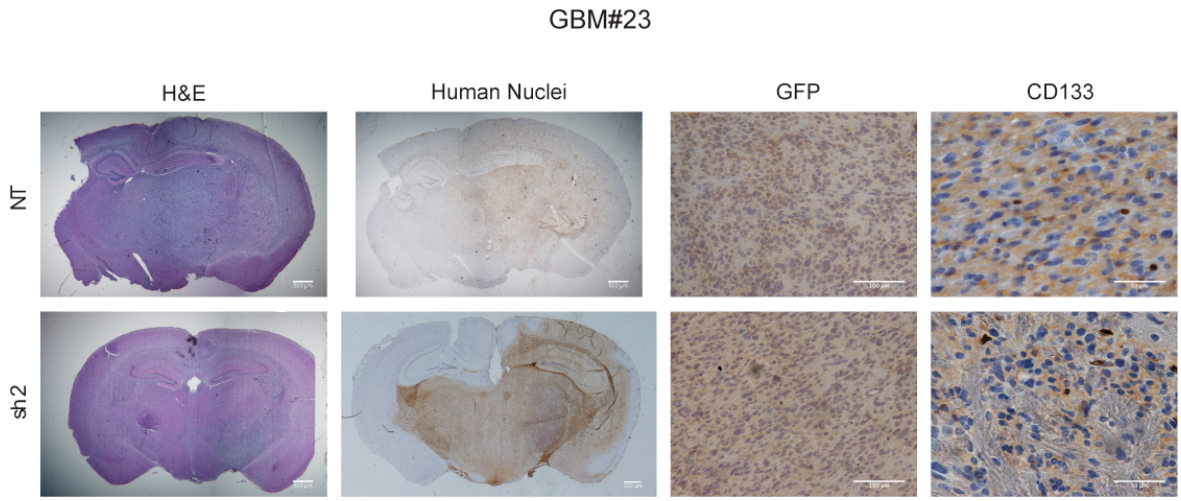

Figure 38. Immunohistochemistry of xenograft tumors derived from infected neurospheres. Representative images of brains of immunocompromised mice implanted with cells isolated from the glioblastoma specimen GBM#9, GBM#10, GBM#18, GBM#23 and infected with non-targeting shRNA (NT) or CD133 shRNAs are shown. 72 hours after infection and puromycin selection identical numbers of viable cells (10^5 cells/mouse) were implanted and brains examined when mice showed neurological signs. Gross images for H&E staining and coronal sections from representative brains bearing glioma xenografts are displayed. GFP and CD133 staining showed that the tumors were formed by infected cells Human Nuclei staining was shown in xenografts derived from GBM#23 infected neurospheres, since these cells formed more invasive tumors with no visible mass with H&E staining. Scale bar, 500µm (H&E and Human Nuclei), 100µm (GFP), 50µm (CD133).

Interestingly, when we looked at CD133 expression levels in these tumors we did not find any difference compared to the controls. This was demonstrated by immunohistochemical staining of CD133 on tissue slices (Figure) and by quantitative PCR on RNA extracted from formalin-fixed paraffin-embedded tissue samples (Figure 39).

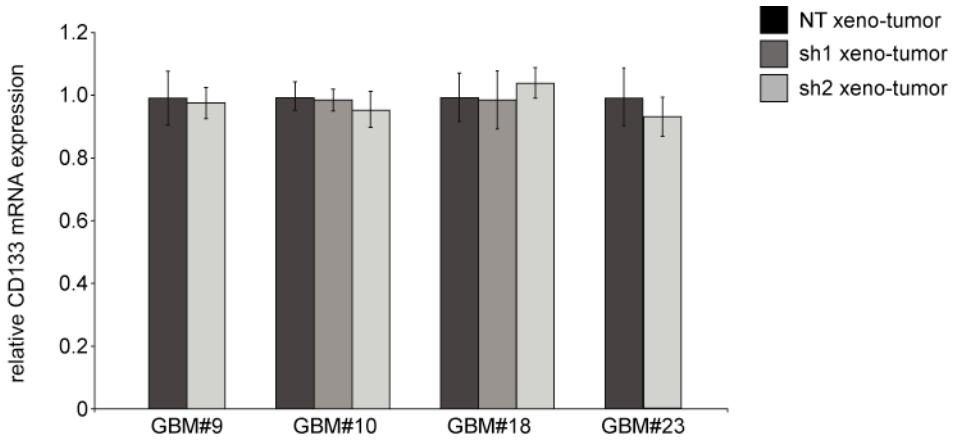

Figure 39. CD133 expression in xeno-tumors formed by infected cells. CD133 mRNA levels are assessed by qRT-PCR in total RNA extracted from FFPE tissue samples (n=2 mice per group). HPRT1 (human

specific) is used as reference gene for normalization of human CD133 expression levels. Bars show mean values and corresponding standard deviation of two mice.

Moreover, neurospheres were isolated from xeno-tumors formed by CD133 silenced and control cells and CD133 protein expression was analyzed on total cell lysates by Western blotting. In all type of xeno-tumors the neurosphere isolated expressed the same level of CD133 (Figure 40).

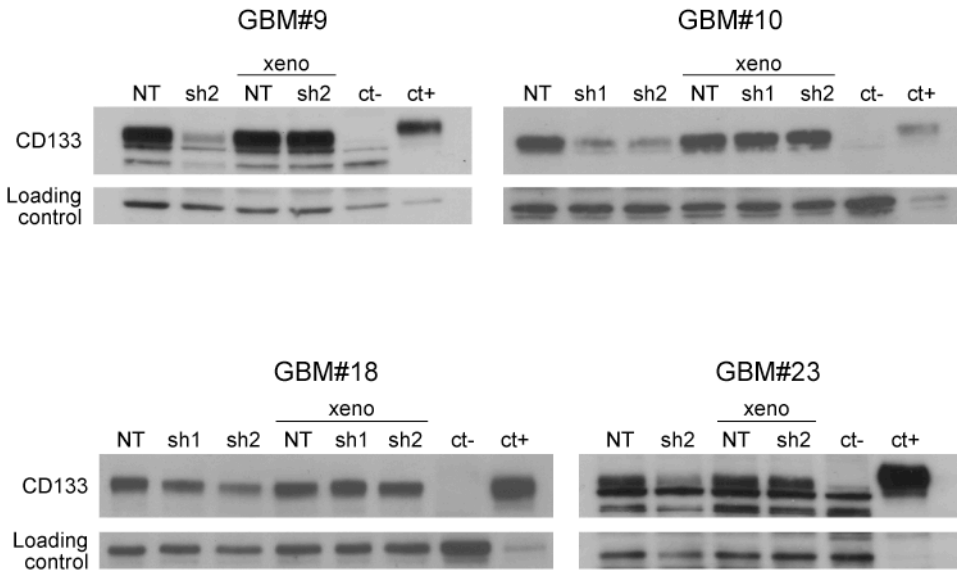

Figure 40. Analysis of CD133 expression in neurosphere isolated from xeno-tumors. Total lysates of NT (not targeting), sh1 and sh2 cells were collected before injection into nude mice and in neurosphere isolated from xeno-tumors. Western blotting with AC133 mAb was performed with neurosphere cells derived from four different patients. . 10 micrograms of total cell lysate were loaded on a 10% polyacrylamide gel. 2 micrograms total cell lysate of Caco2 are used as positive control. 10 micrograms of Hela total cell lysate are used as negative control. Actin is used as loading control.

These results could be explained in different ways: either the tumors were formed by the cells infected with the sh2 that failed to correctly express the silencing shRNA, or the infected and silenced cells escaped the CD133 down-modulation, re-expressing the protein and becoming able to form the tumor, just like the control cells. Thus, CD133 might be important in GBM-neurospheres to form tumors.

5. DISCUSSION

In glioblastomas, the most common primary brain tumors, CD133 identifies a subpopulation of stem-like tumor cells, named cancer stem cells, which drive tumor formation and are highly resistant to conventional chemo- and radiotherapy.

However, several studies report the existence of glioma stem cells not expressing CD133 able to self-renew and retain tumorigenic potential.

These discrepancies result in the reconsideration of CD133 as a universal marker for cancer stem cells in gliomas. Thus, an in-depth characterization of the complex CD133 phenotype in glioblastomas is much needed to re-evaluate the significance of CD133 in these tumors.

Furthermore, questioning the utility of CD133 in the identification of CSCs implies the study of its possible functional role in gliomagenesis and in stem cell properties, since its function in normal and cancer cells is not clearly defined.

We choose the neurosphere system as a good surrogate for *in vitro* study of glioma stem and progenitor cells (Lee et al, 2006; Rietze & Reynolds, 2006). A recent study indicates that *in vitro* expansion of GBM stem/progenitor cells as neurospheres does not alter the differentiation ability and the tumorigenic potential of these cells, neither their karyotype and gene expression pattern (Vik-Mo et al, 2010). Thus, each neurosphere cell line reflects an image of the tumor from which it was derived and remains representative after moderate expansion.

The major findings of this investigation relate to the localization of CD133, reversibly modulated between plasmamembrane and cytoplasm by several factors not yet determinated, and to the functional role of CD133 in the maintenance of human GBM stem/progenitor cells.

We found distinct expression patterns of CD133 both in neurospheres and in freshly dissociated tumors. Substantial amounts of membrane-bound CD133 were detectable only in a fraction of neurosphere lines, that we called CD133-high, whereas CD133 mRNA and intracellular CD133 protein were found expressed at higher levels in almost all neurosphere lines examined (except GBM#24 and GBM#8). The existence of an intracellular pool of CD133 in addition to the one at the cell surface, has been demonstrated in human hematopoietic stem cells and in established

glioblastoma cell lines in two very recent studies (Bauer et al, 2011; Campos et al, 2011), confirming our results.

Inside the cell, CD133 is located primarily in membrane vesicles within multivesicular bodies, endosomes, endoplasmic reticulum and Golgi apparatus (Bauer et al, 2011; Campos et al, 2011). Whether CD133 is localized in the same sub-cellular compartments in the neurosphere cells will be subject of our future investigations.

Cell sorting, based on cell surface CD133 expression, allowed the isolation of a CD133-negative cell fraction composed of cells with an exclusive cytoplasmic expression of CD133. These cells were less clonogenic and formed tumors with a longer latency than the CD133-positive cells did. Notably the impairment in self-renewal capacity and tumorigenic potential of CD133-negative cells was lost when these cells re-expressed CD133 on the plasmamembrane. These results suggest that the localization of CD133 on the plasmamembrane is functionally related to the cancer stem cell biology and characterizes cell populations with enhanced self-renewal and tumorigenic capacity. These results are supported by the recent demonstrations that the cell surface location of CD133 has been related to a higher proliferation rate of GBM cells (Wang et al, 2008). Hence, we can hypothesize that the cell surface CD133 activates a signaling cascade transduced into an activation of proliferation and self-renewal of the GBM stem/progenitor cells.

Our experiments of blocking the cell-surface CD133 using an anti-CD133 antibody with consequent reduction of viability, strongly support the hypothesis of an essential role of plasmamembrane CD133 in the maintenance of glioma stem/progenitor cells.

Our findings confirm the observation that cell-surface associated CD133 is a marker for self-renewing and tumor-initiating GBM cells (Singh et al, 2004), but add the notion that the mere isolation of CD133-positive cells is not sufficient to enrich for a stem cell population. We indeed observed that also neurospheres with low cell surface CD133 expression are able to grown and propagate the tumor, strengthening the idea of CD133 as a non essential element for stem cell properties in all GBM cases.

A recent study shows that self-renewing CD133-negative cells are present in neurosphere cultures derived from human GBM (Chen et al, 2010). These cells can be divided in two different types: (i) CD133-negative cells that generate aggressive tumors comprising a mixture of CD133-positive and

CD133-negative cells, (ii) CD133-negative cells that give rise to slow-growing circumscribed tumors formed of CD133-negative cells alone. They proposed that these cells are lineally related and represent different stages of differentiation. However, it was not reported any type of observation about a possible intracellular localization of CD133 in these two types of CD133-negative cells. They suggested indeed a possible transcriptional regulation of CD133 rather than changes in sub-cellular localization.

Through clonal analysis, we have been able to describe the intrinsic capabilities of individual tumor cells and their progeny. We found that every clone formed by a single CD133-negative cell contain cells with a considerable expression of plasmamembrane associated CD133, although in some cases to a lesser extent.

Our results indicate that there is not a hierarchical relation between CD133-positive and CD133-negative cells. Indeed, CD133 appears in an inter-convertible state, changing its expression levels and sub-cellular localization between the cytoplasm and the plasmamembrane. These changes might be regulated by several kinds of stimuli, such as the progression through the cell cycle phases or the supply of oxygen and nutrients. It has been demonstrated that the CD133 expression is strongly influenced by hypoxic conditions and is associated with alterations in mitochondrial function (Griguer et al, 2008).

Additional studies are needed to determine whether the observations we are reporting occur in all patient tumors and may help to bridge the gap between CD133-positive and CD133-negative glioma stem cells.

It remains obscure whether a population of cells that do not express CD133 at all does exist in the neurosphere. Interestingly, the intracellular staining of CD133 in the plasmamembrane-negative-CD133 cell fraction reveals the existence of a cell population that does not express any CD133. It might be relevant the analysis of the stem cell properties of these cells, although it is impossible to isolate them using the FACS sorting.

In order to identify and purify these totally CD133-negative cells, we propose to trace the activity of CD133 promoter in GBM-derived neurospheres. Using a lentiviral vector we could follow the expression of a reporter gene (*e.g* GFP) controlled by the human CD133 promoter. The infected

neurospheres could be then sorted on the basis of GFP-expression and analyzed for self-renewal capacity *in vitro* and tumorigenic potential *in vivo* (see APPENDIX I).

5.1 Targeting CD133 expression *in vivo* using lentiviral mediated shRNA as new therapeutic approach

The present study shows that CD133 expression is critical for several biological properties of human glioblastoma stem/progenitor cells. We targeted CD133 in the entire cell population of neurospheres derived from four different patients, using lentiviral mediated shRNA interference.

Silencing of CD133 reduces the proliferation rate of neurosphere cells that cannot be serially passaged anymore. This result is in accordance to the demonstration that CD133 expression is down-regulated in G0/G1 phase of the cell cycle in neural stem cells (Sun et al, 2009). Most importantly, depletion of CD133 reduces the self-renewal and the tumorigenic potential of GBM-derived neurospheres, implicating that CD133 has a direct function in the initiation and progression of tumors. Taken together, our results indicate a functional role of CD133 in gliomagenesis, giving further significance to its use in the therapy of glioblastoma.

To determine if targeting CD133 was sufficient to reduce glioma stem cell tumor growth *in vivo*, we targeted CD133 in glioma cells before injection into immunocompromised mice.

However, to determine if targeting CD133 could represent a potential therapeutic paradigm, we could also target CD133 directly in established tumors. In order to test this possibility we intracranially implanted neurosphere cells into immunocompromised mice and allowed tumors to grow for 4 weeks. Tumor-bearing mice were then intracranially injected with lentivirus expressing non-targeting shRNA, as a control, or CD133 shRNA as a novel therapy. The shRNA targeting CD133 expression *in vivo* increased the survival of tumor-bearing animals. The tumor growth was not reduced by the shRNA directed against CD133, since the brain tumor xenografts were already well established and have formed a big and invasive tumor mass before lentivirus injection. Furthermore we observed expression of the reporter gene GFP in the tumor cells, confirming the infection with the lentivirus and we found a reduction of CD133 expression in mice receiving the shRNA targeting CD133 (Appendix II).

Although this experiment was performed only once using GBM neurospheres derived from one single patient, it gives us a very promising result. Much more effort will be made in the re-production of this result and testing of CD133 *in vivo* targeting in several GBM-neurospheres lines.

Taken together, our results indicate a functional role of CD133 in gliomagenesis, giving further significance to its use in the therapy of glioblastoma.

It has to be taken in consideration that cytoplasmic CD133 is re-localized on the plasmamembrane, rendering the anti-CD133 therapy based exclusively on the targeting of cell surface-CD133, not effective in every case. Targeting CD133 using shRNAs might be more effective.

5.2 Gene expression array suggests genes and pathways involved in the biological effects caused by CD133 down-regulation

Our results suggest that CD133 influences crucial biological properties of GSCs. It is conceivable that CD133, directly or through its interaction with signaling pathways transducers, influences the maintenance and the tumorigenic potential of GSCs.

Gene expression analysis was performed to gain insights on the identification of genes and pathways that might be involved in the biological effects associated with CD133 down-regulation.

We used the Gene ST 1.0 array on RNA isolated from neurospheres derived from four different patients and infected with lentiviruses transducing NT and sh2 shRNAs. Slight differences in gene expression, common to the four samples, were found, since we observed a maximum fold change of 1.3 in gene expression levels between interfered and control cells.

However, an interaction between CD133 and the Clathrin-mediated endocytosis signaling is strongly suggested by the finding that 6 genes belonging to this signaling pathway were found significantly down-regulated ($p < 0.05$) in all CD133 silenced neurospheres (see Appendix III A). The differential expression of these genes needs to be confirmed by qPCR and at protein level by Western blotting.

A link between CD133 and the endocytic pathway is supported by the observation that CD133 is associated with the endosomal compartment of mitotic human hematopoietic stem cells (hHSCs) (Fonseca et al, 2008). CD133 is also associated with cholesterol-based lipid rafts whose presence in the endosomal compartments was recently demonstrated (Sobo et al, 2007).

Moreover, CD133, as well as four endosomal-associated proteins (CD53, CD62L, CD63 and CD71) (Beckmann et al, 2007), can be either symmetrically or asymmetrically distributed in mitotic hHSCs (Corbeil et al, 1998; Roper et al, 2000)

Thus, a link between CD133, the endosomal compartment and symmetric/asymmetric cell division in rare primitive mammalian cells (Giebel & Beckmann, 2007) could exist. The endosomal compartment could host potential stem cell determinants and thus might play an active role in the maintenance of certain stem cell properties. Furthermore, CD133-containg lipid rafts might include other stem cell determinants (Fonseca et al, 2008; Kosodo et al, 2004). Thus, the concept of 'stem cell-specific lipid rafts or membrane microdomains' holding molecular determinants necessary to maintain the stem cell properties is attractive in this context (Marzesco et al, 2005).

More recently, Lathia et al demonstrated that the majority of CSCs in the GBM neurospheres were generated through expansive symmetric cell division and not through asymmetric cell division. CD133, and not any other CSC marker, segregates asymmetrically in a fraction of mitoses, some of which were associated with Numb asymmetry. Under growth factor withdrawal conditions, the proportion of asymmetric CD133 distribution increases, consistently with the increase in asymmetric cell divisions (Lathia et al, 2011). Of note, Numb is significantly down-regulated in our CD133-interfered neurospheres.

These results further suggest a link between CD133 and symmetric/asymmetric cell division of glioma stem cells.

As a general consideration, our results show that CD133 alone can not be considered essential as cell surface marker in human glioblastomas, in agreement with the notions that cancer stem cells are not represented by one particular phenotype and different glioma stem cell populations (based on the expression of various markers) are present in this heretogeneous tumor. This conclusion is supported also by the fact that CD133 expression in the tumor is not related to the patients' survival time; in same manner CD133 expression in the neurospheres is not related to the survival time of tumor bearing mice. Thus, a variety of markers has to be used to better identify stem cells in all tumor cases. As consequence our results do not contradict the theory of a hierarchical organization of glioma cells.

APPENDIX I

A

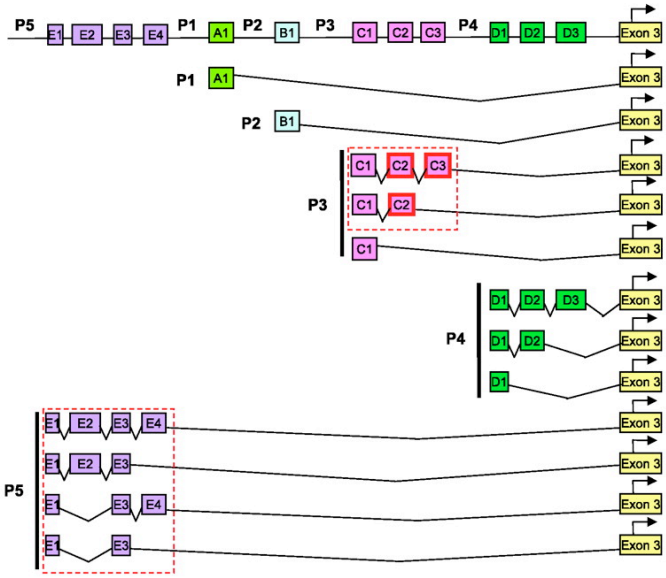

B

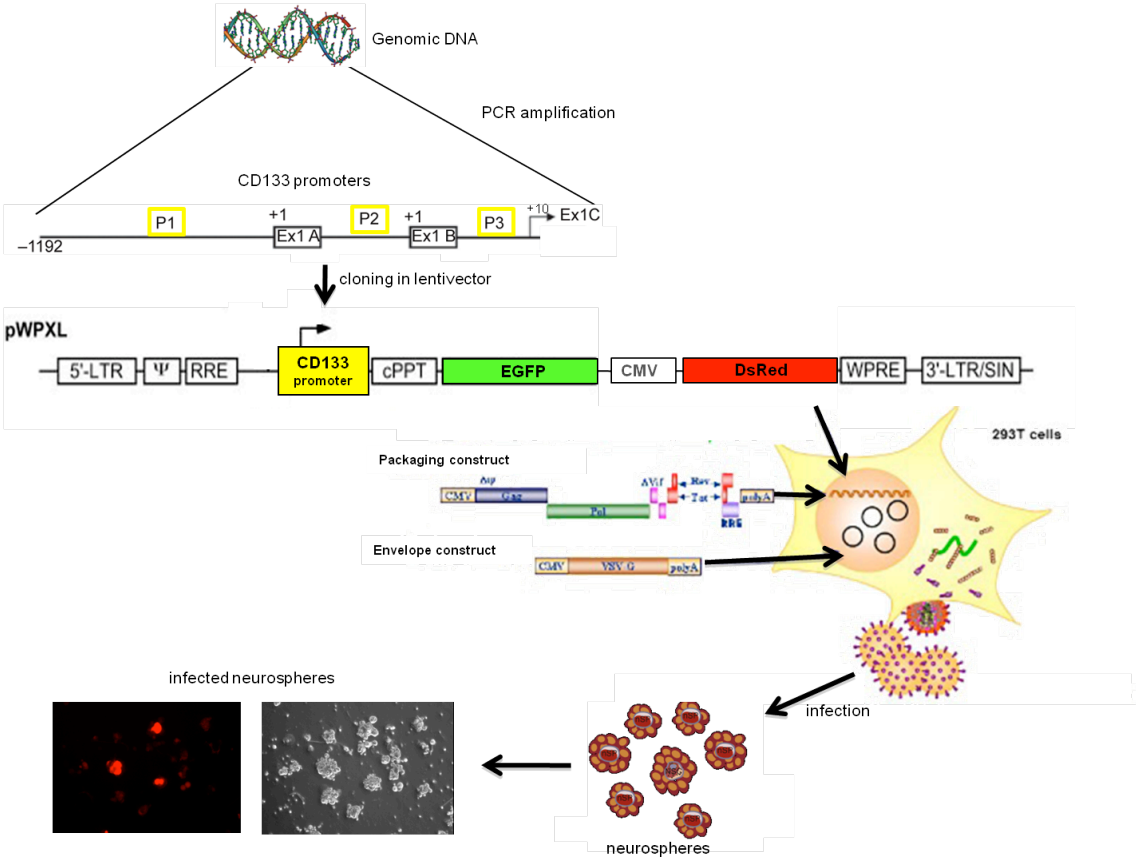

CD133 mRNA expression and promoter activity based on Kemper et al.
(A) Schematic representation of the 5′ region of CD133. Human CD133 is a highly complex gene that contains five alternative promoters, each containing one or multiple corresponding exons (Shmelkov et al, 2004). Promoter regulation exists for human CD133 and could result in seven different splice variants, which differ in coding exons and generate distinct protein isoforms. (B) Schematic representation of our working flow. To analyze promoter activity in GBM-derived neurospheres, promoters P1, P2, P3 active in glioma cells are amplified from genomic DNA and cloned into a lentiviral vector to drive the expression of the reported gene GFP. A selection gene (dsRED) is used to select the infected cells. The GBM-derived neurospheres are infected and selected on the basis of dsRED expression and the CD133 promoter activity followed by the GFP expression. The stem cell properties (self-renewal and tumorigenic potential) of GFP+ and GFP- cells will be studied *in vitro* and *in vivo*.

APPENDIX II

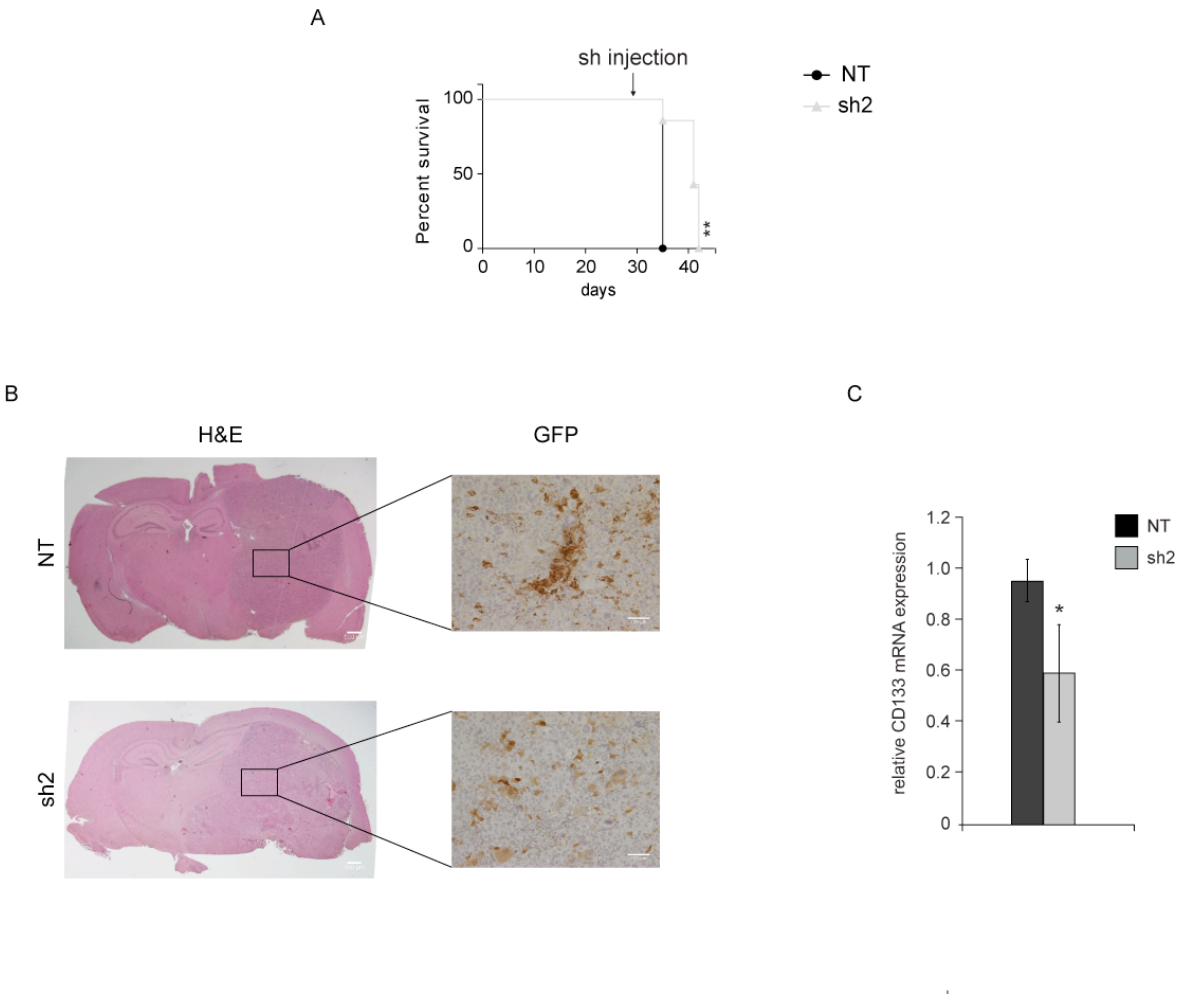

Lentiviral shRNA targeting CD133 increased survival of mice bearing intracranial xenograft tumors. (A) Targeting CD133 *in vivo* through lentiviral mediated shRNA significantly increased the survival of mice bearing intracranial glioma xenografts, Seven mice per group. (**) $p < 0.01$. (B) Representative images of coronal sections of brains of mice implanted with GBM#18 neurospheres and then infected with lentivirus expressing non-targeting shRNA (NT) or CD133 shRNA (sh2) are shown. Identical numbers of cells (10^5 cells/mouse) were implanted into mice brains to establish intracranial tumors. After 30 days to allow the tumor to grow, lentivirus expressing non-targeting shRNA (NT) or shRNA directed against CD133 were delivered to the tumor site through direct injection. Staining of GFP indicated that the tumor cells were infected. (C) CD133 expression was slightly reduced in xenografts treated with shRNA directed against CD133. CD133 expression was analyzed by qRT-PCR in tumor xenografts. HPRT1 (human specific) was used as reference gene for normalization of CD133 expression levels. Bars show mean values and corresponding standard deviation of results derived from three mice/group. (*) $p \leq 0.05$ calculated with two sided Student's t test.

APPENDIX III

Probe ID	Entrez Gene	Entrez Gene Symbol	GBM#9 FC	GBM#10 FC	GBM#18 FC	GBM#23 FC
7942204	2017	CTTN	0.801	0.864	0.932	0.923
7956088	5869	RAB5B	0.909	0.843	0.811	0.908
7910398	5867	RAB4A	0.857	0.751	0.903	0.801
7980005	8650	NUMB	0.8	0.903	0.909	0.891
8052803	22848	AAK1	0.862	0.815	0.892	0.817
8091009	5291	PIK3CB	0.857	0.835	0.843	0.779
8099476	8842	PROM1	0.563	0.485	0.926	0.581

Microarray data. Fold change (FC) in expression for 6 genes involved in the Clathrin-mediated endocytic signaling differentially regulated in non-targeting shRNA (NT) cells and CD133 shRNA (sh2) cells by microarray. Fold change (FC) in expression for CD133 (PROM1 in blue) is shown.

REFERENCES

Abounader R, Laterra J (2005) Scatter factor/hepatocyte growth factor in brain tumor growth and angiogenesis. *Neuro Oncol* **7**(4)**:** 436-451

Aimone JB, Wiles J, Gage FH (2006) Potential role for adult neurogenesis in the encoding of time in new memories. *Nat Neurosci* **9**(6)**:** 723-727

Al-Hajj M, Wicha MS, Benito-Hernandez A, Morrison SJ, Clarke MF (2003) Prospective identification of tumorigenic breast cancer cells. *Proc Natl Acad Sci U S A* **100**(7)**:** 3983-3988

Bachoo RM, Maher EA, Ligon KL, Sharpless NE, Chan SS, You MJ, Tang Y, DeFrances J, Stover E, Weissleder R, Rowitch DH, Louis DN, DePinho RA (2002) Epidermal growth factor receptor and Ink4a/Arf: convergent mechanisms governing terminal differentiation and transformation along the neural stem cell to astrocyte axis. *Cancer Cell* **1**(3)**:** 269-277

Bao S, Wu Q, McLendon RE, Hao Y, Shi Q, Hjelmeland AB, Dewhirst MW, Bigner DD, Rich JN (2006) Glioma stem cells promote radioresistance by preferential activation of the DNA damage response. *Nature* **444**(7120)**:** 756-760

Barabe F, Kennedy JA, Hope KJ, Dick JE (2007) Modeling the initiation and progression of human acute leukemia in mice. *Science* **316**(5824)**:** 600-604

Batchelor TT, Sorensen AG, di Tomaso E, Zhang WT, Duda DG, Cohen KS, Kozak KR, Cahill DP, Chen PJ, Zhu M, Ancukiewicz M, Mrugala MM, Plotkin S, Drappatz J, Louis DN, Ivy P, Scadden DT, Benner T, Loeffler JS, Wen PY, Jain RK (2007) AZD2171, a pan-VEGF receptor tyrosine kinase inhibitor, normalizes tumor vasculature and alleviates edema in glioblastoma patients. *Cancer Cell* **11**(1)**:** 83-95

Bauer N, Fonseca AV, Florek M, Freund D, Jaszai J, Bornhauser M, Fargeas CA, Corbeil D (2008) New insights into the cell biology of hematopoietic progenitors by studying prominin-1 (CD133). *Cells Tissues Organs* **188**(1-2)**:** 127-138

Bauer N, Wilsch-Brauninger M, Karbanova J, Fonseca AV, Strauss D, Freund D, Thiele C, Huttner WB, Bornhauser M, Corbeil D (2011) Haematopoietic stem cell differentiation promotes the release of prominin-1/CD133-containing membrane vesicles--a role of the endocytic-exocytic pathway. *EMBO Mol Med* **3**(7)**:** 398-409

Beckmann J, Scheitza S, Wernet P, Fischer JC, Giebel B (2007) Asymmetric cell division within the human hematopoietic stem and progenitor cell compartment: identification of asymmetrically segregating proteins. *Blood* **109**(12)**:** 5494-5501

Beier D, Hau P, Proescholdt M, Lohmeier A, Wischhusen J, Oefner PJ, Aigner L, Brawanski A, Bogdahn U, Beier CP (2007) CD133(+) and CD133(-) glioblastoma-derived cancer stem cells show differential growth characteristics and molecular profiles. *Cancer Res* **67**(9)**:** 4010-4015

Beier D, Wischhusen J, Dietmaier W, Hau P, Proescholdt M, Brawanski A, Bogdahn U, Beier CP (2008) CD133 expression and cancer stem cells predict prognosis in high-grade oligodendroglial tumors. *Brain Pathol* **18**(3)**:** 370-377

Bhatia M (2001) AC133 expression in human stem cells. *Leukemia* **15**(11)**:** 1685-1688

Bidlingmaier S, Zhu X, Liu B (2008) The utility and limitations of glycosylated human CD133 epitopes in defining cancer stem cells. *J Mol Med* **86**(9)**:** 1025-1032

Bleau AM, Hambardzumyan D, Ozawa T, Fomchenko EI, Huse JT, Brennan CW, Holland EC (2009) PTEN/PI3K/Akt pathway regulates the side population phenotype and ABCG2 activity in glioma tumor stem-like cells. *Cell Stem Cell* **4**(3)**:** 226-235

Bonnefoix T, Bonnefoix P, Verdiel P, Sotto JJ (1996) Fitting limiting dilution experiments with generalized linear models results in a test of the single-hit Poisson assumption. *J Immunol Methods* **194**(2)**:** 113-119

Bonnet D, Dick JE (1997) Human acute myeloid leukemia is organized as a hierarchy that originates from a primitive hematopoietic cell. *Nat Med* **3**(7)**:** 730-737

Brennan C, Momota H, Hambardzumyan D, Ozawa T, Tandon A, Pedraza A, Holland E (2009) Glioblastoma subclasses can be defined by activity among signal transduction pathways and associated genomic alterations. *PLoS One* **4**(11)**:** e7752

Brescia P, Richichi C, Pelicci G (2011) Identification of glioma stem cells: what is already known and how far do we still need to go? The biomarkers dilemma. *JCM* **in press**

Calabrese C, Poppleton H, Kocak M, Hogg TL, Fuller C, Hamner B, Oh EY, Gaber MW, Finklestein D, Allen M, Frank A, Bayazitov IT, Zakharenko SS, Gajjar A, Davidoff A, Gilbertson RJ (2007) A perivascular niche for brain tumor stem cells. *Cancer Cell* **11**(1)**:** 69-82

Cameron HA, McKay RD (2001) Adult neurogenesis produces a large pool of new granule cells in the dentate gyrus. *J Comp Neurol* **435**(4)**:** 406-417

Campbell LL, Polyak K (2007) Breast tumor heterogeneity: cancer stem cells or clonal evolution? *Cell Cycle* **6**(19)**:** 2332-2338

Campos B, Zeng L, Daotrong PH, Eckstein V, Unterberg A, Mairbaurl H, Herold-Mende C (2011) Expression and regulation of AC133 and CD133 in glioblastoma. *Glia*

Carro MS, Lim WK, Alvarez MJ, Bollo RJ, Zhao X, Snyder EY, Sulman EP, Anne SL, Doetsch F, Colman H, Lasorella A, Aldape K, Califano A, Iavarone A (2010) The transcriptional network for mesenchymal transformation of brain tumours. *Nature* **463**(7279)**:** 318-325

Castillo L, Etienne-Grimaldi MC, Fischel JL, Formento P, Magne N, Milano G (2004) Pharmacological background of EGFR targeting. *Ann Oncol* **15**(7)**:** 1007-1012

Chaichana K, Zamora-Berridi G, Camara-Quintana J, Quinones-Hinojosa A (2006) Neurosphere assays: growth factors and hormone differences in tumor and nontumor studies. *Stem Cells* **24**(12)**:** 2851-2857

Chen R, Nishimura MC, Bumbaca SM, Kharbanda S, Forrest WF, Kasman IM, Greve JM, Soriano RH, Gilmour LL, Rivers CS, Modrusan Z, Nacu S, Guerrero S, Edgar KA, Wallin JJ, Lamszus K, Westphal M, Heim S, James CD, VandenBerg SR, Costello JF, Moorefield S, Cowdrey CJ, Prados M, Phillips HS (2010) A hierarchy of self-renewing tumor-initiating cell types in glioblastoma. *Cancer Cell* **17**(4)**:** 362-375

Christensen K, Schroder HD, Kristensen BW (2008) CD133 identifies perivascular niches in grade II-IV astrocytomas. *J Neurooncol* **90**(2)**:** 157-170

Clarke ID, Dirks PB (2003) A human brain tumor-derived PDGFR-alpha deletion mutant is transforming. *Oncogene* **22**(5)**:** 722-733

Clement V, Dutoit V, Marino D, Dietrich PY, Radovanovic I (2009) Limits of CD133 as a marker of glioma self-renewing cells. *Int J Cancer* **125**(1)**:** 244-248

Collins AT, Berry PA, Hyde C, Stower MJ, Maitland NJ (2005) Prospective identification of tumorigenic prostate cancer stem cells. *Cancer Res* **65**(23)**:** 10946-10951

Colman H, Zhang L, Sulman EP, McDonald JM, Shooshtari NL, Rivera A, Popoff S, Nutt CL, Louis DN, Cairncross JG, Gilbert MR, Phillips HS, Mehta MP, Chakravarti A, Pelloski CE, Bhat K, Feuerstein BG, Jenkins RB, Aldape K (2010) A multigene predictor of outcome in glioblastoma. *Neuro Oncol* **12**(1)**:** 49-57

Corbeil D, Marzesco AM, Fargeas CA, Huttner WB (2010) Prominin-1: a distinct cholesterol-binding membrane protein and the organisation of the apical plasma membrane of epithelial cells. *Subcell Biochem* **51:** 399-423

Corbeil D, Roper K, Fargeas CA, Joester A, Huttner WB (2001) Prominin: a story of cholesterol, plasma membrane protrusions and human pathology. *Traffic* **2**(2)**:** 82-91

Corbeil D, Roper K, Hellwig A, Tavian M, Miraglia S, Watt SM, Simmons PJ, Peault B, Buck DW, Huttner WB (2000) The human AC133 hematopoietic stem cell antigen is also expressed in epithelial cells and targeted to plasma membrane protrusions. *J Biol Chem* **275**(8)**:** 5512-5520

Corbeil D, Roper K, Weigmann A, Huttner WB (1998) AC133 hematopoietic stem cell antigen: human homologue of mouse kidney prominin or distinct member of a novel protein family? *Blood* **91**(7)**:** 2625-2626

Costello JF, Plass C, Arap W, Chapman VM, Held WA, Berger MS, Su Huang HJ, Cavenee WK (1997) Cyclin-dependent kinase 6 (CDK6) amplification in human gliomas identified using two-dimensional separation of genomic DNA. *Cancer Res* **57**(7)**:** 1250-1254

Curtis MA, Kam M, Nannmark U, Anderson MF, Axell MZ, Wikkelso C, Holtas S, van Roon-Mom WM, Bjork-Eriksson T, Nordborg C, Frisen J, Dragunow M, Faull RL, Eriksson PS (2007) Human neuroblasts migrate to the olfactory bulb via a lateral ventricular extension. *Science* **315**(5816)**:** 1243-1249

Dalerba P, Dylla SJ, Park IK, Liu R, Wang X, Cho RW, Hoey T, Gurney A, Huang EH, Simeone DM, Shelton AA, Parmiani G, Castelli C, Clarke MF (2007) Phenotypic characterization of human colorectal cancer stem cells. *Proc Natl Acad Sci U S A* **104**(24)**:** 10158-10163

Dubreuil V, Marzesco AM, Corbeil D, Huttner WB, Wilsch-Brauninger M (2007) Midbody and primary cilium of neural progenitors release extracellular membrane particles enriched in the stem cell marker prominin-1. *J Cell Biol* **176**(4)**:** 483-495

Eramo A, Lotti F, Sette G, Pilozzi E, Biffoni M, Di Virgilio A, Conticello C, Ruco L, Peschle C, De Maria R (2008) Identification and expansion of the tumorigenic lung cancer stem cell population. *Cell Death Differ* **15**(3)**:** 504-514

Eramo A, Ricci-Vitiani L, Zeuner A, Pallini R, Lotti F, Sette G, Pilozzi E, Larocca LM, Peschle C, De Maria R (2006) Chemotherapy resistance of glioblastoma stem cells. *Cell Death Differ* **13**(7)**:** 1238-1241

Fargeas CA, Corbeil D, Huttner WB (2003) AC133 antigen, CD133, prominin-1, prominin-2, etc.: prominin family gene products in need of a rational nomenclature. *Stem Cells* **21**(4)**:** 506-508

Fargeas CA, Joester A, Missol-Kolka E, Hellwig A, Huttner WB, Corbeil D (2004) Identification of novel Prominin-1/CD133 splice variants with alternative C-termini and their expression in epididymis and testis. *J Cell Sci* **117**(Pt 18)**:** 4301-4311

Ferrandina G, Martinelli E, Petrillo M, Prisco MG, Zannoni G, Sioletic S, Scambia G (2009) CD133 antigen expression in ovarian cancer. *BMC Cancer* **9:** 221

Florek M, Haase M, Marzesco AM, Freund D, Ehninger G, Huttner WB, Corbeil D (2005) Prominin-1/CD133, a neural and hematopoietic stem cell marker, is expressed in adult human differentiated cells and certain types of kidney cancer. *Cell Tissue Res* **319**(1)**:** 15-26

Fonseca AV, Bauer N, Corbeil D (2008) The stem cell marker CD133 meets the endosomal compartment--new insights into the cell division of hematopoietic stem cells. *Blood Cells Mol Dis* **41**(2)**:** 194-195

Frederick L, Eley G, Wang XY, James CD (2000) Analysis of genomic rearrangements associated with EGRFvIII expression suggests involvement of Alu repeat elements. *Neuro Oncol* **2**(3)**:** 159-163

Freije WA, Castro-Vargas FE, Fang Z, Horvath S, Cloughesy T, Liau LM, Mischel PS, Nelson SF (2004) Gene expression profiling of gliomas strongly predicts survival. *Cancer Res* **64**(18)**:** 6503-6510

Fuller GN, Hess KR, Rhee CH, Yung WK, Sawaya RA, Bruner JM, Zhang W (2002) Molecular classification of human diffuse gliomas by multidimensional scaling analysis of gene expression profiles parallels morphology-based classification, correlates with survival, and reveals clinically-relevant novel glioma subsets. *Brain Pathol* **12**(1)**:** 108-116

Furnari FB, Fenton T, Bachoo RM, Mukasa A, Stommel JM, Stegh A, Hahn WC, Ligon KL, Louis DN, Brennan C, Chin L, DePinho RA, Cavenee WK (2007) Malignant astrocytic glioma: genetics, biology, and paths to treatment. *Genes Dev* **21**(21)**:** 2683-2710

Galli R, Binda E, Orfanelli U, Cipelletti B, Gritti A, De Vitis S, Fiocco R, Foroni C, Dimeco F, Vescovi A (2004) Isolation and characterization of tumorigenic, stem-like neural precursors from human glioblastoma. *Cancer Res* **64**(19)**:** 7011-7021

Giebel B, Beckmann J (2007) Asymmetric cell divisions of human hematopoietic stem and progenitor cells meet endosomes. *Cell Cycle* **6**(18)**:** 2201-2204

Godard S, Getz G, Delorenzi M, Farmer P, Kobayashi H, Desbaillets I, Nozaki M, Diserens AC, Hamou MF, Dietrich PY, Regli L, Janzer RC, Bucher P, Stupp R, de Tribolet N, Domany E, Hegi ME (2003) Classification of human astrocytic gliomas on the basis of gene expression: a correlated group of genes with angiogenic activity emerges as a strong predictor of subtypes. *Cancer Res* **63**(20)**:** 6613-6625

Gomez-Manzano C, Holash J, Fueyo J, Xu J, Conrad CA, Aldape KD, de Groot JF, Bekele BN, Yung WK (2008) VEGF Trap induces antiglioma effect at different stages of disease. *Neuro Oncol* **10**(6)**:** 940-945

Griguer CE, Oliva CR, Gobin E, Marcorelles P, Benos DJ, Lancaster JR, Jr., Gillespie GY (2008) CD133 is a marker of bioenergetic stress in human glioma. *PLoS One* **3**(11)**:** e3655

Grossman SA, Phuphanich S, Lesser G, Rozental J, Grochow LB, Fisher J, Piantadosi S (2001) Toxicity, efficacy, and pharmacology of suramin in adults with recurrent high-grade gliomas. *J Clin Oncol* **19**(13)**:** 3260-3266

Hanahan D, Weinberg RA (2000) The hallmarks of cancer. *Cell* **100**(1)**:** 57-70

Harris MA, Yang H, Low BE, Mukherjee J, Guha A, Bronson RT, Shultz LD, Israel MA, Yun K (2008) Cancer stem cells are enriched in the side population cells in a mouse model of glioma. *Cancer Res* **68**(24)**:** 10051-10059

Hartmann C, Hentschel B, Wick W, Capper D, Felsberg J, Simon M, Westphal M, Schackert G, Meyermann R, Pietsch T, Reifenberger G, Weller M, Loeffler M, von Deimling A (2010) Patients with IDH1 wild type anaplastic astrocytomas exhibit worse prognosis than IDH1-mutated

glioblastomas, and IDH1 mutation status accounts for the unfavorable prognostic effect of higher age: implications for classification of gliomas. *Acta Neuropathol* **120**(6)**:** 707-718

Hartmann C, Meyer J, Balss J, Capper D, Mueller W, Christians A, Felsberg J, Wolter M, Mawrin C, Wick W, Weller M, Herold-Mende C, Unterberg A, Jeuken JW, Wesseling P, Reifenberger G, von Deimling A (2009) Type and frequency of IDH1 and IDH2 mutations are related to astrocytic and oligodendroglial differentiation and age: a study of 1,010 diffuse gliomas. *Acta Neuropathol* **118**(4)**:** 469-474

Hegi ME, Diserens AC, Gorlia T, Hamou MF, de Tribolet N, Weller M, Kros JM, Hainfellner JA, Mason W, Mariani L, Bromberg JE, Hau P, Mirimanoff RO, Cairncross JG, Janzer RC, Stupp R (2005) MGMT gene silencing and benefit from temozolomide in glioblastoma. *N Engl J Med* **352**(10)**:** 997-1003

Hemmati HD, Nakano I, Lazareff JA, Masterman-Smith M, Geschwind DH, Bronner-Fraser M, Kornblum HI (2003) Cancerous stem cells can arise from pediatric brain tumors. *Proc Natl Acad Sci U S A* **100**(25)**:** 15178-15183

Henson JW, Schnitker BL, Correa KM, von Deimling A, Fassbender F, Xu HJ, Benedict WF, Yandell DW, Louis DN (1994) The retinoblastoma gene is involved in malignant progression of astrocytomas. *Ann Neurol* **36**(5)**:** 714-721

Hermansen SK, Christensen KG, Jensen SS, Kristensen BW (2011) Inconsistent immunohistochemical expression patterns of four different CD133 antibody clones in glioblastoma. *J Histochem Cytochem* **59**(4)**:** 391-407

Holland EC, Celestino J, Dai C, Schaefer L, Sawaya RE, Fuller GN (2000) Combined activation of Ras and Akt in neural progenitors induces glioblastoma formation in mice. *Nat Genet* **25**(1)**:** 55-57

Huse JT, Holland EC (2009) Genetically engineered mouse models of brain cancer and the promise of preclinical testing. *Brain Pathol* **19**(1)**:** 132-143

Huse JT, Phillips HS, Brennan CW (2011) Molecular subclassification of diffuse gliomas: seeing order in the chaos. *Glia* **59**(8)**:** 1190-1199

Huttner HB, Corbeil D, Thirmeyer C, Coras R, Kohrmann M, Mauer C, Kuramatsu JB, Kloska SP, Doerfler A, Weigel D, Klucken J, Winkler J, Pauli E, Schwab S, Hamer HM, Kasper BS (2005) Increased membrane shedding - indicated by an elevation of CD133-enriched membrane particles - into the CSF in partial epilepsy. *Epilepsy Res*

Huttner HB, Janich P, Kohrmann M, Jaszai J, Siebzehnrubl F, Blumcke I, Suttorp M, Gahr M, Kuhnt D, Nimsky C, Krex D, Schackert G, Lowenbruck K, Reichmann H, Juttler E, Hacke W, Schellinger PD, Schwab S, Wilsch-Brauninger M, Marzesco AM, Corbeil D (2008) The stem cell marker prominin-1/CD133 on membrane particles in human cerebrospinal fluid offers novel approaches for studying central nervous system disease. *Stem Cells* **26**(3)**:** 698-705

Ignatova TN, Kukekov VG, Laywell ED, Suslov ON, Vrionis FD, Steindler DA (2002) Human cortical glial tumors contain neural stem-like cells expressing astroglial and neuronal markers in vitro. *Glia* **39**(3)**:** 193-206

Immervoll H, Hoem D, Sakariassen PO, Steffensen OJ, Molven A (2008) Expression of the "stem cell marker" CD133 in pancreas and pancreatic ductal adenocarcinomas. *BMC Cancer* **8:** 48

Janich P, Corbeil D (2007) GM1 and GM3 gangliosides highlight distinct lipid microdomains within the apical domain of epithelial cells. *FEBS Lett* **581**(9)**:** 1783-1787

Joo KM, Kim SY, Jin X, Song SY, Kong DS, Lee JI, Jeon JW, Kim MH, Kang BG, Jung Y, Jin J, Hong SC, Park WY, Lee DS, Kim H, Nam DH (2008) Clinical and biological implications of CD133-positive and CD133-negative cells in glioblastomas. *Lab Invest* **88**(8)**:** 808-815

Kang MK, Kang SK (2007) Tumorigenesis of chemotherapeutic drug-resistant cancer stem-like cells in brain glioma. *Stem Cells Dev* **16**(5)**:** 837-847

Karbanova J, Missol-Kolka E, Fonseca AV, Lorra C, Janich P, Hollerova H, Jaszai J, Ehrmann J, Kolar Z, Liebers C, Arl S, Subrtova D, Freund D, Mokry J, Huttner WB, Corbeil D (2008) The stem cell marker CD133 (Prominin-1) is expressed in various human glandular epithelia. *J Histochem Cytochem* **56**(11)**:** 977-993

Kemper K, Sprick MR, de Bree M, Scopelliti A, Vermeulen L, Hoek M, Zeilstra J, Pals ST, Mehmet H, Stassi G, Medema JP (2010) The AC133 epitope, but not the CD133 protein, is lost upon cancer stem cell differentiation. *Cancer Res* **70**(2)**:** 719-729

Kern SE, Shibata D (2007) The fuzzy math of solid tumor stem cells: a perspective. *Cancer Res* **67**(19)**:** 8985-8988

Kilic T, Alberta JA, Zdunek PR, Acar M, Iannarelli P, O'Reilly T, Buchdunger E, Black PM, Stiles CD (2000) Intracranial inhibition of platelet-derived growth factor-mediated glioblastoma cell growth by an orally active kinase inhibitor of the 2-phenylaminopyrimidine class. *Cancer Res* **60**(18)**:** 5143-5150

Kosodo Y, Roper K, Haubensak W, Marzesco AM, Corbeil D, Huttner WB (2004) Asymmetric distribution of the apical plasma membrane during neurogenic divisions of mammalian neuroepithelial cells. *EMBO J* **23**(11)**:** 2314-2324

Laks DR, Masterman-Smith M, Visnyei K, Angenieux B, Orozco NM, Foran I, Yong WH, Vinters HV, Liau LM, Lazareff JA, Mischel PS, Cloughesy TF, Horvath S, Kornblum HI (2009) Neurosphere formation is an independent predictor of clinical outcome in malignant glioma. *Stem Cells* **27**(4)**:** 980-987

Lapidot T, Sirard C, Vormoor J, Murdoch B, Hoang T, Caceres-Cortes J, Minden M, Paterson B, Caligiuri MA, Dick JE (1994) A cell initiating human acute myeloid leukaemia after transplantation into SCID mice. *Nature* **367**(6464)**:** 645-648

Lardon J, Corbeil D, Huttner WB, Ling Z, Bouwens L (2008) Stem cell marker prominin-1/AC133 is expressed in duct cells of the adult human pancreas. *Pancreas* **36**(1)**:** e1-6

Lathia JD, Gallagher J, Heddleston JM, Wang J, Eyler CE, Macswords J, Wu Q, Vasanji A, McLendon RE, Hjelmeland AB, Rich JN (2010) Integrin alpha 6 regulates glioblastoma stem cells. *Cell Stem Cell* **6**(5)**:** 421-432

Lathia JD, Hitomi M, Gallagher J, Gadani SP, Adkins J, Vasanji A, Liu L, Eyler CE, Heddleston JM, Wu Q, Minhas S, Soeda A, Hoeppner DJ, Ravin R, McKay RD, McLendon RE, Corbeil D, Chenn A, Hjelmeland AB, Park DM, Rich JN (2011) Distribution of CD133 reveals glioma stem cells self-renew through symmetric and asymmetric cell divisions. *Cell Death Dis* **2:** e200

Lee J, Kotliarova S, Kotliarov Y, Li A, Su Q, Donin NM, Pastorino S, Purow BW, Christopher N, Zhang W, Park JK, Fine HA (2006) Tumor stem cells derived from glioblastomas cultured in bFGF and EGF more closely mirror the phenotype and genotype of primary tumors than do serum-cultured cell lines. *Cancer Cell* **9**(5)**:** 391-403

Lee J, Son MJ, Woolard K, Donin NM, Li A, Cheng CH, Kotliarova S, Kotliarov Y, Walling J, Ahn S, Kim M, Totonchy M, Cusack T, Ene C, Ma H, Su Q, Zenklusen JC, Zhang W, Maric D, Fine HA (2008) Epigenetic-mediated dysfunction of the bone morphogenetic protein pathway inhibits differentiation of glioblastoma-initiating cells. *Cancer Cell* **13**(1)**:** 69-80

Li A, Walling J, Ahn S, Kotliarov Y, Su Q, Quezado M, Oberholtzer JC, Park J, Zenklusen JC, Fine HA (2009) Unsupervised analysis of transcriptomic profiles reveals six glioma subtypes. *Cancer Res* **69**(5)**:** 2091-2099

Ligon KL, Huillard E, Mehta S, Kesari S, Liu H, Alberta JA, Bachoo RM, Kane M, Louis DN, Depinho RA, Anderson DJ, Stiles CD, Rowitch DH (2007) Olig2-regulated lineage-restricted pathway controls replication competence in neural stem cells and malignant glioma. *Neuron* **53**(4)**:** 503-517

Liu C, Sage JC, Miller MR, Verhaak RG, Hippenmeyer S, Vogel H, Foreman O, Bronson RT, Nishiyama A, Luo L, Zong H (2011) Mosaic analysis with double markers reveals tumor cell of origin in glioma. *Cell* **146**(2)**:** 209-221

Liu G, Yuan X, Zeng Z, Tunici P, Ng H, Abdulkadir IR, Lu L, Irvin D, Black KL, Yu JS (2006) Analysis of gene expression and chemoresistance of CD133+ cancer stem cells in glioblastoma. *Mol Cancer* **5:** 67

Liu Q, Nguyen DH, Dong Q, Shitaku P, Chung K, Liu OY, Tso JL, Liu JY, Konkankit V, Cloughesy TF, Mischel PS, Lane TF, Liau LM, Nelson SF, Tso CL (2009) Molecular properties of CD133+ glioblastoma stem cells derived from treatment-refractory recurrent brain tumors. *J Neurooncol* **94**(1)**:** 1-19

Lois C, Garcia-Verdugo JM, Alvarez-Buylla A (1996) Chain migration of neuronal precursors. *Science* **271**(5251)**:** 978-981

Lottaz C, Beier D, Meyer K, Kumar P, Hermann A, Schwarz J, Junker M, Oefner PJ, Bogdahn U, Wischhusen J, Spang R, Storch A, Beier CP (2010) Transcriptional profiles of CD133+ and CD133- glioblastoma-derived cancer stem cell lines suggest different cells of origin. *Cancer Res* **70**(5)**:** 2030-2040

Louis DN, Ohgaki H, Wiestler OD, Cavenee WK, Burger PC, Jouvet A, Scheithauer BW, Kleihues P (2007) The 2007 WHO classification of tumours of the central nervous system. *Acta Neuropathol* **114**(2)**:** 97-109

Louis SA, Rietze RL, Deleyrolle L, Wagey RE, Thomas TE, Eaves AC, Reynolds BA (2008) Enumeration of neural stem and progenitor cells in the neural colony-forming cell assay. *Stem Cells* **26**(4)**:** 988-996

Luskin MB (1993) Restricted proliferation and migration of postnatally generated neurons derived from the forebrain subventricular zone. *Neuron* **11**(1)**:** 173-189

Marzesco AM, Janich P, Wilsch-Brauninger M, Dubreuil V, Langenfeld K, Corbeil D, Huttner WB (2005) Release of extracellular membrane particles carrying the stem cell marker prominin-1 (CD133) from neural progenitors and other epithelial cells. *J Cell Sci* **118**(Pt 13)**:** 2849-2858

Marzesco AM, Wilsch-Brauninger M, Dubreuil V, Janich P, Langenfeld K, Thiele C, Huttner WB, Corbeil D (2009) Release of extracellular membrane vesicles from microvilli of epithelial cells is enhanced by depleting membrane cholesterol. *FEBS Lett* **583**(5)**:** 897-902

Maw MA, Corbeil D, Koch J, Hellwig A, Wilson-Wheeler JC, Bridges RJ, Kumaramanickavel G, John S, Nancarrow D, Roper K, Weigmann A, Huttner WB, Denton MJ (2000) A frameshift mutation in prominin (mouse)-like 1 causes human retinal degeneration. *Hum Mol Genet* **9**(1)**:** 27-34

Mayer-Proschel M, Kalyani AJ, Mujtaba T, Rao MS (1997) Isolation of lineage-restricted neuronal precursors from multipotent neuroepithelial stem cells. *Neuron* **19**(4)**:** 773-785

Metellus P, Nanni-Metellus I, Delfino C, Colin C, Tchogandjian A, Coulibaly B, Fina F, Loundou A, Barrie M, Chinot O, Ouafik L, Figarella-Branger D (2011) Prognostic Impact of CD133 mRNA Expression in 48 Glioblastoma Patients Treated with Concomitant Radiochemotherapy: A Prospective Patient Cohort at a Single Institution. *Ann Surg Oncol*

Miller CR, Perry A (2007) Glioblastoma. *Arch Pathol Lab Med* **131**(3)**:** 397-406

Miraglia S, Godfrey W, Yin AH, Atkins K, Warnke R, Holden JT, Bray RA, Waller EK, Buck DW (1997) A novel five-transmembrane hematopoietic stem cell antigen: isolation, characterization, and molecular cloning. *Blood* **90**(12)**:** 5013-5021

Monzani E, Facchetti F, Galmozzi E, Corsini E, Benetti A, Cavazzin C, Gritti A, Piccinini A, Porro D, Santinami M, Invernici G, Parati E, Alessandri G, La Porta CA (2007) Melanoma contains CD133 and ABCG2 positive cells with enhanced tumourigenic potential. *Eur J Cancer* **43**(5)**:** 935-946

Moore KA, Lemischka IR (2006) Stem cells and their niches. *Science* **311**(5769)**:** 1880-1885

Nigro JM, Misra A, Zhang L, Smirnov I, Colman H, Griffin C, Ozburn N, Chen M, Pan E, Koul D, Yung WK, Feuerstein BG, Aldape KD (2005) Integrated array-comparative genomic hybridization and expression array profiles identify clinically relevant molecular subtypes of glioblastoma. *Cancer Res* **65**(5)**:** 1678-1686

Norden AD, Drappatz J, Wen PY (2008) Novel anti-angiogenic therapies for malignant gliomas. *Lancet Neurol* **7**(12)**:** 1152-1160

Noushmehr H, Weisenberger DJ, Diefes K, Phillips HS, Pujara K, Berman BP, Pan F, Pelloski CE, Sulman EP, Bhat KP, Verhaak RG, Hoadley KA, Hayes DN, Perou CM, Schmidt HK, Ding L, Wilson RK, Van Den Berg D, Shen H, Bengtsson H, Neuvial P, Cope LM, Buckley J, Herman JG, Baylin SB, Laird PW, Aldape K (2010) Identification of a CpG island methylator phenotype that defines a distinct subgroup of glioma. *Cancer Cell* **17**(5)**:** 510-522

Nowell PC (1976) The clonal evolution of tumor cell populations. *Science* **194**(4260)**:** 23-28

Nutt CL, Mani DR, Betensky RA, Tamayo P, Cairncross JG, Ladd C, Pohl U, Hartmann C, McLaughlin ME, Batchelor TT, Black PM, von Deimling A, Pomeroy SL, Golub TR, Louis DN (2003) Gene expression-based classification of malignant gliomas correlates better with survival than histological classification. *Cancer Res* **63**(7)**:** 1602-1607

O'Brien CA, Pollett A, Gallinger S, Dick JE (2007) A human colon cancer cell capable of initiating tumour growth in immunodeficient mice. *Nature* **445**(7123)**:** 106-110

Ogden AT, Waziri AE, Lochhead RA, Fusco D, Lopez K, Ellis JA, Kang J, Assanah M, McKhann GM, Sisti MB, McCormick PC, Canoll P, Bruce JN (2008) Identification of A2B5+CD133- tumor-initiating cells in adult human gliomas. *Neurosurgery* **62**(2)**:** 505-514; discussion 514-505

Ohgaki H, Kleihues P (2007) Genetic pathways to primary and secondary glioblastoma. *Am J Pathol* **170**(5)**:** 1445-1453

Pallini R, Ricci-Vitiani L, Banna GL, Signore M, Lombardi D, Todaro M, Stassi G, Martini M, Maira G, Larocca LM, De Maria R (2008) Cancer stem cell analysis and clinical outcome in patients with glioblastoma multiforme. *Clin Cancer Res* **14**(24)**:** 8205-8212

Parsons DW, Jones S, Zhang X, Lin JC, Leary RJ, Angenendt P, Mankoo P, Carter H, Siu IM, Gallia GL, Olivi A, McLendon R, Rasheed BA, Keir S, Nikolskaya T, Nikolsky Y, Busam DA, Tekleab H, Diaz LA, Jr., Hartigan J, Smith DR, Strausberg RL, Marie SK, Shinjo SM, Yan H, Riggins GJ, Bigner DD, Karchin R, Papadopoulos N, Parmigiani G, Vogelstein B, Velculescu VE,

Kinzler KW (2008) An integrated genomic analysis of human glioblastoma multiforme. *Science* **321**(5897)**:** 1807-1812

Pelloski CE, Ballman KV, Furth AF, Zhang L, Lin E, Sulman EP, Bhat K, McDonald JM, Yung WK, Colman H, Woo SY, Heimberger AB, Suki D, Prados MD, Chang SM, Barker FG, 2nd, Buckner JC, James CD, Aldape K (2007) Epidermal growth factor receptor variant III status defines clinically distinct subtypes of glioblastoma. *J Clin Oncol* **25**(16)**:** 2288-2294

Phillips HS, Kharbanda S, Chen R, Forrest WF, Soriano RH, Wu TD, Misra A, Nigro JM, Colman H, Soroceanu L, Williams PM, Modrusan Z, Feuerstein BG, Aldape K (2006) Molecular subclasses of high-grade glioma predict prognosis, delineate a pattern of disease progression, and resemble stages in neurogenesis. *Cancer Cell* **9**(3)**:** 157-173

Piccirillo SG, Reynolds BA, Zanetti N, Lamorte G, Binda E, Broggi G, Brem H, Olivi A, Dimeco F, Vescovi AL (2006) Bone morphogenetic proteins inhibit the tumorigenic potential of human brain tumour-initiating cells. *Nature* **444**(7120)**:** 761-765

Prados MD, Lamborn KR, Chang S, Burton E, Butowski N, Malec M, Kapadia A, Rabbitt J, Page MS, Fedoroff A, Xie D, Kelley SK (2006) Phase 1 study of erlotinib HCl alone and combined with temozolomide in patients with stable or recurrent malignant glioma. *Neuro Oncol* **8**(1)**:** 67-78

Quintana E, Shackleton M, Sabel MS, Fullen DR, Johnson TM, Morrison SJ (2008) Efficient tumour formation by single human melanoma cells. *Nature* **456**(7222)**:** 593-598

Rao MS, Noble M, Mayer-Proschel M (1998) A tripotential glial precursor cell is present in the developing spinal cord. *Proc Natl Acad Sci U S A* **95**(7)**:** 3996-4001

Rappa G, Fodstad O, Lorico A (2008) The stem cell-associated antigen CD133 (Prominin-1) is a molecular therapeutic target for metastatic melanoma. *Stem Cells* **26**(12)**:** 3008-3017

Raso A, Mascelli S, Biassoni R, Nozza P, Kool M, Pistorio A, Ugolotti E, Milanaccio C, Pignatelli S, Ferraro M, Pavanello M, Ravegnani M, Cama A, Garre ML, Capra V (2011) High levels of PROM1 (CD133) transcript are a potential predictor of poor prognosis in medulloblastoma. *Neuro Oncol* **13**(5)**:** 500-508

Raymond E, Brandes AA, Dittrich C, Fumoleau P, Coudert B, Clement PM, Frenay M, Rampling R, Stupp R, Kros JM, Heinrich MC, Gorlia T, Lacombe D, van den Bent MJ (2008) Phase II study of imatinib in patients with recurrent gliomas of various histologies: a European Organisation for Research and Treatment of Cancer Brain Tumor Group Study. *J Clin Oncol* **26**(28)**:** 4659-4665

Rebetz J, Tian D, Persson A, Widegren B, Salford LG, Englund E, Gisselsson D, Fan X (2008) Glial progenitor-like phenotype in low-grade glioma and enhanced CD133-expression and neuronal lineage differentiation potential in high-grade glioma. *PLoS One* **3**(4)**:** e1936

Reya T, Morrison SJ, Clarke MF, Weissman IL (2001) Stem cells, cancer, and cancer stem cells. *Nature* **414**(6859)**:** 105-111

Reynolds BA, Rietze RL (2005) Neural stem cells and neurospheres--re-evaluating the relationship. *Nat Methods* **2**(5)**:** 333-336

Reynolds BA, Weiss S (1992) Generation of neurons and astrocytes from isolated cells of the adult mammalian central nervous system. *Science* **255**(5052)**:** 1707-1710

Reynolds BA, Weiss S (1996) Clonal and population analyses demonstrate that an EGF-responsive mammalian embryonic CNS precursor is a stem cell. *Dev Biol* **175**(1)**:** 1-13

Ricci-Vitiani L, Lombardi DG, Pilozzi E, Biffoni M, Todaro M, Peschle C, De Maria R (2007) Identification and expansion of human colon-cancer-initiating cells. *Nature* **445**(7123)**:** 111-115

Ricci-Vitiani L, Pallini R, Biffoni M, Todaro M, Invernici G, Cenci T, Maira G, Parati EA, Stassi G, Larocca LM, De Maria R (2010) Tumour vascularization via endothelial differentiation of glioblastoma stem-like cells. *Nature* **468**(7325)**:** 824-828

Rich JN, Reardon DA, Peery T, Dowell JM, Quinn JA, Penne KL, Wikstrand CJ, Van Duyn LB, Dancey JE, McLendon RE, Kao JC, Stenzel TT, Ahmed Rasheed BK, Tourt-Uhlig SE, Herndon JE, 2nd, Vredenburgh JJ, Sampson JH, Friedman AH, Bigner DD, Friedman HS (2004) Phase II trial of gefitinib in recurrent glioblastoma. *J Clin Oncol* **22**(1)**:** 133-142

Richardson GD, Robson CN, Lang SH, Neal DE, Maitland NJ, Collins AT (2004) CD133, a novel marker for human prostatic epithelial stem cells. *J Cell Sci* **117**(Pt 16)**:** 3539-3545

Rickman DS, Bobek MP, Misek DE, Kuick R, Blaivas M, Kurnit DM, Taylor J, Hanash SM (2001) Distinctive molecular profiles of high-grade and low-grade gliomas based on oligonucleotide microarray analysis. *Cancer Res* **61**(18)**:** 6885-6891

Rietze RL, Reynolds BA (2006) Neural stem cell isolation and characterization. *Methods Enzymol* **419:** 3-23

Roper K, Corbeil D, Huttner WB (2000) Retention of prominin in microvilli reveals distinct cholesterol-based lipid micro-domains in the apical plasma membrane. *Nat Cell Biol* **2**(9)**:** 582-592

Sagrinati C, Netti GS, Mazzinghi B, Lazzeri E, Liotta F, Frosali F, Ronconi E, Meini C, Gacci M, Squecco R, Carini M, Gesualdo L, Francini F, Maggi E, Annunziato F, Lasagni L, Serio M, Romagnani S, Romagnani P (2006) Isolation and characterization of multipotent progenitor cells from the Bowman's capsule of adult human kidneys. *J Am Soc Nephrol* **17**(9)**:** 2443-2456

Sakariassen PO, Immervoll H, Chekenya M (2007) Cancer stem cells as mediators of treatment resistance in brain tumors: status and controversies. *Neoplasia* **9**(11)**:** 882-892

Salmaggi A, Boiardi A, Gelati M, Russo A, Calatozzolo C, Ciusani E, Sciacca FL, Ottolina A, Parati EA, La Porta C, Alessandri G, Marras C, Croci D, De Rossi M (2006) Glioblastoma-derived tumorospheres identify a population of tumor stem-like cells with angiogenic potential and enhanced multidrug resistance phenotype. *Glia* **54**(8)**:** 850-860

Sampson JH, Archer GE, Mitchell DA, Heimberger AB, Bigner DD (2008) Tumor-specific immunotherapy targeting the EGFRvIII mutation in patients with malignant glioma. *Semin Immunol* **20**(5)**:** 267-275

Sanai N, Tramontin AD, Quinones-Hinojosa A, Barbaro NM, Gupta N, Kunwar S, Lawton MT, McDermott MW, Parsa AT, Manuel-Garcia Verdugo J, Berger MS, Alvarez-Buylla A (2004) Unique astrocyte ribbon in adult human brain contains neural stem cells but lacks chain migration. *Nature* **427**(6976)**:** 740-744

Sasaki A, Kamiyama T, Yokoo H, Nakanishi K, Kubota K, Haga H, Matsushita M, Ozaki M, Matsuno Y, Todo S (2010) Cytoplasmic expression of CD133 is an important risk factor for overall survival in hepatocellular carcinoma. *Oncol Rep* **24**(2)**:** 537-546

Scadden DT (2006) The stem-cell niche as an entity of action. *Nature* **441**(7097)**:** 1075-1079

Sennino B, Falcon BL, McCauley D, Le T, McCauley T, Kurz JC, Haskell A, Epstein DM, McDonald DM (2007) Sequential loss of tumor vessel pericytes and endothelial cells after inhibition of platelet-derived growth factor B by selective aptamer AX102. *Cancer Res* **67**(15)**:** 7358-7367

Shackleton M, Quintana E, Fearon ER, Morrison SJ (2009) Heterogeneity in cancer: cancer stem cells versus clonal evolution. *Cell* **138**(5)**:** 822-829

Shah NP, Skaggs BJ, Branford S, Hughes TP, Nicoll JM, Paquette RL, Sawyers CL (2007) Sequential ABL kinase inhibitor therapy selects for compound drug-resistant BCR-ABL mutations with altered oncogenic potency. *J Clin Invest* **117**(9)**:** 2562-2569

Shai R, Shi T, Kremen TJ, Horvath S, Liau LM, Cloughesy TF, Mischel PS, Nelson SF (2003) Gene expression profiling identifies molecular subtypes of gliomas. *Oncogene* **22**(31)**:** 4918-4923

Shaked Y, Ciarrocchi A, Franco M, Lee CR, Man S, Cheung AM, Hicklin DJ, Chaplin D, Foster FS, Benezra R, Kerbel RS (2006) Therapy-induced acute recruitment of circulating endothelial progenitor cells to tumors. *Science* **313**(5794)**:** 1785-1787

Shirahata M, Iwao-Koizumi K, Saito S, Ueno N, Oda M, Hashimoto N, Takahashi JA, Kato K (2007) Gene expression-based molecular diagnostic system for malignant gliomas is superior to histological diagnosis. *Clin Cancer Res* **13**(24)**:** 7341-7356

Shmelkov SV, Butler JM, Hooper AT, Hormigo A, Kushner J, Milde T, St Clair R, Baljevic M, White I, Jin DK, Chadburn A, Murphy AJ, Valenzuela DM, Gale NW, Thurston G, Yancopoulos GD, D'Angelica M, Kemeny N, Lyden D, Rafii S (2008) CD133 expression is not restricted to stem cells, and both CD133+ and CD133- metastatic colon cancer cells initiate tumors. *J Clin Invest* **118**(6)**:** 2111-2120

Shmelkov SV, Jun L, St Clair R, McGarrigle D, Derderian CA, Usenko JK, Costa C, Zhang F, Guo X, Rafii S (2004) Alternative promoters regulate transcription of the gene that encodes stem cell surface protein AC133. *Blood* **103**(6)**:** 2055-2061

Shu Q, Wong KK, Su JM, Adesina AM, Yu LT, Tsang YT, Antalffy BC, Baxter P, Perlaky L, Yang J, Dauser RC, Chintagumpala M, Blaney SM, Lau CC, Li XN (2008) Direct orthotopic transplantation of fresh surgical specimen preserves CD133+ tumor cells in clinically relevant mouse models of medulloblastoma and glioma. *Stem Cells* **26**(6)**:** 1414-1424

Singh SK, Clarke ID, Terasaki M, Bonn VE, Hawkins C, Squire J, Dirks PB (2003) Identification of a cancer stem cell in human brain tumors. *Cancer Res* **63**(18)**:** 5821-5828

Singh SK, Hawkins C, Clarke ID, Squire JA, Bayani J, Hide T, Henkelman RM, Cusimano MD, Dirks PB (2004) Identification of human brain tumour initiating cells. *Nature* **432**(7015)**:** 396-401

Sobo K, Le Blanc I, Luyet PP, Fivaz M, Ferguson C, Parton RG, Gruenberg J, van der Goot FG (2007) Late endosomal cholesterol accumulation leads to impaired intra-endosomal trafficking. *PLoS One* **2**(9)**:** e851

Son MJ, Woolard K, Nam DH, Lee J, Fine HA (2009) SSEA-1 is an enrichment marker for tumor-initiating cells in human glioblastoma. *Cell Stem Cell* **4**(5)**:** 440-452

Soroceanu L, Kharbanda S, Chen R, Soriano RH, Aldape K, Misra A, Zha J, Forrest WF, Nigro JM, Modrusan Z, Feuerstein BG, Phillips HS (2007) Identification of IGF2 signaling through phosphoinositide-3-kinase regulatory subunit 3 as a growth-promoting axis in glioblastoma. *Proc Natl Acad Sci U S A* **104**(9)**:** 3466-3471

Stiles CD, Rowitch DH (2008) Glioma stem cells: a midterm exam. *Neuron* **58**(6)**:** 832-846

Stupp R, Hegi ME, Gilbert MR, Chakravarti A (2007) Chemoradiotherapy in malignant glioma: standard of care and future directions. *J Clin Oncol* **25**(26)**:** 4127-4136

Stupp R, Mason WP, van den Bent MJ, Weller M, Fisher B, Taphoorn MJ, Belanger K, Brandes AA, Marosi C, Bogdahn U, Curschmann J, Janzer RC, Ludwin SK, Gorlia T, Allgeier A, Lacombe D, Cairncross JG, Eisenhauer E, Mirimanoff RO (2005) Radiotherapy plus concomitant and adjuvant temozolomide for glioblastoma. *N Engl J Med* **352**(10)**:** 987-996

Suetsugu A, Nagaki M, Aoki H, Motohashi T, Kunisada T, Moriwaki H (2006) Characterization of CD133+ hepatocellular carcinoma cells as cancer stem/progenitor cells. *Biochem Biophys Res Commun* **351**(4)**:** 820-824

Sun Y, Kong W, Falk A, Hu J, Zhou L, Pollard S, Smith A (2009) CD133 (Prominin) negative human neural stem cells are clonogenic and tripotent. *PLoS One* **4**(5)**:** e5498

Suslov ON, Kukekov VG, Ignatova TN, Steindler DA (2002) Neural stem cell heterogeneity demonstrated by molecular phenotyping of clonal neurospheres. *Proc Natl Acad Sci U S A* **99**(22)**:** 14506-14511

Taylor MD, Poppleton H, Fuller C, Su X, Liu Y, Jensen P, Magdaleno S, Dalton J, Calabrese C, Board J, Macdonald T, Rutka J, Guha A, Gajjar A, Curran T, Gilbertson RJ (2005) Radial glia cells are candidate stem cells of ependymoma. *Cancer Cell* **8**(4)**:** 323-335

TCGA (2008) Comprehensive genomic characterization defines human glioblastoma genes and core pathways. *Nature* **455**(7216)**:** 1061-1068

Thon N, Damianoff K, Hegermann J, Grau S, Krebs B, Schnell O, Tonn JC, Goldbrunner R (2010) Presence of pluripotent CD133+ cells correlates with malignancy of gliomas. *Mol Cell Neurosci* **43**(1)**:** 51-59

Toma JG, Akhavan M, Fernandes KJ, Barnabe-Heider F, Sadikot A, Kaplan DR, Miller FD (2001) Isolation of multipotent adult stem cells from the dermis of mammalian skin. *Nat Cell Biol* **3**(9)**:** 778-784

Uchida N, Buck DW, He D, Reitsma MJ, Masek M, Phan TV, Tsukamoto AS, Gage FH, Weissman IL (2000) Direct isolation of human central nervous system stem cells. *Proc Natl Acad Sci U S A* **97**(26)**:** 14720-14725

Uhrbom L, Dai C, Celestino JC, Rosenblum MK, Fuller GN, Holland EC (2002) Ink4a-Arf loss cooperates with KRas activation in astrocytes and neural progenitors to generate glioblastomas of various morphologies depending on activated Akt. *Cancer Res* **62**(19)**:** 5551-5558

van den Boom J, Wolter M, Kuick R, Misek DE, Youkilis AS, Wechsler DS, Sommer C, Reifenberger G, Hanash SM (2003) Characterization of gene expression profiles associated with glioma progression using oligonucleotide-based microarray analysis and real-time reverse transcription-polymerase chain reaction. *Am J Pathol* **163**(3)**:** 1033-1043

Verhaak RG, Hoadley KA, Purdom E, Wang V, Qi Y, Wilkerson MD, Miller CR, Ding L, Golub T, Mesirov JP, Alexe G, Lawrence M, O'Kelly M, Tamayo P, Weir BA, Gabriel S, Winckler W, Gupta S, Jakkula L, Feiler HS, Hodgson JG, James CD, Sarkaria JN, Brennan C, Kahn A, Spellman PT, Wilson RK, Speed TP, Gray JW, Meyerson M, Getz G, Perou CM, Hayes DN (2010) Integrated genomic analysis identifies clinically relevant subtypes of glioblastoma characterized by abnormalities in PDGFRA, IDH1, EGFR, and NF1. *Cancer Cell* **17**(1)**:** 98-110

Vescovi AL, Galli R, Reynolds BA (2006) Brain tumour stem cells. *Nat Rev Cancer* **6**(6)**:** 425-436

Vik-Mo EO, Sandberg C, Olstorn H, Varghese M, Brandal P, Ramm-Pettersen J, Murrell W, Langmoen IA (2010) Brain tumor stem cells maintain overall phenotype and tumorigenicity after in vitro culturing in serum-free conditions. *Neuro Oncol*

Vital AL, Tabernero MD, Castrillo A, Rebelo O, Tao H, Gomes F, Nieto AB, Resende Oliveira C, Lopes MC, Orfao A (2010) Gene expression profiles of human glioblastomas are associated with both tumor cytogenetics and histopathology. *Neuro Oncol* **12**(9)**:** 991-1003

von Deimling A, Korshunov A, Hartmann C (2011) The next generation of glioma biomarkers: MGMT methylation, BRAF fusions and IDH1 mutations. *Brain Pathol* **21**(1)**:** 74-87

Vredenburgh JJ, Desjardins A, Herndon JE, 2nd, Marcello J, Reardon DA, Quinn JA, Rich JN, Sathornsumetee S, Gururangan S, Sampson J, Wagner M, Bailey L, Bigner DD, Friedman AH, Friedman HS (2007) Bevacizumab plus irinotecan in recurrent glioblastoma multiforme. *J Clin Oncol* **25**(30)**:** 4722-4729

Wang J, Sakariassen PO, Tsinkalovsky O, Immervoll H, Boe SO, Svendsen A, Prestegarden L, Rosland G, Thorsen F, Stuhr L, Molven A, Bjerkvig R, Enger PO (2008) CD133 negative glioma cells form tumors in nude rats and give rise to CD133 positive cells. *Int J Cancer* **122**(4)**:** 761-768

Wang R, Chadalavada K, Wilshire J, Kowalik U, Hovinga KE, Geber A, Fligelman B, Leversha M, Brennan C, Tabar V (2010) Glioblastoma stem-like cells give rise to tumour endothelium. *Nature* **468**(7325)**:** 829-833

Weigmann A, Corbeil D, Hellwig A, Huttner WB (1997) Prominin, a novel microvilli-specific polytopic membrane protein of the apical surface of epithelial cells, is targeted to plasmalemmal protrusions of non-epithelial cells. *Proc Natl Acad Sci U S A* **94**(23)**:** 12425-12430

Wen PY, Kesari S (2008) Malignant gliomas in adults. *N Engl J Med* **359**(5)**:** 492-507

Westermark B, Heldin CH, Nister M (1995) Platelet-derived growth factor in human glioma. *Glia* **15**(3)**:** 257-263

Yan H, Parsons DW, Jin G, McLendon R, Rasheed BA, Yuan W, Kos I, Batinic-Haberle I, Jones S, Riggins GJ, Friedman H, Friedman A, Reardon D, Herndon J, Kinzler KW, Velculescu VE, Vogelstein B, Bigner DD (2009) IDH1 and IDH2 mutations in gliomas. *N Engl J Med* **360**(8)**:** 765-773

Yin AH, Miraglia S, Zanjani ED, Almeida-Porada G, Ogawa M, Leary AG, Olweus J, Kearney J, Buck DW (1997) AC133, a novel marker for human hematopoietic stem and progenitor cells. *Blood* **90**(12)**:** 5002-5012

Yu JW, Zhang P, Wu JG, Wu SH, Li XQ, Wang ST, Lu RQ, Ni XC, Jiang BJ (2010) Expressions and clinical significances of CD133 protein and CD133 mRNA in primary lesion of gastric adenocacinoma. *J Exp Clin Cancer Res* **29:** 141

Yuan H, Corbi N, Basilico C, Dailey L (1995) Developmental-specific activity of the FGF-4 enhancer requires the synergistic action of Sox2 and Oct-3. *Genes Dev* **9**(21)**:** 2635-2645

Yuan X, Curtin J, Xiong Y, Liu G, Waschsmann-Hogiu S, Farkas DL, Black KL, Yu JS (2004) Isolation of cancer stem cells from adult glioblastoma multiforme. *Oncogene* **23**(58)**:** 9392-9400

Zacchigna S, Oh H, Wilsch-Brauninger M, Missol-Kolka E, Jaszai J, Jansen S, Tanimoto N, Tonagel F, Seeliger M, Huttner WB, Corbeil D, Dewerchin M, Vinckier S, Moons L, Carmeliet P (2009) Loss of the cholesterol-binding protein prominin-1/CD133 causes disk dysmorphogenesis and photoreceptor degeneration. *J Neurosci* **29**(7)**:** 2297-2308

Zeppernick F, Ahmadi R, Campos B, Dictus C, Helmke BM, Becker N, Lichter P, Unterberg A, Radlwimmer B, Herold-Mende CC (2008) Stem cell marker CD133 affects clinical outcome in glioma patients. *Clin Cancer Res* **14**(1)**:** 123-129

Zhang M, Song T, Yang L, Chen R, Wu L, Yang Z, Fang J (2008) Nestin and CD133: valuable stem cell-specific markers for determining clinical outcome of glioma patients. *J Exp Clin Cancer Res* **27:** 85

Zhu L, Gibson P, Currle DS, Tong Y, Richardson RJ, Bayazitov IT, Poppleton H, Zakharenko S, Ellison DW, Gilbertson RJ (2009) Prominin 1 marks intestinal stem cells that are susceptible to neoplastic transformation. *Nature* **457**(7229)**:** 603-607